

Towards Continuous User Authentication by exploring Physiological Multimodality: ECG and BVP

Miguel Jorge Saragoça Martinho

Thesis to obtain the Master of Science Degree in

Biomedical Engineering

Supervisor(s): Prof. Ana Luísa Nobre Fred
M.D. Rui Cruz Ferreira

Examination Committee

Chairperson: Prof. Maria Margarida Campos da Silveira

Supervisor: Prof. Ana Luísa Nobre Fred

Members of the Committee: Prof. Paulo Luís Serras Lobato Correia

May 2018

Acknowledgments

The work underlying this thesis was developed with the support of people who gave some of their time to be involved actively in the project and for that I thank and acknowledge them here.

Foremost, my acknowledgment goes to Professor Ana Fred, for her insights on the research topics and guidance through the work developed.

I also have to thank all my colleagues and friends with whom I shared many experiences during the last five years. I need to thank especially to the following friends that closely worked with me during the thesis: André Manso, for the discussions and help devising and making the acquisition system; Francisco Sargo, for the exchange of knowledge and issues regarding the work developed; and Rita Cóias, that was able to gather many participants to perform the experiment and was responsible for overseeing many of the acquisition sessions.

My acknowledgment also extends to Diana Batista and Helena Aidós, for their help and knowledge regarding signal processing and pattern recognition algorithms, and to Joana Santos, for her expertise in the study of ECG physiology and morphology.

I also have to thank Hugo Silva for always being available to provide advices and for the time spent assisting, creating and fixing the acquisition modules.

I have to thank all those people who participated in the experiments: friends, graduate and undergraduate students that took some of their time to help in the development of the work.

To my family, parents and sister, who provided a great support during all these years, I deeply thank them.

Lastly, an acknowledgment to Instituto de Telecomunicações (IT) for providing the logistics required to develop this thesis. This work has been conducted with the financial support of Fundação para a Ciência e Tecnologia (FCT) under the project PTDC/EEI-SII/7092/2014.

Abstract

Multibiometrics and the development of pervasive systems for performing continuous identity recognition have become a major topic of research. The work conducted in this thesis addresses the broad issue of behavioral biometrics applied to a specific environment that is common to many people in their daily routines: interaction with a computer setup.

Two physiological signals, the Electrocardiogram (ECG) and the Blood Volume Pulse (BVP), were collected in a semi off-the-person approach.

Several signal processing and classification techniques were applied and developed, which include a method for the segmentation of the signals based on the heart rate, algorithms for outlier removal and a probabilistic fusion classifier. The Error of Identification (EID) and Equal Error Rate (EER) were used as performance metrics for the identification and authentication tests, respectively.

Amplitude waveform values were extracted as features and k-Nearest Neighbors and Naive-Bayes decision level fusion classifiers were used to perform identification and authentication tests. The results show that the BVP signal degrades the performance of the multimodal approach, but the combined use of windows of different lengths for the ECG modality can yield an increase in the performance. EID of approximately 2% and 8% were achieved for the ECG in within and across-session tests, respectively. As for the EER, the values were approximately 4% and 13%, respectively.

The use of the ECG and BVP as biometric traits in the given context is limited. Although further improvements regarding sensor integration and signal processing techniques must be conducted, this work lays the foundations for exploring continuous ECG and multimodality based biometrics in a computer interaction setup.

Keywords: Multimodality; ECG; BVP; Continuous biometrics; Off-the-person; Pervasiveness

Resumo

Multibiometria e o desenvolvimento de sistemas pervasivos para reconhecimento contínuo de identidade tornaram-se tópicos importantes de investigação. O trabalho realizado nesta tese foca-se na questão principal de biometria comportamental aplicada a um ambiente específico que é comum a muitas pessoas no dia-a-dia: interacção com um computador.

Dois sinais fisiológicos, o Electrocardiograma (ECG) e o Pulso de Volume Sanguíneo (BVP), foram adquiridos numa abordagem semi “off-the-person”.

Várias técnicas de processamento de sinal e de classificação foram aplicadas e desenvolvidas, incluindo um método para a segmentação dos sinais baseado no ritmo cardíaco, algoritmos para a remoção de outliers e um classificador de fusão probabilístico. O Erro de Identificação (EID) e a Taxa de Erro Igual (EER) foram usados como métricas de avaliação da performance dos testes de identificação e autenticação, respectivamente.

Os valores de amplitude das ondas foram extraídos como features e os classificadores k-Nearest Neighbors e de fusão ao nível da classificação Naive-Bayes foram usados para realizar testes de identificação e autenticação. Os resultados indicam que o sinal de BVP degrada a performance da abordagem multimodal, mas o uso combinado de diferentes janelas na modalidade ECG pode levar a um aumento da performance. EID de aproximadamente 2% e 8% foram obtidos para o ECG nos testes dentro e entre sessões, respectivamente. Relativamente ao EER, os valores obtidos foram de aproximadamente 4% e 13%, respectivamente.

O uso do ECG e do BVP como traços biométricos neste contexto é limitado. Embora melhoramentos adicionais em termos de integração de sensores e técnicas de processamento de sinal tenham de ser realizados, este trabalho estabelece as fundações para explorar biometria contínua baseada em ECG e multimodalidade num setup de interacção com um computador.

Palavras-chave: Multimodalidade; ECG; BVP; Biometria contínua; Off-the-person; Ubiquidade

Contents

1	Introduction	1
1.1	Context	1
1.2	Problem Definition and Objectives	2
1.3	Proposed Methodology	2
1.4	Contributions	3
1.5	Research Context	3
1.6	Thesis Structure	4
2	Information Sources	5
2.1	ECG	5
2.2	BVP	8
3	Basic Concepts and State of the Art	10
3.1	Biometrics Concepts	11
3.2	Behavioral Biometrics	14
3.2.1	ECG	14
3.2.2	BVP	20
3.3	Multimodal Biometrics	21
3.4	Continuous Biometrics	25
4	Acquisition System and Experimental Setup	27
4.1	Acquisition System	27
4.1.1	Sensor Modules	27
4.1.2	Software Application for Signal Acquisition	28
4.2	Experimental Setup	29
4.2.1	Acquisition Protocol	30
4.2.2	Preliminary Considerations	31
4.3	Participants	32

5 Signal Processing	33
5.1 Denoising	34
5.1.1 ECG	34
5.1.2 BVP	34
5.1.3 Additional Denoising Techniques	34
5.2 Segmentation	37
5.2.1 Fiducial Point Detection in ECG	38
5.2.2 Fiducial Point Detection in BVP	39
5.2.3 Segmentation Methods	39
5.3 Outlier Removal	44
5.3.1 Tested Methods	44
5.3.2 Proposed Method	50
5.4 Amplitude Normalization	53
6 Feature Extraction and Classification	57
6.1 Feature Extraction	57
6.2 Classification: Identification and Authentication Techniques	58
6.2.1 Single Modality Biometrics	58
6.2.2 Multimodal Biometrics	59
7 Experimental Results and Discussion	61
7.1 Test Protocol	61
7.2 System's Usability	62
7.2.1 User Acceptability	63
7.2.2 User Satisfaction	64
7.3 Identification Results: Single Modalities	65
7.3.1 Averaging and ECG Cutoff Frequency	65
7.3.2 Normalization Techniques and Dissimilarity Measures	67
7.3.3 Comparison Between Tasks	68
7.4 Authentication Results: Single Modalities	71
7.5 Identification Results: Multimodality	71
7.5.1 Forearm ECG and BVP	71
7.5.2 Forearm ECG	72
7.6 Benchmarking	73
8 Conclusions	75
8.1 Main Results	75
8.2 Future Work	76

A Tools	78
A.1 Thesis Writing	78
A.2 Scientific Computation	78
B Acquisition System and Experimental Setup	79
B.1 Interface of the Signal Acquisition Application	79
B.2 Text Associated with the Task Typing 1	80
B.3 Informed Consent Form	81
C Additional Results	82
C.1 Test Protocol	82
C.2 User Acceptability	84
C.3 Identification Results: Single Modalities	86
C.3.1 Averaging and ECG Cutoff Frequency	86
C.3.2 Comparison Between Tasks	88
C.4 Authentication Results	88

List of Figures

1.1	Overview of the proposed methodology.	3
2.1	Standard electrode placement and leads for the ECG.	6
2.2	Formation of the heartbeat waveform.	7
2.3	BVP waveform and main characteristic points.	8
3.1	Representation of a biometric system.	12
3.2	Categorization of ECG recognition methods based on features.	16
3.3	Categorization of the fusion methods performed at different levels.	23
4.1	Sensor modules.	29
4.2	Placement of the sensors and electrodes on a subject.	30
4.3	Setup used in the experiment.	31
4.4	Segments of raw EDA and filtered ECG acquired at the collar bones.	32
5.1	Signal processing pipeline.	33
5.2	Filtering method applied to the ECG signal.	35
5.3	Noise and artifacts in ECG recordings.	35
5.4	Denoising of the BVP signal and a segment contaminated with noise.	36
5.5	Use of ICA with BVP and ACC signals.	37
5.6	Forearm ECG signal obtained after EKS based filtering.	38
5.7	Detected R-peaks of segments of ECG using the modified Engelse-Zeelenberg algorithm.	39
5.8	Detected systolic peaks in a segment of BVP signal.	40
5.9	Segmentation performed using fixed time windows.	41
5.10	Effect of HRV in uniform heart rate based resampling and morphology of the waves.	42
5.11	Segmentation performed using a heart rate based resampling.	43
5.12	KL divergence method applied to a segment of chest ECG.	48
5.13	Cross-correlation and Pearson correlation coefficient methods applied to a segment of chest ECG.	48
5.14	Example of flat beat.	51

5.15 Outlier removal pipeline.	52
5.16 Outlier removal results for the BVP data.	54
5.17 Outlier removal results for the forearm ECG data.	55
5.18 Outlier removal results for chest ECG data.	56
5.19 Example where the proposed outlier removal method failed.	56
7.1 Results of the answers to the user satisfaction questionnaire.	65
7.2 Identification results of averaging consecutive waves when performing WS-AT analysis.	66
7.3 Example of mean waves of chest ECG and ECG collected at the collar bones.	69
7.4 Results obtained for the AS analysis for the forearm ECG modality.	70
7.5 ROC curves obtained when performing WS-AT and AS analyses.	72
B.1 Real-time plots produced by the application.	79
B.2 Excerpt used in task Typing 1.	80
B.3 Informed consent form and questionnaire about user satisfaction given to the subjects involved in the experiment.	81
C.1 Identification results of averaging consecutive waves when performing WS-WT analysis.	86
C.2 Identification results of averaging consecutive waves when performing AS analysis.	87

List of Tables

4.1	Resolution of the channels of the acquisition system.	28
5.1	Performance of the modified Engelse-Zeelenberg and Christov R-peak detection algorithms.	39
7.1	Summary of the types of analysis conducted.	61
7.2	Labels assigned to the tasks.	62
7.3	Composition of the used balanced data sets.	62
7.4	Summary of the information regarding the performance evaluation tests conducted.	62
7.5	Averaged fraction of recording effectively used and total time of acquisition in the first session.	63
7.6	Average EID results when testing different normalization techniques and dissimilarity measures for WS-AT analysis.	67
7.7	Average EID results obtained for each task when conducting a WS-AT analysis using a fixed time window segmentation	68
7.8	Average EID results obtained for each task when conducting an AS analysis using a fixed time window segmentation.	68
7.9	Average EID results obtained when conducting WS-AT and AS analyses using fixed time windows with different lengths for the forearm ECG modality.	69
7.10	Average global EER results obtained when conducting WS-AT and AS analyses using a fixed time window segmentation.	71
7.11	Average EID results obtained when conducting single modality and multimodality tests using the forearm ECG and BVP as input modalities.	73
7.12	Average EID results obtained when conducting single modality and multimodality tests using the forearm ECG modality with a combination of different fixed time windows.	73
C.1	Data collected for each subject in each task and session and elapsed time between sessions.	82
C.2	Information regarding the number of waves extracted and waves accepted as valid after outlier removal for the total population in the first session using a fixed time window segmentation.	84
C.3	Information regarding the duration of the signal acquisitions in the first session using a fixed time window segmentation.	85

C.4	Average EID results obtained for each activity when conducting an WS-AT analysis using the heart rate based resampling segmentation.	88
C.5	Average EID results obtained for each activity when conducting an AS analysis using the heart rate based resampling segmentation.	88
C.6	Average global EER results obtained when conducting WS-WT and AS analyses using the heart rate based resampling segmentation.	88

Acronyms

ACC Accelerometer

ADC Analog-to-digital Converter

ANN Artificial Neural Network

ANS Autonomic Nervous System

AS Across-session

BVP Blood Volume Pulse

CMC Cumulative Match Characteristic

CV Cross-validation

DCT Discrete Cosine Transform

DET Detection Error Tradeoff

DWT Discrete Wavelet Transform

EAC Ensemble Accumulation Clustering

ECG Electrocardiogram

EDA Electrodermal activity

EEG Electroencephalogram

EER Equal Error Rate

EID Error of Identification

EMD Empirical Mode Decomposition

EMG Electromyography

FAR False Accept Rate

FIR Finite Impulse Response

FTA Failure to Acquire

FTE Failure to Enroll

FRR False Reject Rate

GAR Genuine Accept Rate

GMC Generative Model Classifier

HRV Heart Rate Variability

ICA Independent Component Analysis

IoT Internet of Things

IT Instituto de Telecomunicações

KL Kullback-Leibler

LDA Linear Discriminant Analysis

LED Light-emitting Diode

LLR Log-likelihood Ratio

LMS Least-mean-squares

LOOCV Leave-one-out Cross-validation

LPC Linear Predictive Coding

MFA Multi-factor Authentication

MFCC Mel-frequency Cepstral Coefficients

ML Maximum likelihood

MNPD Mutual Nearest Point Distance

MNPM Mutual Nearest Point Match

NIST National Institute of Standards and Technology

NN Nearest Neighbor

nSC Normalized Spatial Correlation

PCA Principal Component Analysis

PCG Phonocardiogram

PIA Pattern and Image Analysis group

PPG Photoplethysmography

PRD Percent Residual Difference

ROC Receiver Operating Curve

SAECG Signal Averaged ECG

SCR Skin Conductance Response

SIMCA Soft Independent Modeling of Class Analogy

STFT Short-time Fourier Transform

TPR True Positive Rate

TPIR True Positive Identification Rate

VQ Vector Quantization

WS Within-session

WS-AT Within-session across-task

WS-WT Within-session within-task

ZMCP Ziv-Merhav Cross Parsing

Chapter 1

Introduction

1.1 Context

Over the last two decades we have seen a growing trend in the ubiquity of sensors in many fields of the society that include security, health care, lifestyle, communications and even fashion. The advancements done in the area of Internet of Things (IoT) and cloud-based services allow developers to propose new solutions that are able to extract more meaningful information from the larger amounts of data collected to provide better and more personalized experiences and benefits to the users. However, these developments raise concerns regarding privacy and the security of sensitive data, and thus the development of secure systems is crucial. In this context, biometrics, *i.e.*, the use of physical or behavioral characteristics as a means of verifying personal identity, becomes more relevant when compared to the use of passwords and tokens that can be lost, shared, and stolen.

Biometrics research has been focused on exploring new modalities to increase the performance of biometric systems, but also on studying and developing more pervasive processes that do not require active collaboration of users and experts while, at the same time, do not interfere with the user experience. This work is essential when considering the development of techniques for continuous identity recognition and of systems which are less susceptible to attacks that try to compromise them by directly simulating the user's biometric trait or by tampering the system at other levels. Although there has been an improvement in the sensors and acquisition systems, there are many challenges that need to be addressed, and which include the quality and variability of the biometric traits.

This thesis is focused on the study of continuously identifying subjects using a devised biometric system that is integrated on a computer interaction setup, inhibiting access to the computer resources when an impostor is detected.

1.2 Problem Definition and Objectives

Biometrics studies the development of techniques used to find the identity of subjects by extracting and combining relevant information of biological and behavioral traits. This field poses significant challenges that include: (i) which characteristics should be extracted from the traits produced by the highly dynamic and complex systems that compose the human body? (ii) how to process, update and combine the information obtained to better distinguish subjects from each other?

With this in mind, we studied two physiological signals to assert the possibility of combining these two traits to perform continuous identity recognition in the context of a biometric system integrated on a computer interaction setup with a semi off-the-person approach. A semi off-the-person approach consists of the combined use of wearables, *i.e.*, detachable electronic devices that are worn on the body, and devices that are integrated in objects or surfaces, for example, with which the user interacts with, without requiring any specific preparation, which in turn increases the user acceptability and ease of use. The selected signals were the Electrocardiogram (ECG), the electrical manifestation of the heart's activity, and the Blood Volume Pulse (BVP), which results from the interaction between the heart and the circulatory system. The biosignals were collected while the subjects used a computer, and signal processing algorithms were applied to extract significant characteristics of both signals for performing identity recognition.

The main goals of the thesis are the following:

- proposal and test of a prototype biometric system to continuously authenticate subjects through fusion of two modalities, ECG and BVP, acquired using a semi off-the-person approach where the system is integrated on a computer interaction setup;
- address the challenging issues associated with such a scenario, including robust denoising of signals;
- creation of a database with acquisitions from a set of subjects using the proposed system in different contexts of use of a computer;
- evaluation of the performance of the system using the created database;
- evaluation of the system's usability;
- test and implementation of identification and authentication techniques for single modality and multi-modality biometrics;
- address the problem of trait permanence and changes promoted by a varying heart rate.

1.3 Proposed Methodology

This thesis addresses the problem of identity recognition based on physiological data and proposes a holistic system that comprises the biosignals acquisition modules, the signal processing and biometric recognition

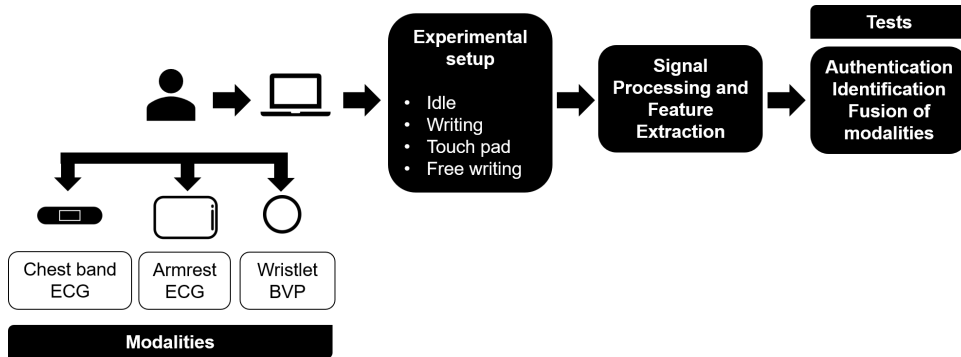


Figure 1.1: Overview of the proposed methodology.

techniques and the set of experiments conducted to test and validate them. Figure 1.1 shows a summary overview of the methodology. The ECG and BVP modalities were acquired in a pervasive on and semi off-the-person approaches. Considering the system designed and the use of dry electrodes, the quality of the signals poses additional challenges, particularly in terms of signal processing. Denoising and outlier removal techniques were applied to reduce and eliminate some noise and artifact components. Regarding the biometric application component, solutions for the following challenges are proposed: representation and selection of discriminative characteristics and fusion of modalities to increase the performance. The system and techniques used and developed were finally tested using a set of experiments based on the interaction with a computer.

1.4 Contributions

The major contributions are the following:

- acquisition system for integration in a computer setup in a semi off-the-person approach;
- novel outlier removal methodology and algorithms for severely noisy ECG and BVP signals;
- development of a heart rate based segmentation for the ECG and BVP;
- implementation of a decision level fusion probabilistic classifier.

1.5 Research Context

The work developed in this thesis is part of a wider research that is being followed by the Pattern and Image Analysis (PIA) group at Instituto de Telecomunicações (IT) in Lisbon. One of the main areas of research is the acquisition of physiological data and the extraction of information pertaining to the identity of the subject as well to his or her affective, cognitive and physical states while conducting tasks that promote changes in these states. The group has focused in the last years on off-the-person approaches by developing pervasive and non-intrusive devices, and the work produced in this thesis is included in this context.

1.6 Thesis Structure

This thesis is divided into eight chapters. The current chapter introduced the problem, explaining briefly the motivations behind it and the contributions of the present thesis. Chapter 2 describes the signal sources used in the work in terms of their physiological background and Chapter 3 provides a review of the state of the art on biometrics involving the behavioral traits that are object of study, giving an overview of biometrics concepts, and also focusing on topics such as multibiometrics and continuous biometrics.

Chapter 4 describes the acquisition process, the system used to collect the data and the details of the experiment conducted. After that, Chapter 5 details the signal processing algorithms that were tested and applied to each of the physiological signals acquired in terms of the denoising and outlier removal techniques considered. Chapter 6 starts by describing the feature extraction process, and then the type of classification algorithms considered and implemented for performing identification and authentication tests in the case of single modality and multimodal biometrics.

The results in terms of performance and usability of the system developed, and respective discussion, are described in Chapter 7. The last chapter, Chapter 8, provides the conclusions and addresses future work.

Chapter 2

Information Sources

In this chapter, we describe briefly the two main information sources used in this work: the ECG and the BVP. These two physiological signals are manifestations of intrinsic aspects of the human body and due to the interaction of the heart with the circulatory system, they share some characteristics.

2.1 ECG

The accurate measurement of the electrical activity of the heart started in the early 1900s with the work of Einthoven [22]. Since then, the ECG has become a standard method of studying the heart and the cardiovascular system, yielding relevant information for the diagnosis of heart related diseases, but also for the study of physical and emotional states. Characteristics such as the position, size and shape of the heart, and the functional and structural properties of the cardiac tissues result in manifestations of activity that can be highly individualized and thus used in identity recognition systems. Although there is active research in the use of other signals produced by the heart as biometric traits, such as the sounds generated during the cardiac cycle [63], the main focus of research for the last fifteen years has been the ECG.

The ECG consists on the recording of the electrical activity of the heart using electrodes placed on the surface of the body, usually at chest level, or on the heart, although the last option is highly intrusive. These electrodes capture the electrical signals that are produced at the myocardium by the cardiac cells, and are then propagated through the body, eventually reaching the skin with enough amplitude to be acquired and amplified by appropriate circuitry found in an ECG sensor.

The most common recordings of ECG, especially in clinical conditions, are the 12-leads ECG recordings, acquired using ten electrodes: four extremity electrodes, where two are placed on the left and right arms, the neutral electrode is placed on the right leg and the last one on the left leg; and six chest electrodes: V1, which is placed on the 4th intercostal space to the right of the sternum, V2, which is placed on the 4th intercostal space but to the left of the sternum, V3, which is placed between V2 and V4, V4, which is placed on the 5th intercostal space, V5, which is placed between V4 and V6, and finally V6, which is placed on the mid-axillary line at the same height as V4. Using these ten electrodes one can derive twelve

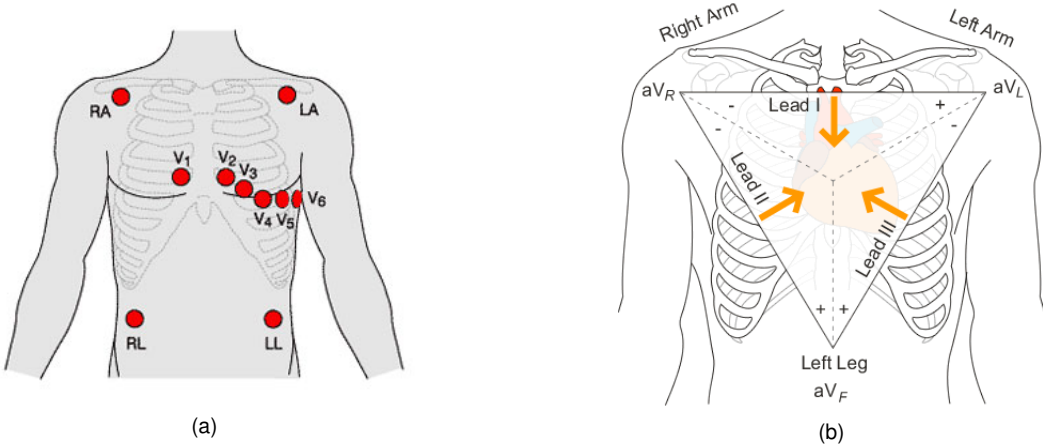


Figure 2.1: (a) Placement of the extremity and chest electrodes and (b) the six extremity leads [59].

leads, six extremity and six precordial leads. There are variants of the 12-leads ECG that use a subset of leads depending on the application. Figure 2.1 shows the standard placement of the electrodes and the configuration of the extremity leads.

The ECG is a non-stationary and quasi-periodic signal [17] whose properties depend on the conductivity and metabolic conditions of the cardiac tissue, and the interaction with the autonomic nervous system (ANS). One heartbeat, which corresponds to a cycle in the ECG signal, is characterized by a defined sequence of waves: the P wave, the QRS complex, which comprises the Q, R and S waves, and the T wave. There is an additional wave, called the U wave, that has a small amplitude and as a consequence is difficult to observe. During one heartbeat, the P wave is generated by the atrial depolarization, followed by the QRS complex, which is formed due to the ventricular depolarization and masks the small wave produced by the atrial repolarization. Lastly, the T wave is caused by the repolarization of the ventricles at the end of the cardiac cycle. Figure 2.2 illustrates the contribution of different regions and structures of the heart to the generation of the heartbeat waveform during one cycle.

The width and amplitude of these waves depend on the heart rate variability (HRV), which can be affected by many factors such as the respiration. Changes in the mental, emotional and physical states of an individual lead to an impact on the morphology of the heartbeat, via ANS activity, contributing to the intrasubject variability. In [20] the authors create a dataset of ECG recordings to investigate the impact of emotional and cognitive states on the morphology of the ECG. Porée *et al* [71] conducted experiments with 12-leads ECG recordings from 11 healthy subjects acquired at supine rest, standing and exercise, using the correlation coefficient as similarity measure between heartbeats. The authors evaluated the recording conditions, the size of the window around the R-peak and the number of leads used. Besides the aspects already mentioned, posture, gender, age, substances ingested and clinical conditions also have an impact on the morphology of the heartbeat, especially on the QT segment [17]. A more detailed analysis of the ECG can be found in [89].

For diagnostic studies based on the ECG, the commonly analyzed frequency range is from 0.05 Hz to 40

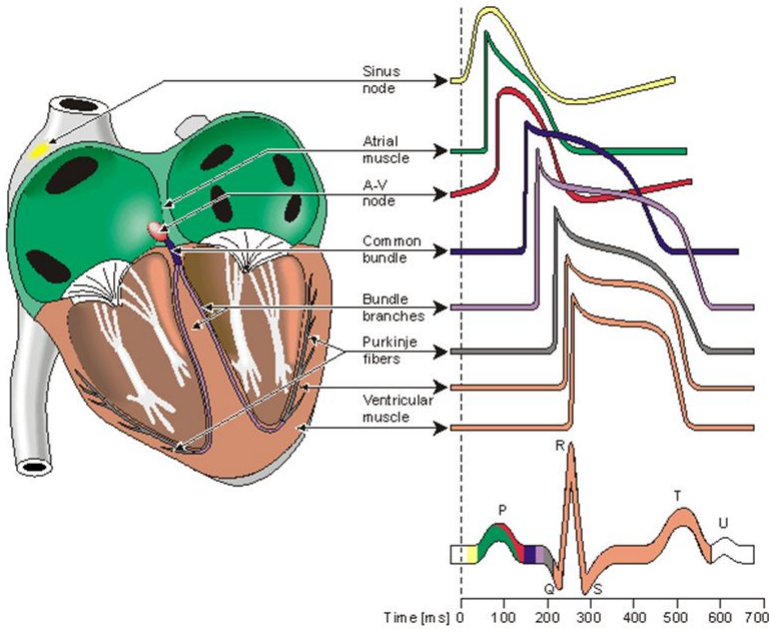


Figure 2.2: Contribution of each group of specialized cardiac muscle cells to the generation of the heartbeat waveform [54].

or 100 Hz, although some additional information can be possibly found out of this range. The selected range depends on the kind of cardiovascular disease that is investigated and how it changes the morphology of the heartbeat. For biometric research, a lower maximum bound is usually used, such as 20 and 40 Hz. The noise and artifact components that contaminate the ECG signal include [17]:

- Power line interference: 50 ± 0.2 Hz mains noise. The periodic interference is present not only at 50 Hz, but also at the higher harmonics;
- Contact noise: loss of contact between the electrodes and the skin that produces sharp changes leading to the saturation of the sensor;
- Motion artifacts: relative movement between the electrodes and the skin, leading to changes in the impedance between the former, which translates in fast but continuous changes of the baseline or complete saturation;
- Electromyography (EMG): the contraction of muscles generates electrical activity with a frequency that can range from 0 to 10 kHz.
- Baseline wandering: low frequency signal, ranging from 0.15 to 0.3 Hz, that is caused by respiration;
- Data collecting device noise: caused by the acquisition and signal processing hardware;
- Quantization noise, aliasing and signal processing artifacts.

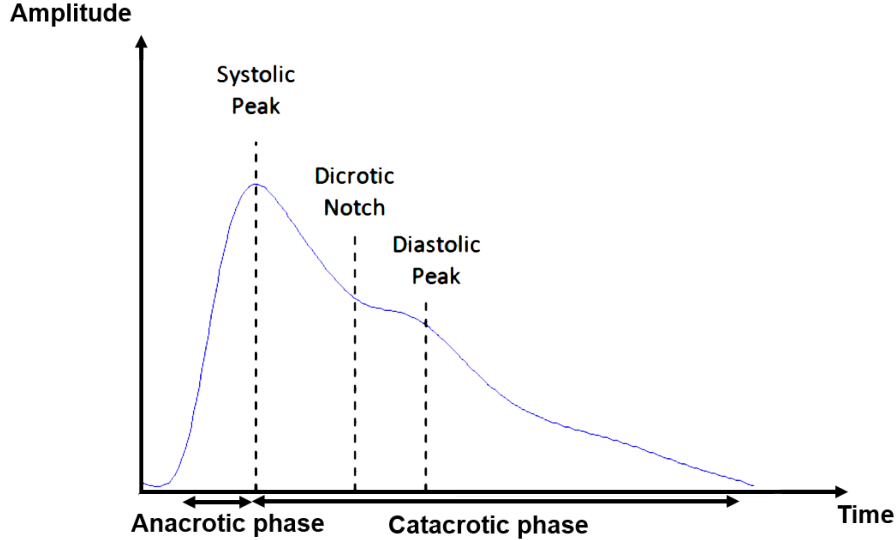


Figure 2.3: BVP waveform and main characteristic points [25].

2.2 BVP

The BVP signal measures the changes in blood volume in the capillaries and arteries by using a light-emitting diode (LED) that emits light with a determined wavelength through the tissues [62]. This light suffers scattering, reflection, transmission and absorption by the different tissues and blood, and only a partial amount of the light returns to the photodetector of the photoplethysmography (PPG) sensor. The amount of light that reaches the detector is inversely proportional to the volume of blood present in the near capillaries and arteries, given that the composition and thickness of the other tissues do not change, and neither the position of the source of light. The AC component of the signal is an indirect measure of the blood flow that changes depending on the heart's activity and on the characteristics of the local and global vascular bed, mainly their elasticity and level of dilation.

There are several types of PPG sensors. Some use only one LED that emits visible light, while others use two: one that emits light in the red spectrum and another one that emits infrared.

The BVP signal can be acquired at several places on the body such as the fingertips, the base of the fingers, wrists, earlobes and toes. The site chosen to place the sensor should be translucent and present a reasonable degree of vascularization close to the surface of the skin.

Similar to the ECG, the BVP is a non-stationary and quasi-periodic signal whose information can be useful in the discrimination between different individuals. Due to the contractions and dilations of the heart, the blood is propelled through the blood vessels, leading to the pulsatile nature of the BVP signal. A single pulse comprises two phases [79]: the anacrotic and catacrotic phases. In the anacrotic phase, the systolic pressure increases, and so does the signal, which reaches the systolic peak shortly after the systole. After this phase, there is a diastole and a wave reflection from the peripheral vessels, which produce the waveform

that characterizes the catacrotic phase, where the dicrotic notch and the diastolic peak appear.

The amplitude of the systolic peak is related to the stroke volume and to the vascular distensibility over a significant range of cardiac output [24]. Factors such as the local temperature, the relative elevation of the measurement site, local perfusion, sympathetic activity, and vasoconstrictors affect the systolic amplitude. As the BVP signal depends on the heart's activity, the signal is affected by many factors that influence the ECG, which were referred in Section 2.1. In [24] is described more particularly the morphology of the BVP acquired at the fingertips and the factors that lead to the variations observed in the signal. A more detailed analysis of the history of photoplethysmography, in terms of instrumentation and measurement protocols, and of the physiology and applications of the signal can be found in [8].

The main frequency range of the BVP is from 0.05 to 10 Hz [76]. The noise and artifact components that contaminate the BVP signal include [24]:

- Power line interference: 50 ± 0.2 Hz mains noise. The periodic interference is present not only at 50 Hz, but also at the higher harmonics;
- Motion artifacts: poor contact between the photosensor and the skin, which can be caused by vibrations and movements of the subject. The frequency of the motion artifacts is directly related to the frequency of the vibrations, and usually share the same frequency band of the BVP;
- Baseline wandering: changes in the local temperature, bias in the instrumentation amplifiers and respiration can produce variations in the baseline that usually resemble low frequency sine waves;
- Low amplitude signal: can be caused by the automatic gain controller, which adjusts the gain of the amplifier based on the amplitude of the signal, and this can lead to the saturation of the signal. A low amplitude signal can also be due to loss of central blood pressure or to loss of local perfusion induced by the constriction or dilation of the vessels;
- Ambient light interference: produced by light sources other than the LED that can affect the readings of the photodetector if this component is not effectively covered.
- Data collecting device noise: caused by the acquisition and signal processing hardware;
- Quantization noise, aliasing and signal processing artifacts.

Chapter 3

Basic Concepts and State of the Art

In this chapter we introduce the main concepts of biometrics, with emphasis on the recent work developed in the area of behavioral biometrics, more concretely the research regarding the two physiological signals that were studied. We also present an overview of the current trends in multimodal and continuous biometrics.

Biometric recognition can be described as the ability to discriminate individuals based on their physical or behavioral characteristics in an automated approach. By using intrinsic characteristics of an individual, the use of passwords and tokens can become complementary, as in multi-factor authentication (MFA) [60], or obsolete provided that the biometric systems are robust [61]. Since biometric traits are difficult to share, simulate and cannot be forgotten or lost, biometric systems have the potential of being more secure than systems based on passwords and tokens [39].

The research field of biometrics has been developing for over 50 years, starting with the pioneering work of Mitchell Trauring [86] regarding fingerprint patterns, and significant advances have led to the successful deployment of biometric applications in many different contexts, ranging from industries such as banking and military to commercial and personal use cases due to the ubiquity of laptops and smartphones and their increased connectivity, computing power and range of sensors. With the development of more compact and efficient sensors, especially in the field of fingerprint scanners, the integration of biometric systems in many different devices has become a reality and opened the possibility of using biometrics in new applications such as mobile commerce and transactions.

Initially, the research developed in this field was more focused on physical traits such as fingerprint, face, and iris. However, more recently the research community began to gain interest in behavioral traits and on the combination of traits to increase the performance of biometric systems, creating an area that is known as multibiometrics.

Behavioral traits differ from physical traits in the sense that they result from the interaction of an individual with the environment. Different stimuli promote different responses by the human body that vary with time. These dynamic responses are caused by the behavior of highly complex, nonlinear and time-variant systems that compose the human body, such as the nervous and cardiovascular systems. Behavioral traits give

insight on affective, cognitive and physical states of an individual, and can be used to extract information to characterize individuals across time. Naturally, the diversified behavior and interaction of these systems lead to an increase in the variability of patterns that are possible to be collected from each individual. Failure to capture these changes with time may result in a poor ability to discriminate. Examples of behavioral traits include voice, keystroke, gait, heart and brain [32].

In this thesis we consider two manifestations of heart activity and hemodynamics: the ECG and the BVP, respectively.

3.1 Biometrics Concepts

A biometric system is a system that acquires biometric data from an individual, pertaining to one or more traits, extracts from the data a set of relevant features that are then compared with feature sets stored in a database, and the result of the matching process elicits an action that consists, usually, in granting or removing access to certain resources. A generic biometric system is composed by four main modules [74]: a sensor module; a quality assessment and feature extraction module; a matching and decision module; and a database module. Figure 3.1 illustrates the architecture of a biometric system. A brief description of each module is done below.

1. Sensor module: this module is responsible for the acquisition of the raw biometric data of an individual and defines the interface between the user and the biometric system. A system whose point of entry is ill devised can result in low rates of raw data acquisition, which ultimately reflects in poor user acceptability.
2. Feature extraction module: the acquired raw data is usually processed using signal processing algorithms that remove noise and artifacts and enhance components of interest in the data. If the quality of the data is poor, the user may be asked to present more data until sufficient data with quality are acquired. After processing the data, a relevant set of features is generated as a compact and expressive representation of the subject. If the subject is presenting data for the first time, the process is described as enrollment and the feature set, referred as template, is stored in the database.
3. Matching and decision module: during the recognition phase, the query biometric sample of the subject is compared against templates stored in the database using a matcher. The matcher produces match scores that reflect the similarity (or dissimilarity) between the feature sets. Based on these match scores a decision is made: either validate a claimed identity or provide a ranking of the enrolled identities.
4. Database module: the database contains the templates stored for all subjects enrolled in the system. Given that a database can store many identities, larger databases are commonly structured in such a

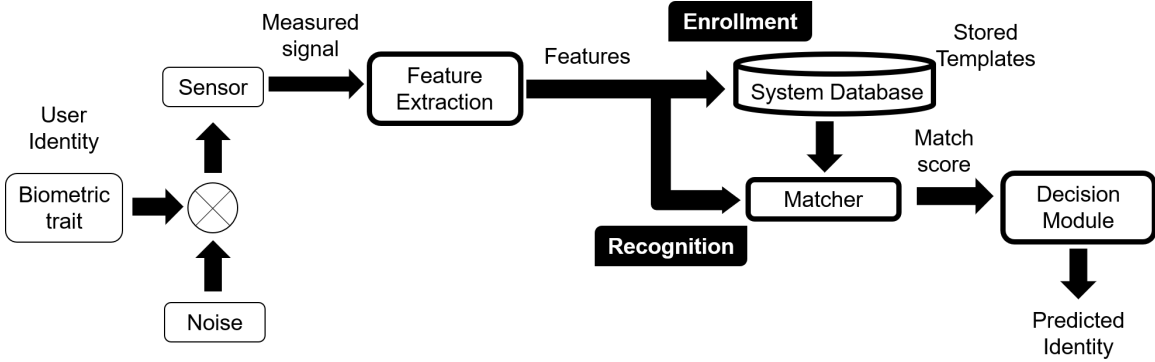


Figure 3.1: Representation of a biometric system.

way to enable a fast access to a claimed identity information or subset of identities. The data that is stored during the enrollment, depending on the application, can be analyzed by a human expert.

Given the description of the several modules that compose a biometric system, the primary challenge is to design a sensor, a signal processing and feature extraction framework, and a similarity measure to minimize the error of recognition. The raw biometric data acquired at the sensor level may present intra-subject variations across measurements due to several causes [38]: (i) limitations of the sensor module, (ii) changes in the interaction of the subject with the biometric system, (iii) intrinsic variations of the trait, (iv) changes in the acquisition environment and (v) trait specific sources of noise. By designing sensors that integrate better with the context of the application, by controlling the conditions of acquisition, if possible, and by using signal processing algorithms to remove noise and artifacts, one can decrease the intrasubject variability and thus increase the performance of the biometric system. Intrasubject variability refers to the variability between feature sets of the same individual. On the other hand, intersubject variability refers to the variability between feature sets that come from different individuals. When considering feature representation schemes, the main goal is choosing feature sets that exhibit small intrasubject variability and large intersubject variability, since these feature sets present more discriminative capacity and are less variant to changes at the individual level.

The choice of a biometric trait to be used in a certain application depends on the degree to which the trait satisfies the following properties [40]:

- universality: every individual must possess the biometric trait;
- uniqueness: any pair of individuals can be distinguished based on the biometric trait. Since uniqueness is hard to achieve, the property that is more commonly analyzed is the distinctiveness;
- collectability: the biometric trait must be a measurable quantity that is possible to be acquired and from which sets of representative features can be extracted;
- permanence: the biometric trait should be time invariant. Traits that change considerably in a short period of time are not useful in biometrics;

- performance: the biometric system should present sufficient discriminative ability given the conditions and constraints that are imposed;
- acceptability: the biometric system should present a high user acceptance, *i.e.* the users should be willing to present the biometric trait to the system;
- circumvention: the biometric trait should be hard to mimic and simulate.

Although there is a plethora of biometric traits that have been proposed, only a few are deployed in biometric systems. Fingerprint, face and iris are the most used traits [38] given the high accuracy shown in several applications, the extensive databases, produced by governments and related agencies all over the world, and the evaluations conducted by entities such as the National Institute of Standards and Technology (NIST) [73]. Traits like DNA and palmprint are used by law enforcement and forensics [56], while other traits such as voice, signature and hand geometry have been deployed in commercial applications, but with limited use. Other traits, mentioned as soft biometrics (as opposed to hard biometrics), are traits that individually do not have significant discriminative ability, because of intrinsic characteristics or because the traits have yet to reach a reasonable degree of performance and technology advancement. Soft biometrics comprise traits such as gender, ethnicity, and height that can assist other modalities in the recognition process [37]. Novel and immature soft biometric traits that are object of active research include the ECG, electroencephalogram (EEG), BVP and keystroke dynamics.

Depending on the context, a biometric system can operate in two modes [74]: verification (or authentication) and identification. In the verification mode, the system validates a subject's identity by comparing the extracted feature set with the template(s) stored in the database that belong to the claimed identity. There is an one-to-one match and the identity claim is accepted if the match score is above a defined threshold. In the case of identification, the query is compared against all templates in the database, in an one-to-many match, and the result will be the closest identity (or set of identities) whose templates exhibit the highest degree of similarity with the query sample, or a reject response when no suitable identity can be matched to the input. If there is no reject response, the system is operating in closed-set identification, otherwise the system assumes that the input can come from an identity that is not represented in the database, and this is referred as open-set identification.

When a biometric system operates in verification or identification modes, different sets of metrics are used to evaluate the performance of the system. In verification mode the biometric system can output one of two decisions: classify the individual as a genuine or an impostor individual. If the user identity matches the claimed identity but is rejected by the system, a false rejection occurs, and is described as a type 1 error; on the other hand, if the user is an impostor and is accepted by the system, that is referred to a false acceptance and classified as a type 2 error. The number of rejected genuine and accepted impostor subjects is expressed in terms of the ratio of attempts. These ratios are designated as False Reject Rate (FRR) and False Accept Rate (FAR), respectively, and can be computed globally or for each subject in

the database. Other performance metrics include the Equal Error Rate (EER), which is the value at which the FAR and FRR curves intersect, and the Receiver Operating Curve (ROC) that consists of plotting the FAR as a function of the Genuine Accept Rate (GAR), also termed True Positive Rate (TPR), which is the complement of the FRR. Alternatively to ROC curves, there are Detection Error Tradeoff (DET) curves that are similar to the former, but the axes are scaled nonlinearly.

When a biometric system operates in identification mode, the most commonly used performance metric is the Error of Identification (EID), which consists of the ratio between the number of misclassified biometric samples and the total number of biometric samples that were provided for identification. Another useful identification metric is the Cumulative Match Characteristic (CMC) curve that describes the identification accuracy as a function of rank. Each biometric test sample is compared against all template samples and the resulting scores are sorted and ranked. Then, the rank at which a correct match occurs is determined and this is used to compute the True Positive Identification Rate (TPIR) for each rank value, thus generating the CMC curve.

The metric Failure to Enroll (FTE) expresses the ratio of individuals that are not accepted by the system at the enrollment phase, while Failure to Acquire (FTA) represents the proportion of verification or identification failed attempts due to lack of data with sufficient quality. These failures can arise due to problems related to the availability of the trait, limitations of the acquisition system, changes in the environmental conditions and noncompliance of the user. These factors impact the amount of data available and their quality. Additionally, security issues, ease of use and the comfort provided by the system must be considered for an effective deployment of the biometric system.

3.2 Behavioral Biometrics

Since characteristics that describe human behavior can change with time, a biometric system that relies on these kind of traits must be designed to account for this variability. As a consequence, behavioral biometric systems are confronted with a higher degree of variability than those using physical traits. On the other hand, some behavioral traits are able to capture more information about the individual than physical traits and can be more difficult to simulate due to their higher degree of complexity. Additionally, behavioral traits can be less intrusive, which leads to increased user acceptance [33]. Traits such as the physiological signals also provide liveness detection, as opposed to fingerprint and face. Although a fingerprint sample or a photo can be easily obtained and used to perform spoofing attacks, physiological traits require the presence of the individual or the use of specialized instrumentation that can generate either data previously recorded from the individual, which was stolen, or a synthetic signal that resembles the original one.

3.2.1 ECG

The first study on the use of ECG as a biometric trait was conducted by Biel and colleagues [10], where they tested different combinations of features in 12-leads ECG recordings from 20 subjects. In order to

increase the usability of biometric applications, many studies have investigated the use of one-lead ECG for personal identification, such as the work developed by Lourenço *et al* [52], that used ECG signals acquired at the thumbs. Despite the less amount of discriminative information present in ECG signals obtained using only one lead, this configuration has shown potential in terms of performance and is more suitable to be integrated in deployable biometric systems. Other studies have used two or more ECG channels to increase the performance of recognition. These studies include those where two [94], three [26] and twelve channels [5] were used.

A significant number of studies perform the segmentation of ECG recordings into single heartbeats. This approach leads to a more coherent feature extraction and allows the application of ensemble averaging (EA) to remove noise. Santos *et al* [78] segment the ECG signal into individual heartbeats, using Principal Component Analysis (PCA) to produce eigen-templates that characterize each subject. Alternatives to this approach include the work developed by Plataniotis *et al* [65] and Loong *et al* [49]. Plataniotis *et al* used as features Discrete Cosine Transform (DCT) coefficients of the autocorrelation signal of non-overlapping windows larger than a single heartbeat, while Loong *et al* used spectral coefficients of overlapping windows computed through Linear Predictive Coding (LPC).

The features extracted from the ECG can be divided into fiducial and non-fiducial approaches. The different types of features extracted from the ECG signal are organized in Figure 3.2. Fiducial approaches use specific points of the ECG signal, called fiducial points, to extract relevant features. These features can be divided into temporal, amplitude and morphological features that are generally used in combination. The categorization of the fiducial based approaches is done below.

- Temporal features: these features pertain to the duration of segments defined by the relationships between the different waves that compose a heartbeat. By identifying the onsets, peaks and other relevant points in the waves, one can determine different temporal intervals. The most used include the duration of each wave and the time intervals between the peaks or onsets of the waves;
- Amplitude features: these include the relative amplitudes between peaks of the waves, generally with respect to the R-peak, but also the amplitude of peaks of the 1st and 2nd derivatives of the heartbeat and ratios between them. Examples of studies that use temporal and amplitude features are shown in [10] and [96];
- Morphological features: these features present information regarding the shape of the ECG in terms of each individual wave or the complete heartbeat. The most common morphological feature based approach is to use the ECG waveform, *i.e*, the temporal sequence of amplitude values as features. Other approaches include using slopes between waves, such as the ST slope segment, and the angles of the Q, R and S waves. Some of these approaches can be considered partially fiducial, since these features are not fiducial points but those are used to perform the segmentation of the ECG signal from which the features are extracted and computed. Examples of studies that use this kind of features are

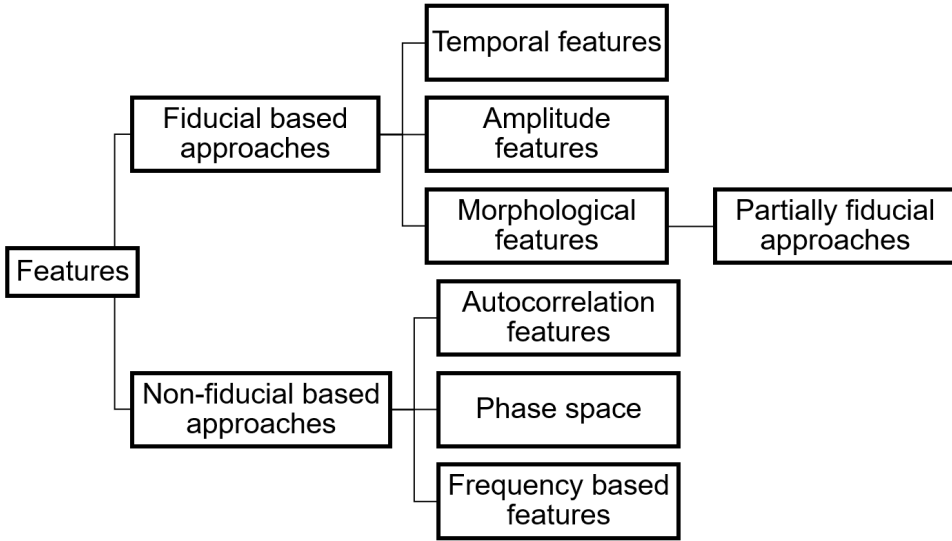


Figure 3.2: Categorization of ECG recognition methods based on features.

described in [15], [52] and [57].

The performance of biometric systems that use fiducial or partially fiducial approaches depends on the accurate localization of the fiducial points and alignment of the heartbeats. The position of the fiducial points and the length of the heartbeat change with the heart rate. Time normalization techniques try to decrease or remove the influence of the HRV in the latency and morphology of the different complexes. These techniques include the non-uniform decimation of segments of the heartbeat defined by fiducial points, such as in [52], where the authors performed decimation of the interval between the onset of the P wave until the R-peak and another decimation of the interval between the R-peak and the end of the T wave. The decimation is done such that each heartbeat has 300 samples. Another time normalization technique is the normalization of the QT segment using correction formulas such as Bazett's [9], Fridericia's [31] and Framingham's [75] formulas. Vandenberk *et al* [87] evaluated the use of these three formulas to correct the QT segment in ECG recordings of patients with sinus rhythm and concluded that Fridericia's and Framingham's corrections were better predictors of 30-day all-cause mortality than Bazett's formula. In [84] the authors used Framingham's correction formula, and introduced an adaptation by leaving the QRS unchanged, since the QRS complex is fairly robust to changes in the heart rate [3]. An alternative to the use of resampling techniques is the use of Dynamic Time Warping (DTW), as in [88], since one does not have to perform a mapping of every heartbeat to a domain of fixed length.

Although the QRS complex carries less discriminative information than the complete heartbeat, some research has been focused in the use of the QRS to perform recognition, given the invariance of the segment to the heart rate. Khalil *et al* [43] proposed the use of Legendre polynomials coefficients derived by fitting the QRS complex. Below, we describe some of the research conducted on ECG biometrics using fiducial

based approaches.

Biel *et al* [10] investigated identity recognition by using 12-leads ECG recordings acquired during rest, done in multiple days across six weeks, from 20 healthy individuals. At least 7 temporal and amplitude features were used depending on the number of leads considered. Features with a relative high correlation with other features were removed. Some tests were conducted to decrease the number of features used. The classification was done using Soft Independent Modeling of Class Analogy (SIMCA), a generative model classifier (GMC) that uses PCA to model each class. The test set consisted of 50 samples and an EID of 0% was achieved using 10 features.

Zhang and Wei [96] proposed an identification method based on Bayes' theorem. A database of 502 ECG recordings of 10 seconds was used. The ECG recordings were divided into two segments: one to build the model and the other to perform identification. 14 temporal and amplitude features were used, with the area of the QRS complex also included. Each class is modeled with a multivariate Gaussian distribution and the prior probabilities are considered equal. Tests were conducted using different leads and the best results were found using lead V2 (EID of 2.6%). For lead I, the EID increased to 14.7%.

In terms of partially fiducial approaches, some examples are described below. Chan *et al* [15] performed person identification using three quantitative measures: percent residual difference (PRD), correlation coefficient and a measure based on wavelet transform (WDIST). ECG data were collected from 50 subjects during three sessions on different days. The sensors were placed at the thumb and index finger of the subjects. Across-session (AS) analysis was performed using the data from the first session as enrollment, and the two other sessions as test sets. Each session consisted in the recording of ECG segments of 90 seconds. PQRST complexes were identified and aligned using correlation coefficients. The complexes that were not removed due to significant noise corruption were used to compute a signal averaged ECG (SAECG). The person associated with the enrollment data with the lowest PRD or the highest correlation coefficient is selected as a match. For the measure based on wavelet transform, detail coefficients up to the 5th level of Daubechies scalar wavelet (Db3) were chosen. The person associated with the enrollment data with the lowest value of this novel measure is selected. Several SAECG segments with different lengths and locations were tested. The results showed that the QRS complex has a high degree of reproducibility and that the classification accuracy is higher for segments associated with the P wave than those with the T wave. The lowest EID was achieved using WDIST (11%).

Lourenço *et al* [52] proposed a finger-based ECG biometric system. The ECG segmentation was performed using an adaptation of the Engelse-Zeelenberg algorithm. After finding the P and T complexes, the segmented heartbeats are normalized in time and amplitude. Two minutes of ECG signals were recorded for 16 subjects. The features consisted in the amplitudes of the waveform. Classification was performed using 1-Nearest Neighbor (NN) classifier with Euclidean distance as the metric. Using cross-validation (CV), 30 runs of enrollment/test sequence for each user were performed. For the enrollment phase, a mean heartbeat was computed for each subject by averaging 30 heartbeats. The same was done to build test templates. An

EID of 5.7% was achieved. As for the authentication scenario, subject-specific thresholds were tested and an EER of 10.1% was attained.

Odinaka *et al* [57] used single-lead ECG signals acquired in a non-standard placement of the electrodes on the lower rib cage and in three sessions of 5 minutes that were separated from two weeks to six months for 269 subjects. The subjects were sitting during the acquisition. Using a fixed time window [-200, 500] (ms) centered at the R peaks, each ECG recording was segmented. The short-time Fourier transform (STFT) of each averaged heartbeat was computed using a Hamming window of 64 ms with a step size of 10 ms, with overlap of 54 ms. The frequency content is truncated at 250 Hz and then the spectrogram is computed. Each point of the spectrogram is considered a time-frequency bin that is modeled as a Gaussian distribution. The parameters are computed using the maximum likelihood (ML) estimates. The symmetric relative entropy between a subject feature set and the nominal feature set, which is obtained using the spectrograms of all subjects, is used to perform feature selection. A log-likelihood ratio (LLR) score is used to validate a test heartbeat if the score is larger than a defined threshold. Tests were conducted within-session and across-session. Regarding AS analysis, the fusion of two sessions to create the training set was also tested. The authors achieved an EER of 5.58% and an EID of 13.1% when testing in heartbeats from different days. When the recognition was performed in the same session, the EER and EID decreased to 0.37% and 1%, respectively.

Non-fiducial approaches are not based on the detection of fiducial points, but use the quasi-periodicity of the ECG to extract relevant patterns. These approaches can be divided into three categories that are described below.

- Autocorrelation features: the ECG has a repetitive structure, but the signal is not periodic neither time invariant. By using the autocorrelation of ECG segments larger than a heartbeat, one can extract information regarding the most relevant characteristics that are preserved across time. Plataniotis *et al* [65] used the data from 14 healthy subjects from the PTB database [34] and computed the normalized autocorrelation of ECG segments of 10 seconds. Each recording has a duration of 100 seconds, leading to 10 windows per subject. Several maximum lags were considered. DCT was applied to the autocorrelation coefficients for dimensionality reduction. Two distance metrics were used: the normalized Euclidean distance and the normalized Gaussian log-likelihood. The classification was done using 1-NN. The best results were achieved for the normalized Gaussian log-likelihood with lags between 100 ms and 200 ms, where an EID of 0% was attained. Agrafioti [4] and Wang [91] also investigated the use of normalized autocorrelation coefficients.
- Phase space analysis: the ECG signal is mapped to two-dimensional or three-dimensional spaces by creating delayed versions of the same signal. This creates a trajectory in the phase-space that can show characteristic structures of the ECG. As an example of phase space analysis in the field of ECG biometrics, we have the work of Fang and Chang [27] that explored the three-dimensional phase-space of ECG segments of 5 seconds from 3-leads ECG recordings of 30 seconds, acquired in

two sessions separated by 30 minutes, for a set of 100 subjects. The single-lead ECG segments of 5 seconds are expanded into a time series of three-components that are normalized and obtained using different time delays τ ($\tau = 4, \dots, 36$ ms). The three-lead ECG segments are assembled into a three-dimensional vector, also normalized. The phase space is divided in a grid to decrease the resolution of the trajectory. Each cell that is traversed by the trajectory at least once is marked with a value of 1. A more detailed trajectory leads to a sparse structure and higher computational demand. Three different metrics are used to describe the similarity or dissimilarity between trajectories: the normalized spatial correlation (nSC), the mutual nearest point distance (MNPD) and the mutual nearest point match (MNPM). A global threshold is tested for the three metrics. The best results were obtained using three leads and using nSC and MNPM as metrics (EID=1%). Using only one lead, the best results were achieved using a lag of 6 ms with MNPD and 8 ms with MNPM, with an EID value of 2% for both methods. These values were attained using 40 partitions in the phase space.

- Frequency based features: use of frequency related information from the ECG signal. Loong *et al* [49] investigated the use of LPC. The authors used single-lead ECG recordings of 60 seconds from 15 healthy subjects. Two sessions were acquired in the same day and used as training and test sets. Each ECG recording was divided into segments of 5 seconds windows with 50% overlap. Then, the LPC spectrum of each window was computed and the first 40 coefficients were used as features. The classification was performed using an artificial neural network (ANN) with one hidden layer. An EID of 0% was achieved. Another example is the work of Kouchaki *et al* [45] that used Empirical Mode Decomposition (EMD) to decompose ECG segments of 1 second and applied the Hilbert Transform to the last component to compute the instantaneous frequency. The classification is performed using a 1-NN classifier. 20 healthy subjects from the PTB database were used. An EID of 7.78% was achieved.

The several works in ECG biometrics that were referred previously are a small set of all the research produced in the field, but illustrate the developments that have been done, the tendencies and the limitations. Most of the studies use small populations which are obtained, in many cases, from private databases. A small population does not allow to infer the applicability of ECG biometrics on large scale contexts, thus the deployment of ECG based biometric systems is not something currently viable. The use of private databases hinders the comparison of the performance by different methods. Although there are guidelines for ECG acquisition [72], a standard is not followed in terms of sampling frequency, type of electrodes, denoising methods and other acquisition and processing parameters. Non-fiducial features based recognition seems to bring an increase in the performance when compared with those using fiducial features. In terms of leads, the focus has been in single-lead recordings, which increase the usability of the system. Few studies analyze ECG permanence, since many works are based on within-session (WS) analysis or on sessions separated by short-time intervals, and do not investigate the variability introduced by posture, exercise, mental and emotional states, and even pathological conditions. Examples of some studies where

permanence is investigated include [2], where the authors propose a methodology for template update and [47], where a permanence analysis of the QRS complex during 24 hours is conducted. In [29] and [58] the authors do an extensive analysis of the research developed in the area of ECG biometrics, referring the main trends, limitations and future of the field.

3.2.2 BVP

Similar to the analysis done in ECG biometrics, there are fiducial and non-fiducial based approaches. Regarding the time-domain, features such as relative amplitudes, slopes, the position of peaks, the interval between characteristic points and first and second derivatives are used as biometric descriptors, but, analogous to the ECG, there are problems in the alignment and matching of waves given the changes in morphology produced by changes in the heart rate. Given this, non-fiducial approaches try to overcome these problems.

Below, several approaches in BVP biometrics are described. Chakraborty and Pal [14] extracted 12 amplitude and temporal features from the BVP and its derivatives. The authors used LDA and the classification was performed in the transformed space using 1-NN and the Euclidean distance. Data were collected from 15 healthy individuals during 3 minutes under a relaxed state. An EID of 0% was achieved.

Kavsaoglu *et al* [42] used 40 features extracted from the BVP signal and derivatives. A feature selection algorithm based on the individual accuracy of the features is used to rank the features. The classification is performed using a NN classifier and different number of neighbors were tested. The data were obtained from 30 healthy subjects. The signal was acquired at their right index finger while the individuals were seated in a calm position. Two sessions were collected in different time spans. In each session a 15-period-signal was acquired. Three configurations of data were considered: using only data from the first session (1st configuration), from the second one (2nd configuration), and fusing the data from the two sessions (3rd configuration). The best performance for the 1st configuration was achieved using 1 neighbor and 25 features, with an EID of 9.66%. For the 2nd configuration, the best results were attained using also 1 neighbor and 20 features, with an EID of 5.66%. As for the 3rd configuration, the best results were achieved using 3 neighbors and 15 features, with an EID of 12.78%.

Spachos *et al* [81] used BVP recordings from 29 healthy subjects, where 15 came from the OpenSignal PPG Dataset and 14 from the BioSec PPG Dataset [12]. The BVP was acquired at the fingertips in one session. Then, the signal was segmented, and the pulses normalized and scaled to 200 samples. The waveform amplitude values were used with Linear Discriminant Analysis (LDA) to build a smaller feature set. Five consecutive test pulses of BVP were projected into LDA space and 1-NN and majority voting was used to determine the matching, depending on the threshold used. An EER of 25% was attained when using the BioSec dataset.

Sarkar *et al* [80] modeled the BVP signal as a sum of Gaussians. A generalization of the dynamical model for the ECG from McSharry *et al* [55] was used to fit the BVP pulses to a limit cycle. From the

fit, a set of parameters were obtained, using two and five Gaussians. LDA and Quadratic Discriminant Analysis (QDA) were used to perform classification. The authors used the DEAP dataset [44] to test their approach. The data from 23 individuals were used. The data is available for 40 sessions, each with one minute, where the subjects were presented with video based stimulus to elicit different emotions. Several tests were conducted using one session as the training set and the rest as the test set. EIDs of 10% and 5% were achieved testing in 2 and 8 seconds of test data using QDA and 5 Gaussians, respectively. Better results were achieved when the test window increased, which shows the possibility of using such a method for continuous authentication.

The research in BVP biometrics is more recent than the one related to the ECG. Additionally, as the BVP shares many characteristics with the ECG, the research in this field suffers from many of the limitations found in the latter. Moreover, there are no standards regarding the materials and methods used in BVP biometrics research and the BVP signal seems to carry less discriminative information than the ECG, although there is some potential in the use of this modality as a biometric trait, individually or by complementing other modalities with higher performance. As an advantage, BVP sensors can be less intrusive and cheaper than other modalities such as the ECG. The fact that the signal can easily be measured from sites such as the index finger and the earlobes increases the user acceptability of a system based on this modality.

3.3 Multimodal Biometrics

A multibiometric system is a system that combines the information from multiple biometric sources to perform recognition and is designed with the aim to increase the performance and overcome the limitations of biometric systems that use only one source of information. In a multibiometric system, one can consider different sources of information, which leads to different types of multibiometric systems. These can be divided into multi-sensor, multi-sample, multi-algorithm, multi-instance, multimodal and hybrid systems. A detailed description of each system is done in [74]. In this thesis, we are mainly focused in multimodal biometric systems that combine the information given by different biometric traits to establish an identity.

These systems can present a better performance and robustness, since even when one or more traits are not available, due to some limitation that affects those traits, the rest can still be used to give an output, which is particularly useful in continuous monitoring. The kinds of limitations that can occur are related to the inability to present a certain trait at a given moment and to the acquisition conditions that lead to a significant noise contamination that degrades the quality of the data recorded, which can result in a small set of biometric samples that is not sufficient to produce an output for that trait. Multimodal systems can use a set of traits that individually do not present enough discriminability or that produce information with a significant degree of intrasubject variability, but that when combined can give complementary information, which can lead to improvements in performance. Additionally, by requesting multiple traits, a multimodal system is less vulnerable to circumvention attacks, since an impostor has to spoof multiple traits.

The central question of multibiometrics is the problem regarding information fusion, *i.e*, how to combine

the information given by two or more biometric sources? Other secondary problems arise such as: the cost benefits of the multibiometric system when compared with the respective individual biometric systems; the choice of traits to be used given the context of use; how the acquisition and processing is made, either in serial or in parallel; and which type of attributes should be extracted given the degree of correlation among the biometric sources used.

In a multibiometric system, the fusion of information can happen at different levels:

- Sensor level: the biometric samples are consolidated before any feature extraction. This can be useful in systems that combine raw data such as fingerprints, where impressions are used to create a composite fingerprint where more minutiae points are revealed. The same method can be used when merging several face images.
- Feature level: the biometric feature sets from the same individual are concatenated to produce a single larger feature set. If the features come from different algorithms and traits, the feature spaces can be different and their relationship unknown. The feature sets might be even incompatible. For example, one can have a fixed length while the other has a variable length. Besides these problems, augmenting a feature set can degrade the performance of the system if the number of samples is small (curse of dimensionality). When concatenating individual feature sets, the values of the features may present significant differences in their range and distribution. In these cases, a normalization step should be applied. There are several normalization techniques such as the min-max and median normalizations. The latter is more robust to outliers, but also less efficient. When combining feature sets, one can perform feature selection to prevent curse of dimensionality. A subset of features is chosen using a feature selection technique that rely on some criterion function. In the case of biometric systems, this criterion can be the EER or the EID. Dimensionality reduction can also be achieved using transformations to lower dimensional subspaces such as PCA and LDA.
- Score level: the most commonly used approach in multibiometrics is combining the scores output by the matchers. The match scores produced by different matchers may follow different distributions, have different ranges and belong to different measures of similarity or dissimilarity. If there is enough data available, one can estimate the distribution of scores for each matcher and subject. Assuming independence between matchers, one can express the conditional joint probability density of the vector of scores for all matchers as the product of the marginal conditional densities. Usually, in multibiometric systems the data available is limited, hence an accurate estimation of these densities is difficult. An alternative is to combine the scores without transforming them into probabilities estimates. To make the individual scores comparable, score normalization must be performed. There are several normalization techniques such as the min-max and the z -score normalizations. Depending on the scores distributions, some normalization techniques are more robust and efficient than others. The most common methods for fusion at the score level are the sum, max and min score fusion rules. When

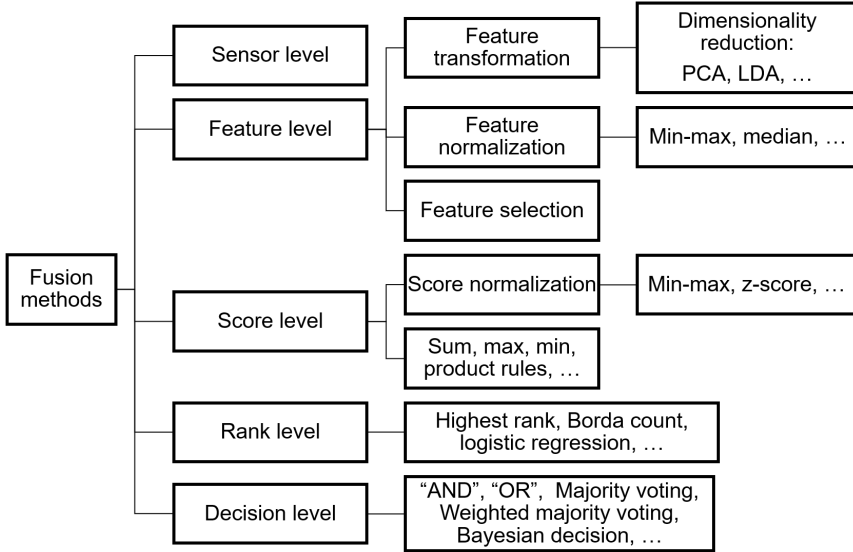


Figure 3.3: Categorization of the fusion methods performed at different levels.

posterior probabilities can be estimated, the product rule is also usually used.

- Rank level: rank fusion level techniques can be applied when the system is operating in identification mode and outputs a rank with the possible matching identities sorted in decreasing order of confidence. The fusion schemes find a consensus ranking from the several individual rankings produced. To achieve a consensus ranking, several fusion schemes can be used such as the highest rank method, where each matching identity is assigned the highest rank and ties are broken randomly; the Borda Count, that sums all individual ranks for each matching identity to achieve a consensus rank; and the logistic regression, which is similar to Borda Count, but the sum is weighted.
- Decision level: the fusion is done using the decisions produced by the set of individual matchers. The simplest method of merging decision outputs is to use the “AND” and “OR” rules. When using the “AND” rule, the matching identity is accepted only when all matchers output the same decision. In the case of the “OR” rule, only one matcher needs to output the matching identity. The use of these rules can degrade the performance of the system when one or more matchers have a much smaller performance than the rest. The most common method is majority voting, where the output identity is the one given by the majority of the matchers. If there is no majority, a reject decision is given as output. This method assumes that all matchers have the same performance. Similarly to the “AND” and “OR” rules, the implementation does not require any training nor any a priori knowledge about the matchers. Weighted majority voting can give more weight to the decisions made by the more accurate matchers. However, the weights may have to be obtained via training. Other methods for fusion at the decision level include Bayesian decision fusion schemes that map the outputs given by the individual matchers into probability values.

Figure 3.3 shows a scheme that represents the different types of fusion that can be implemented at different levels in a biometric system. The performance of multimodal biometric systems depends heavily on the correlation between the traits used. For example, two biometric traits that are not correlated, such as face and fingerprint, do not give the same kind of information, leading to potentially better performance than systems that use traits that present a higher degree of correlation. As the fusion is performed at later stages, the information that is fused is less rich, but the process of fusion is usually less complex. However, fusion at the sensor level can lead to a decrease in performance due to the noise present. Given this, many researchers prefer to perform fusion at the feature or score levels. A more detailed explanation of the methods of fusion used at different levels is done in [74]. Some research conducted in the area of multimodal biometrics is described below.

Trabelsi *et al* [85] proposed a multimodal biometric system based on finger vein and palmprint vein traits. The finger vein data was taken from the multimodal database SDUMLA-HMT [95] that presents data from 106 subjects. This database presents 36 finger vein images of different fingers of both hands for each subject. The hand vein data was taken from the Bosphorus Hand Database [1]. Features related to the finger vein were extracted using a texture descriptor. For the hand vein, vessels are used as features. The classification was performed using ANNs. The classifiers produce scores that are then normalized using min-max normalization and the sum rule is used to combine the scores. EERs of 1.1% and 1.2% were achieved for hand and finger vein, respectively. When combining the traits, an EER of 0.004% was achieved.

Bugdol and Mitas [13] devised a multimodal biometric system using ECG and voice as traits. The fusion was performed at the feature level with no details regarding normalization. In the experiment performed to generate the dataset, the ECG was acquired during 30 seconds, and then the subject was asked to match the sound, on a given pitch, produced by a musical instrument. Two sessions were performed with an interval of one month for 30 subjects. The ECG features were the mean and other statistics of the RR values. For the voice, Mel-frequency cepstral coefficients (MFCC) and the voice timbre were used as features. A 3-NN classifier was used for both traits and the Euclidean distance was used as metric. An averaged EID of 23% was achieved.

Al-Hamdan *et al* [7] proposed a multimodal biometric system that combines phonocardiogram (PCG), ECG and speech. The used database presents 20 genuine users and 70 impostors. After performing ECG and PCG segmentation, MFCC were extracted and used as features for the three signals. Vector Quantization (VQ) was used to perform classification. Fusion was done at the score level with the sum rule using several types of normalization. Using a piecewise-linear normalization an EER of 0.7% was obtained.

Gamboa [32] performed a set of cognitive tests with the purpose of studying the behavior and the physiological reaction under diverse cognitive situations. The dataset comprised the data of several behavioral traits from 27 subjects. The ECG and electrodermal activity (EDA) were collected to explore their use for identity recognition. The ECG features consisted of temporal fiducial features and the resampled mean

heartbeat. As for the EDA, a model was used to fit the skin conductance response (SCR) events. The ECG scores were obtained by template matching, using the Euclidean distance as the metric. For the EDA, a GMC was designed. The product rule was used to perform fusion at the score level. An EER of 4.8% was achieved by considering a sequence of 10 seconds of data. Increasing the time interval to 90 seconds, an EER of 1.1% was attained, while the individual classifiers achieved 1.7% and 6.9% for ECG and EDA, respectively.

3.4 Continuous Biometrics

In a continuous authentication framework, the authentication is performed through time, so the access to resources by a subject is continuously validated as opposed to performing the validation at just one point in time. Over time, changes in the profile of a subject can occur, which is referred to behavior drift. Continuous authentication methods can deal with this problem by updating the subject's template at fixed time intervals or according to the occurrence of some event. This can be useful for biometric traits that are time-variant. As the enrollment phase may not be sufficiently long to acquire a set of biometric samples that fully represents the characteristics of the trait for a given subject, by continuously acquiring new data the system is presented with more information regarding the variability of the trait and hence can adapt the stored templates accordingly. However, by considering template update, the system is more vulnerable to impostors that, if accepted, can change the templates of a valid user to the extent that this genuine user can no longer be accepted by the system. In order to overcome this, research conducted in the field of adversarial machine learning may provide approaches that allow for the design of more robust learning algorithms and, consequently, more secure biometric systems [11]. Continuous biometrics are more user friendly in the case of soft biometrics traits, since these traits can be acquired passively, which increases user acceptability. As for hard biometric traits such as fingerprint, their use in continuous authentication frameworks may be hindered by the low availability of the trait and the low user acceptability.

When devising a continuous authentication biometric system, some additional considerations must be taken into account. There are three main considerations: (i) is the enrollment and further identity verification phases performed passively or actively by the user? (ii) which is the most appropriate time interval to perform identity verification? (iii) should the system update the templates and how is the update performed?

Larger time intervals have the advantage of allowing to collect more data and thus can lead to an increase in the accuracy, but on the other hand, an impostor is able to access the resources for a longer period. Furthermore, when the data collected does not have enough quality, the system must define some behavior as, for example, lock the system and wait for enough valid data. Below, some proposed continuous biometric methods are described summarily.

Guennoun *et al* [35] proposed a simple continuous authentication scheme for ECG biometrics where a template of the ECG wave, based on fiducial features, is stored in a database during enrollment, and during the authentication process the test heartbeats are compared with the stored template using the Mahalanobis

distance. If the resulting score is below a predefined threshold, the system considers as a match and the authentication score increases by 1. This process is repeated for 35 heartbeats. If the authentication score is greater than a threshold, the user is authenticated, otherwise the access to resources is denied.

Coutinho *et al* [18] used a non-fiducial approach that converts the ECG wave into sequences of symbols from an alphabet using 8 bit uniform quantization (string matching). 1-NN was used as classifier with a similarity measure based on Ziv-Merhav cross parsing (ZMCP). During the enrollment phase, the system learns for each user the model and the threshold. During continuous authentication, when the user is accepted the model is updated by simply concatenating a new string. ECG recordings were collected for 19 subjects during a concentration task for an average of 10 minutes. Features were extracted from the mean waves of 10 consecutive heartbeats. LOOCV was performed over 50 runs. The proposed continuous authentication method achieved an EER of 0.36%.

Labati *et al* [46] studied re-enrollment methods for QRS signals, using data collected from Holter devices for 24 hours. During the initial enrollment, a super template is created. This super template consists of a set of QRS templates that are representative of the intrasubject variability. The match and template update are performed when the similarity score produced when comparing the test sample and one template that composes the super template is below a certain threshold. Four types of update methods were tested: in the first, the closest template is replaced by the test sample; in the second, the less similar template is the one that is replaced by the test sample; in the third, the templates that compose the augmented super template, which includes the test sample, are compared with the median template and the template farthest from the median template is removed; the fourth method is similar to the third, but is the closest template that is removed. The authors considered ECG recordings from 185 subjects. The best performance was obtained when using the first update method (minimum EER of 5.68%).

Liu *et al* [48] proposed an eigenspace updating algorithm scheme for continuous face recognition. For each subject, an individual eigenspace is computed using the training images. Each test image is projected into every individual eigenspace and assigned to the one that gives the minimal residue. The update occurs when the residue is smaller than a defined threshold. A confidence measure is computed as a function between the difference in residues of the two top candidates. So that the eigenspace can be more representative of the recent samples than the older ones, decay parameters were used. The best results were achieved using the method with dynamic decay parameters, achieving recognition error rates close to 1%.

Chapter 4

Acquisition System and Experimental Setup

In this chapter, we describe in detail the developed acquisition system and the experimental setup used to collect data from the participants. We also outline the devised protocol that the subjects were asked to follow during the experimental procedure.

4.1 Acquisition System

The acquisition system has two main components: the sensor modules developed to collect the data and the computer application that communicates with these modules. Both components are described below.

4.1.1 Sensor Modules

The acquisition system has two main sensor modules, labeled MOD_ARM and MOD_WRIST, whose primary function is to collect ECG on the forearms and BVP on the index finger, respectively. An additional module, MOD_CHEST, is used to collect the ECG on the chest. Each module is composed by a set of sensors connected to a BITalino device [19]. Each BITalino device uses a Bluetooth connection to send data to a computer and receive instructions. A detailed description of the BITalino board is presented in [67].

The module MOD_ARM (Figure 4.1a) is responsible for the acquisition of the single-lead ECG on the forearms. Two pieces of a conductive fabric [82] were placed on an armrest, and are used as electrodes that are plugged into an ECG sensor. This sensor is connected to a 10-bit analog port of the BITalino board integrated in the armrest, which can be removed for battery recharging. The placement of the electrodes matches lead I.

The module MOD_WRIST (Figure 4.1b) encloses a BVP and an EDA sensors, and an accelerometer (ACC). The module is designed to acquire BVP and ACC data at the base of a finger, while the rest of the module, including the EDA sensor, is placed inside the wristlet. The EDA electrodes are made of the same conductive fabric used in the electrodes of the armrest. The BVP and ACC sensors were integrated in an

Table 4.1: Resolution of the channels of the modules that compose the acquisition system.

Module	Channels	Resolution
MOD_WRIST	ECG	10-bit
	BVP	10-bit
	EDA	10-bit
	ACC-X	10-bit
	ACC-Y	10-bit
	ACC-Z	6-bit
MOD_CHEST	ECG chest band	10-bit
	ECG external electrodes	10-bit
	Respiration	10-bit
	ACC-X	10-bit
	ACC-Y	6-bit
	ACC-Z	6-bit

adjustable ring which is placed around the base of the index finger. Both the wristlet and the ring use Velcro for adjusting the two components to the user's wrist and finger. Every sensor is connected to a 10-bit analog port except the Z-axis signal of the ACC, which is connected to a 6-bit port.

Finally, the additional module MOD_CHEST (Figure 4.1c) is used to acquire a single-lead ECG, ACC and Respiration data at the chest level by integrating the sensors in a band, which can be adjusted to the user. Another ECG sensor was placed inside the band and can be used with an electrode cable to acquire a single-lead ECG. The battery was placed outside the band, using Velcro, for easier access. Once again, every sensor is connected to a 10-bit analog port except the Y- and Z-axes signals of the ACC, which are connected to 6-bit ports. Table 4.1 summarizes the channels of the different modules that compose the acquisition system and their respective resolution. The datasheets of the ECG, BVP, EDA, ACC and Respiration sensors can be found in [68], [23], [69], [66], [70], respectively.

The ACC and Respiration data were collected to test denoising techniques, such as Independent Component Analysis (ICA) and adaptive filtering, that use these signals to remove some noise and motion artifacts that contaminate the ECG and BVP signals, since the signals can be correlated with some noise components.

The ECG signal collected using the module MOD_CHEST is used as reference modality when conducting the performance evaluation tests. As for the EDA signal, the data was acquired to investigate the use of this trait for identity and emotion recognition in future works.

4.1.2 Software Application for Signal Acquisition

A simple application was developed to allow the communication between the computer and the several sensor modules. This application, developed in *Python*, enables the acquisition and online visualization and storage of the acquired signals. Figure B.1 shows the online visualization tool of the application. The user can select the sampling rate (10, 100 or 1000 Hz) and other acquisition parameters such as the channels that are used and the duration of the acquisition. All channels are acquired practically simultaneously, with

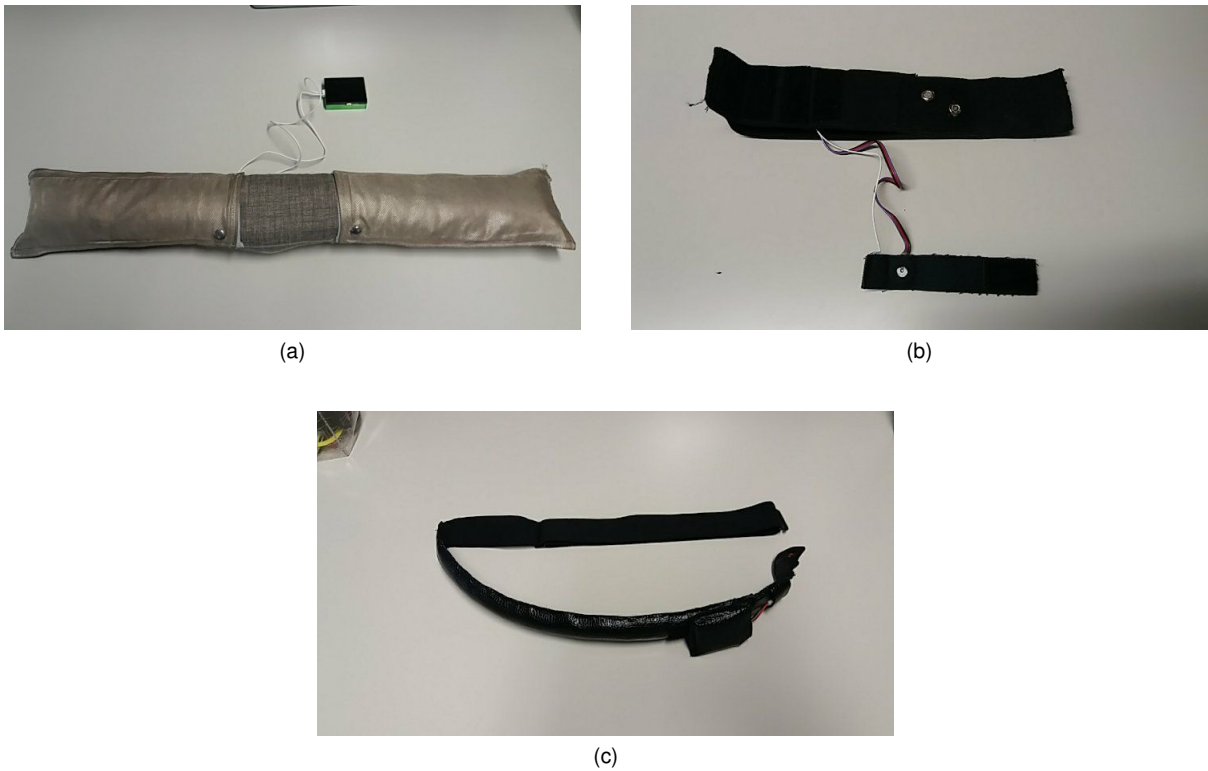


Figure 4.1: Sensor modules (a) MOD_ARM, (b) MOD_WRIST and (c) MOD_CHEST.

time differences smaller than 1 ms. The data collected are saved in HDF5 [28] and txt files that can be posteriorly read to be processed and analyzed.

4.2 Experimental Setup

All acquisitions were made using a sampling rate of 1 kHz. Figure 4.2 illustrates the placement of the electrodes and modules MOD_WRIST and MOD_CHEST.

The ECG was collected on the forearms by placing the left and right forearms over the two pieces of conductive fabric that cover the top of the armrest of module MOD_ARM.

Module MOD_WRIST was placed on the wrist of the non-dominant hand with the EDA sensor integrated in the wristlet on the anterior face of the wrist. The BVP sensor was placed on the anterior face of the base of the index finger and the ACC was positioned on the posterior face.

As for the module MOD_CHEST, using the ECG sensor integrated in the band, the ECG was acquired in a non-standard bipolar lead, with the electrodes placed on each side of the sternum at the 5th intercostal space. The positive electrode was placed to the left of the sternum and the negative to the right, as shown in Figure 4.2. Additionally, using the other ECG sensor connected to the electrode cable, the ECG was acquired at the collar bones, with the positive electrode on the left side (lead I).

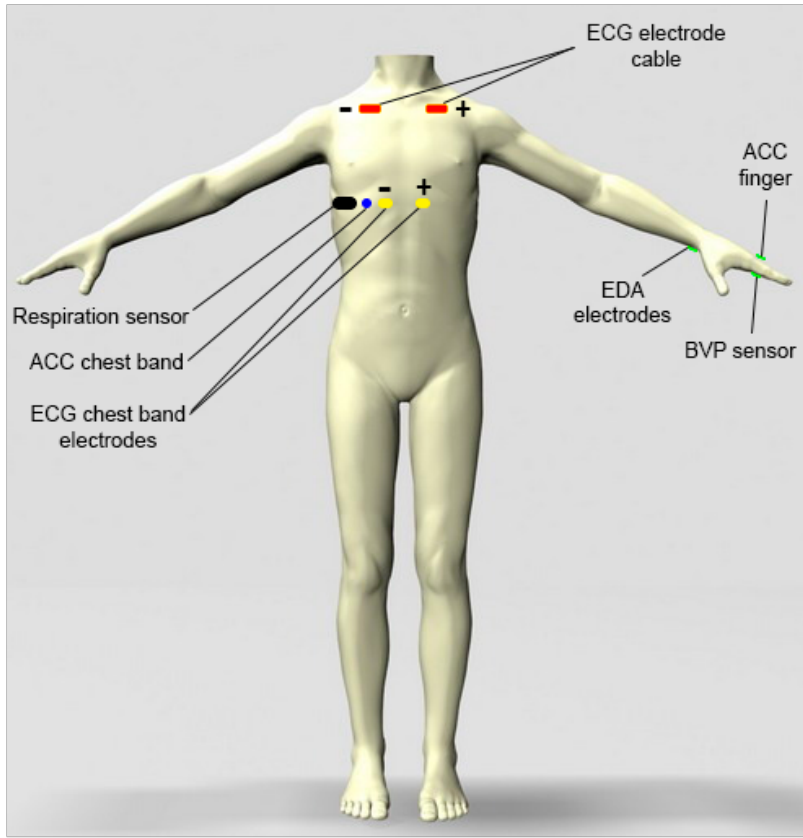


Figure 4.2: Placement of the sensors and electrodes of modules MOD_WRIST and MOD_CHEST on a subject model.

4.2.1 Acquisition Protocol

This experiment was designed to investigate the use of a biometric system in an semi off-the-person approach with the user interacting with a computer setup as shown in Figure 4.3. A set of tasks was developed to simulate this interaction. The subjects were asked to perform two acquisition sessions that were set, on average, eight weeks apart. In each session, the subjects performed four different tasks that are described below. Before performing any task, a preliminary acquisition was done to assure the correct operation and placement of the sensor modules.

The sequence of tasks performed is the following:

1. Idle: the subject places the anterior face of his or her forearms over the armrest without performing any movement and with the hands placed over the keyboard in a relaxed position for 2 minutes;
2. Typing 1: the subject types a predefined text (Figure B.2) shown on a second screen above the computer;



Figure 4.3: Example of the setup used in the experiment.

3. Touch pad: the subject performs a set of predetermined actions using the touch pad. The subject is asked to open a web browser and click on the web page of Instituto Superior Técnico. The user clicks on a news post, reads the post for about 1 minute, scrolling down and up. The subject then copies a paragraph to an open text editor;
4. Typing 2: the subject writes a small and coherent improvised text for 3 minutes.

In addition to this set of tasks, data were also collected in long time intervals with the subjects performing their usual work routine (predominantly composed of programming, writing and reading) on the computer while using the devised system. For a subset of subjects ($n=6$) one to two sessions of 60 or 120 minutes were performed. These recordings can be used in future works to test the performance of the system in terms of trait permanence and adaptive templates.

4.2.2 Preliminary Considerations

A prior analysis of the collected recordings showed that, for a significant fraction of the subjects, the EDA signal either saturated after a short period of time due to the sweating on the wrist promoted by the use of the wristlet, or could not be acquired on the given site. Tests were conducted with an EDA sensor with a lower sensibility, but this sensor was not able to acquire any signal on the wrist. Given these results, the former EDA sensor was maintained.

As for the ECG collected at the collar bones, this signal showed a lower SNR than that collected using the electrodes integrated in the chest band. The movements produced by the subjects cause motions on the cable that contaminate the ECG signal with motion artifacts. Considering these effects, the ECG collected at the collar bones was not used as a reference signal. Figure 4.4 shows two segments of EDA and ECG

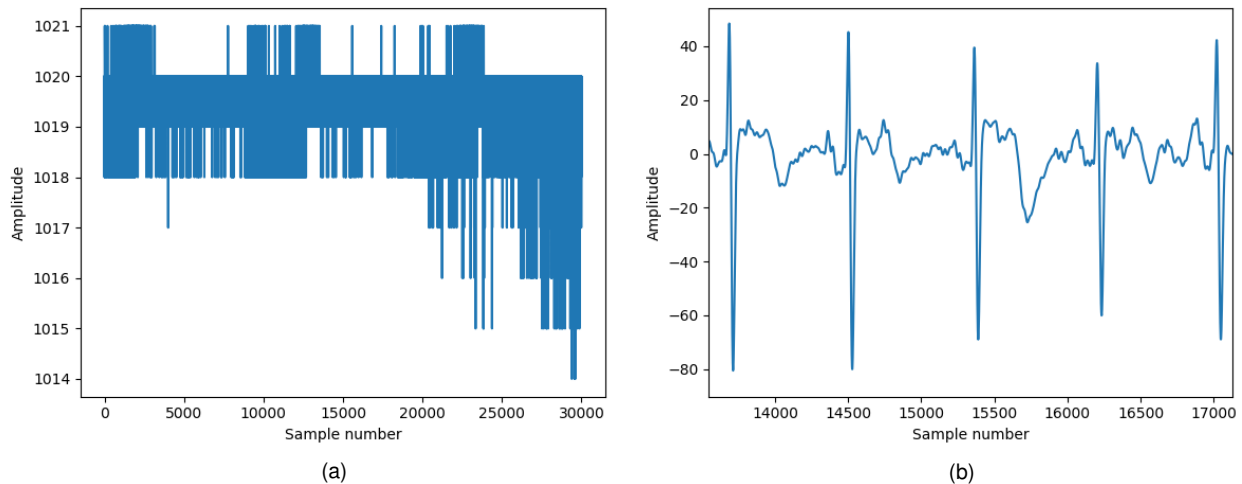


Figure 4.4: Segments of (a) raw EDA and (b) filtered ECG acquired at the collar bones.

acquired at the collar bones.

4.3 Participants

For this study we invited undergraduate and graduate students from Instituto Superior Técnico, University of Lisbon via direct recruitment. The subjects were informed of the type of experiment that we intended to develop and the acquisition sessions were appointed according to their and our availabilities. The acquisition sessions occurred from June 23, 2017 to December 12, 2017. Each acquisition session lasted on average 30 minutes.

The population was composed of 53 subjects from whom 24 were male (45%), and their mean age was 22.9 with a standard deviation of 3.1. The minimum age was 18 and the maximum age was 37.

In the beginning of each acquisition session, the acquisition protocol was explained to each subject: description in detail of the tasks to be performed, the physiological data to be acquired, the goals of the work and how to place the different sensor modules. Each subject was also asked to sign an informed consent form which presented a small questionnaire regarding user acceptability and satisfaction to be filled at the end of the session. Subjects could provide additional commentary about improvements and changes that they thought could lead to a better user experience. The informed consent form is depicted in Figure B.3.

There were some subjects that only performed one session and could not attend a second one, and, in some cases, the acquisition of some or all tasks of the experiment had to be stopped due to unstable Bluetooth connection between the sensor modules and the computer or to non-compliance of the subjects that did not follow the acquisition protocol and were unavailable to repeat the session. For this set of subjects, the data was discarded and so was not considered in the performance evaluation tests.

Chapter 5

Signal Processing

In this chapter we first address the processing of the ECG and BVP that were acquired using the methodology referred in Chapter 4. More concretely, we detail the methods used for denoising and removing outliers in the collected recordings. The amplitude values of the signals shown in the plots are presented either as the values output by the analog-to-digital converter (ADC) of the sensor or are normalized. Lastly, we describe the feature extraction process.

Due to the conditions in which the recordings are performed, the noise is less predictable and more dominant than in other settings such as medical contexts. Additionally, the ECG collected on the forearms presents a lower SNR than in other more standard locations which include the chest and hands. Thus, finding effective methods to remove noise and extract only waves with an acceptable degree of quality is a crucial step. Figure 5.1 depicts the signal processing pipeline.

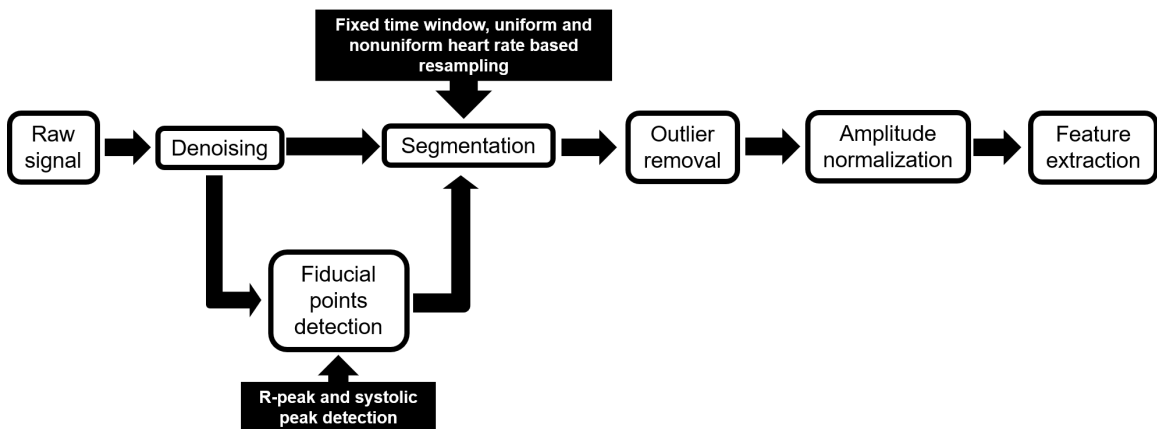


Figure 5.1: Signal processing pipeline.

5.1 Denoising

Raw physiological data contain noise components that modify the structure of the signal and degrade the information that can be extracted, thus affecting the performance of all methods applied downstream. In Chapter 2 an overview of the main types of noise that influence the ECG and BVP was presented. The methods used to remove some of these components for both signals are described below.

5.1.1 ECG

The filtering strategy described in [21] was applied to the ECG recordings acquired on the chest and forearms. The method consists in removing the baseline wandering by subtracting from the raw signal the one obtained by applying a cascade of two median filters of 200 ms and 600 ms windows, respectively, followed by a low-pass finite impulse response (FIR) filter of order 300 with a flat-top window. Two different cutoff frequencies of 20 and 40 Hz were applied to the ECG signal. A segment of filtered ECG following this method is shown in Figure 5.2.

This filtering method can effectively remove the power line interference noise and baseline wandering, but fails to filter the contact noise and motion artifacts shown in Figure 5.3. Furthermore, the low-pass filtering is able to remove some of the EMG noise that affects particularly the signal acquired on the forearms, but some components of this noise are still present, as shown in Figures 5.2a and 5.3, since the EMG frequency band overlaps with the one of the ECG.

Two cutoff frequencies were used to test the influence of this low-pass filtering on the performance of the biometric system. By using a lower cutoff frequency, more components of the EMG can be removed, which leads to a smoother signal. However, as a tradeoff, some frequency components of the ECG, which could provide useful discriminative information, are also removed.

5.1.2 BVP

The BVP signal was filtered using a band-pass Butterworth filter of order 4 with cutoff frequencies of 1 and 8 Hz, as shown in Figure 5.4a. The method is successful in removing baseline wandering, but cannot remove contact noise and motion artifacts generated by the movement of the finger that can distort completely the BVP signal as shown in Figure 5.4b.

5.1.3 Additional Denoising Techniques

The applied filtering method is not able to remove some noise components such as the EMG noise in the ECG and the motion artifacts in both signals. Given this, other strategies were studied and are shortly described below. Although in the end these strategies were not applied in this work, because they were either unsuccessful or needed a more comprehensive analysis and tuning of the parameters, the analysis done below presents a basis for future work in the denoising of these signals.

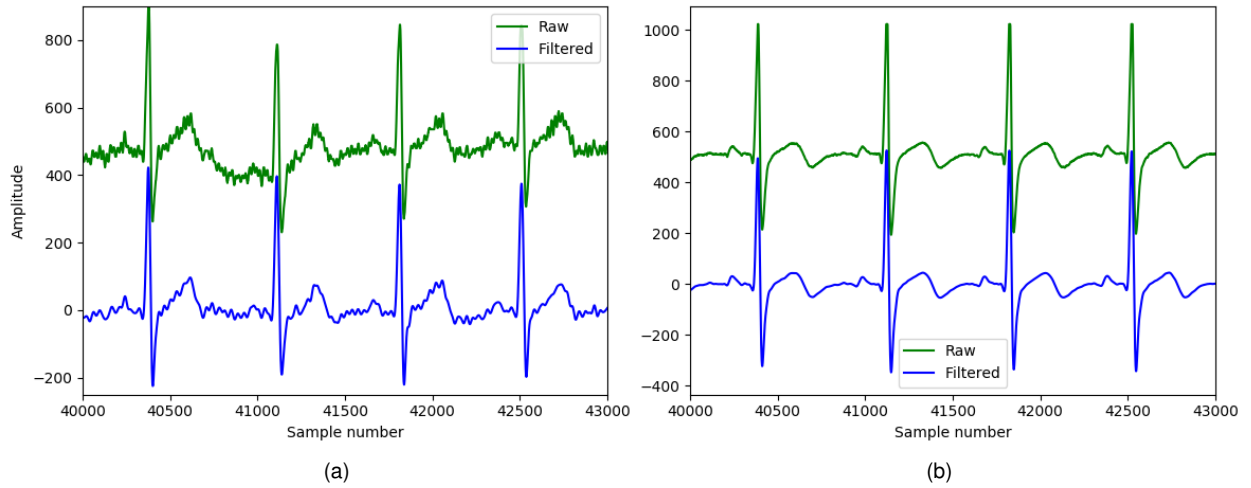


Figure 5.2: Segments of raw and denoised ECG recordings using the adopted filtering strategy. ECG acquired at the forearms (a) and chest (b). Cutoff frequency fixed at 40 Hz.

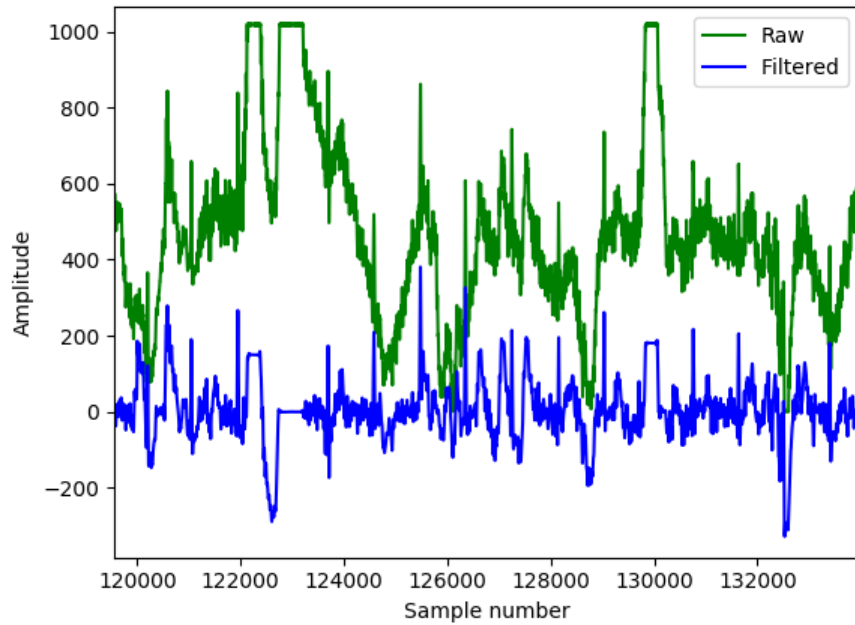


Figure 5.3: Segment of raw and denoised forearm ECG recordings contaminated with contact noise and motion artifact.

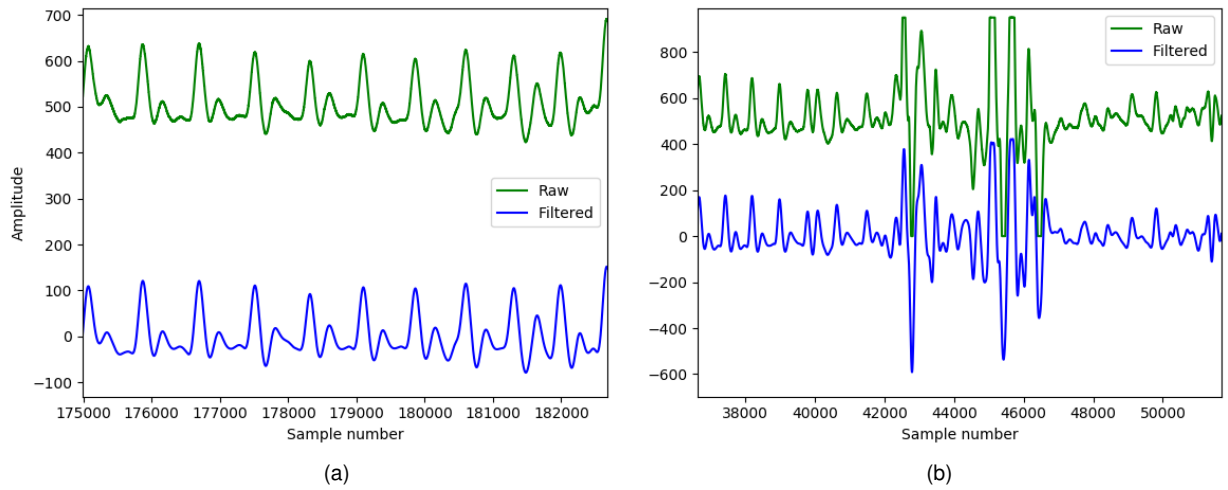


Figure 5.4: (a) Segments of raw and denoised BVP recordings using the adopted filtering strategy and (b) another set of segments contaminated with contact noise and motion artifacts.

Regarding the collected Respiration data, as the applied filtering method was effective in removing the baseline wandering, mainly caused by respiration, this signal was not used for denoising.

ICA and Adaptive Filtering

Tests were conducted by performing ICA using segments of BVP recordings with motion artifacts and ACC data acquired simultaneously, as shown in Figure 5.5. ICA was unsuccessful at separating the motion artifacts from the BVP signal. One reason for that might be that the statistical independence does not hold for BVP signals that are contaminated by motion artifacts [93]. Additionally, some of the works found in the literature that study the use of ICA to remove motion artifacts from the BVP either use multiple PPG sensors or use a PPG sensor that contains more than one channel. However, the results are not satisfactory or are obtained using data where the subjects perform slow movements with low amplitude [97], as opposed to the movements produced by the subjects in this work.

Another technique that is commonly used is adaptive filtering [92], but experiments with Least-mean-squares (LMS) and normalized LMS were also not successful. The transfer dynamics between the motion artifacts and the accelerometer data are unknown and the latter may not provide sufficient information to estimate a model that effectively cancels the motion artifacts. Hence, a thorough study of the dynamics that relate the acceleration acquired on the posterior face of the index finger with the motion artifacts present in the BVP signal acquired on the anterior face must be performed.

Extended Kalman Smoothing

The use of an Extended Kalman Smoother (EKS) [77] for the denoising of the ECG was also tested. The algorithm uses a nonlinear dynamical model of the ECG, based on a mixture of Gaussians, to remove

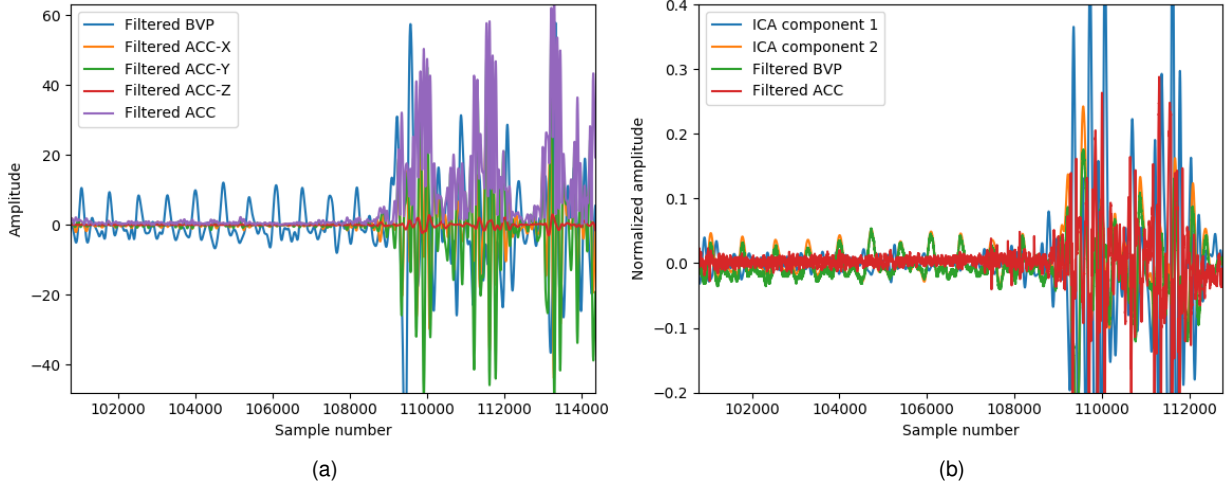


Figure 5.5: (a) Segments of BVP and ACC recordings and (b) respective independent components after performing ICA.

noise such as the EMG. The method presents interesting results. Although computationally expensive and dependent on the accurate localization of the R-peaks, the technique can effectively remove EMG noise without distorting significantly the PQRST complexes, as shown in Figure 5.6. Tests were conducted using 5 Gaussians, one for each wave in the heartbeat. Improvements to the model must be conducted in terms of the number of Gaussians used. For instance, the T wave is not symmetric and thus must be represented by a number of Gaussians greater than one.

5.2 Segmentation

The segmentation of the ECG and BVP was performed at the individual wave cycle. Since the amount of noise present in the data can still be significant after denoising, by extracting individual waves one can use wave based outlier removal methods to extract only waves with a reasonable degree of quality. Furthermore, after aligning the waves, one can perform ensemble averaging to remove EMG noise by averaging across consecutive heartbeats, although this leads to the loss of inter-beat variations that may carry significant information and can produce a distorted average wave if the method is applied to waves with significant differences in morphology caused by factors such as the HRV.

In order to perform segmentation of the signals at the individual wave cycle, one needs to first find fiducial points. The detection of these fiducial points must be accurate to produce an effective segmentation. Ideally, in the case of the ECG, the heartbeat should be segmented between the onset of the P wave and the offset of the T wave, since the PQRST complex encloses the activity of the heart in one cardiac cycle. Unfortunately, detecting automatically the onsets, offsets, and even peaks, of these two waves is a difficult task, especially when the heartbeat is contaminated with noise that distorts the waves. Hence, the focus is on the detection

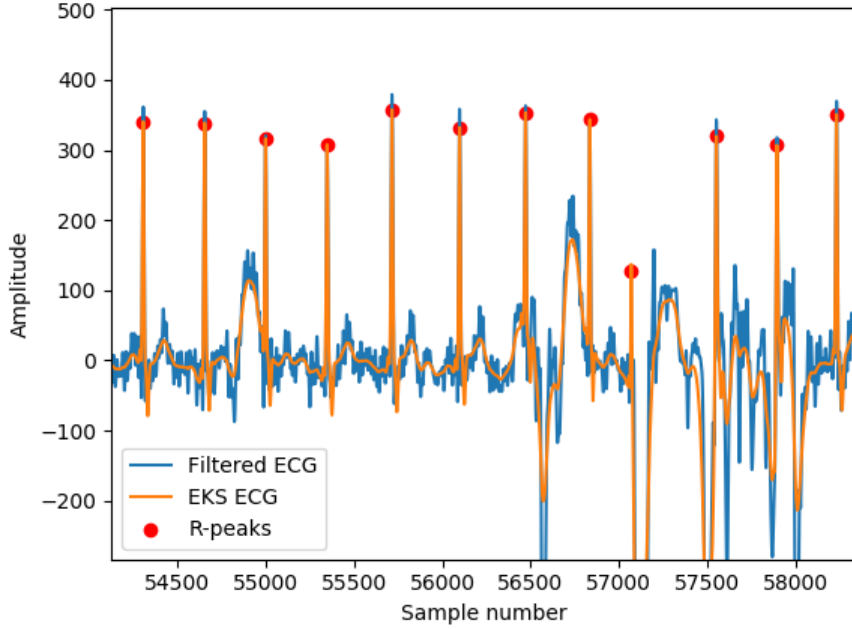


Figure 5.6: Forearm ECG signal obtained after EKS based filtering.

of the R-peaks, which are the easiest fiducial points to detect in the heartbeat given the high signal-to-noise ratio (SNR) of the QRS complex. As for the BVP, ideally the signal should be segmented using the onsets of the systolic waves. However, the accurate detection of this fiducial point can be difficult, leading to a misalignment of the waves in the presence of noise. Given this, the onsets of the waves are determined and used to detect the systolic peaks, which are used as fiducial points.

The algorithms used to detect these fiducial points in the ECG and BVP signals and two segmentation strategies based on the detected fiducial points are described below.

5.2.1 Fiducial Point Detection in ECG

A modified version of the Engelse-Zeelenberg algorithm [53] was used to extract the R-peaks from the filtered ECG signals, as shown in Figure 5.7. The algorithm achieves a good performance and is robust to the different ECG morphologies present in the tested dataset. Two other R-peak detection algorithms were also tested, more concretely, the Christov [16] and Hamilton [36] algorithms. A preliminary analysis showed that the Hamilton algorithm presented a low performance especially when the ECG morphology was characterized by a pronounced S wave, with the algorithm considering S-peaks as R-peaks. For the other two algorithms, a test using a subset of subjects ($n=34$) was conducted to evaluate their performance on the forearm ECG signal. The algorithms were applied to the recordings acquired during the task Idle of the first acquisition session. The R-peaks detected in the ECG signal acquired on the chest were used as reference. In the case of this modality, the R-peaks are well defined and have a significant SNR, so

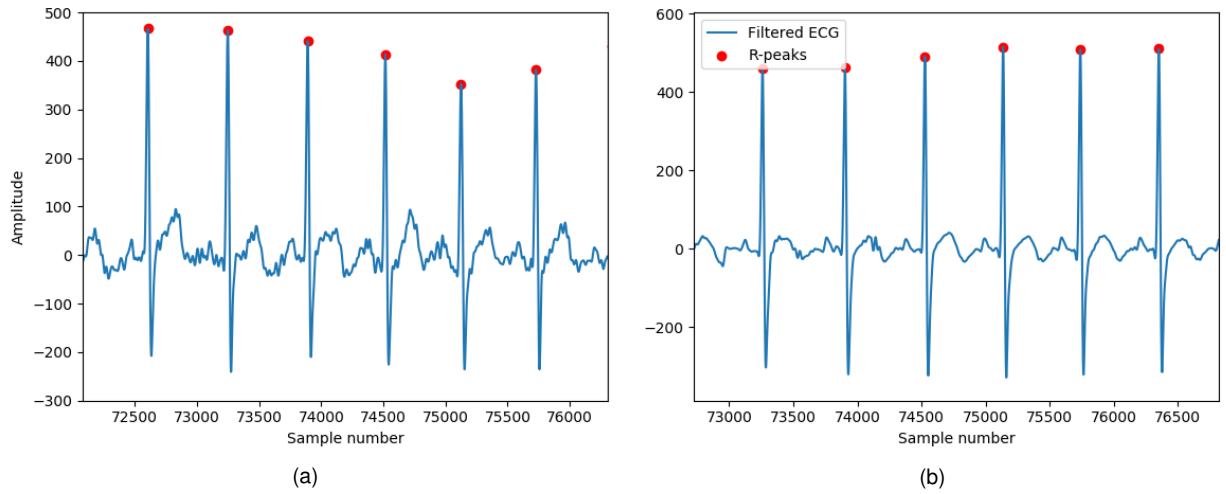


Figure 5.7: Segments of filtered ECG with detected R-peaks using the modified Engelse-Zeelenberg algorithm for the ECG acquired (a) on the forearms and (b) on the chest.

Table 5.1: Performance of the modified Engelse-Zeelenberg and Christov R-peak detection algorithms.

R-peak detection algorithm	Undetected peaks (%)	Erroneous peaks (%)
Modified Engelse-Zeelenberg	7.45%	0.6%
Christov	12.81%	0.4%

both detectors identify correctly all the R-peaks. The results are presented in Table 5.1 and show that the modified version of the Engelse-Zeelenberg algorithm achieves a better performance.

5.2.2 Fiducial Point Detection in BVP

The segmentation of the BVP consisted in detecting the onsets of the BVP pulses using the algorithm proposed in [99]. However, the algorithm incorrectly detected some onsets on the slope of the diastolic pulse after the dicrotic notch. This may be due to the fact that the morphology of the signal output by the sensor is different from the usual morphology of the BVP, which is caused by the filtering performed at the hardware level. To overcome this problem, an additional search using a window of 300 ms around the detected point is performed to find the systolic peak. If the maximum in the search window appears after the detect onset, the point is considered a valid onset and the maximum is marked as the systolic peak. On the other hand, if the maximum comes before the detected point, the point is not considered a valid onset. The result of applying the method to detect the systolic peaks in a segment of BVP signal is shown in Figure 5.8.

5.2.3 Segmentation Methods

When the segmentation of the signal is conducted at the individual wave cycle, the waves must be aligned for performing averaging and coherent feature extraction when the dimension of the feature sets is fixed and depends on the length of the segmented waves. Two methods used to align the waves are described below.

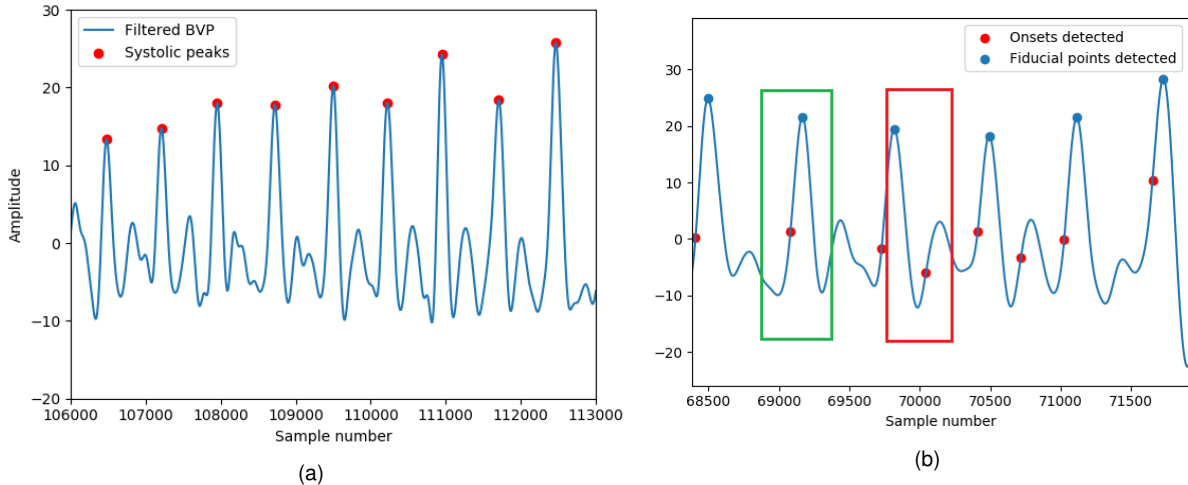


Figure 5.8: (a) Segment of BVP signal with detected systolic peaks and (b) another segment of BVP signal where it is shown, as an example, one correctly identified onset and the respective search window in green, and one incorrectly identified onset and its search window in red.

Fixed Time Window

This method consists of applying a fixed window defined using a fiducial point. In this work, the R-peak and the systolic peak were used as fiducial points. For the ECG, a window of 600 ms, [-200, 400] ms, is defined relative to the R-peak. As for the BVP, the window presents a length of 500 ms, [-100, 400] ms, and is defined relative to the systolic peak. These windows enclose, for a normal rest heart rate, the PQRST complex and the BVP wave. Given this, the method does not consider the complete wave neither the changes in morphology caused by the HRV. For example, if the heart rate increases beyond 110-120 bpm, the window may possibly capture waves of the consecutive heartbeat, such as the P wave and QRS complex in the ECG, as illustrated in Figure 5.9d, or, in the case of the BVP signal, a portion of the systolic pulse of the next wave. Figure 5.9 shows examples of the segmentation produced using the fixed time window method in the three signals.

Heart Rate based Resampling

To overcome the problems of the fixed time window, one alternative is to resample each wave to a fixed number of points. In this case, as only one fiducial point is identified, a wave is defined as the segment between two consecutive R-peaks in the ECG, and two systolic peaks in the BVP. A uniform resampling method assumes that the different segments of the wave change homogeneously, but this is an incorrect assumption, as shown in several works in the literature and illustrated in Figure 5.10a, and as a consequence distorts the waves and introduces intrasubject variability.

During the work performed in this thesis, a brief analysis of the alterations of the different segments of the heartbeat due to changes in the heart rate was conducted based on the analysis of the recordings collected during an additional experiment where the subjects performed physical exercise using a static bicycle. The

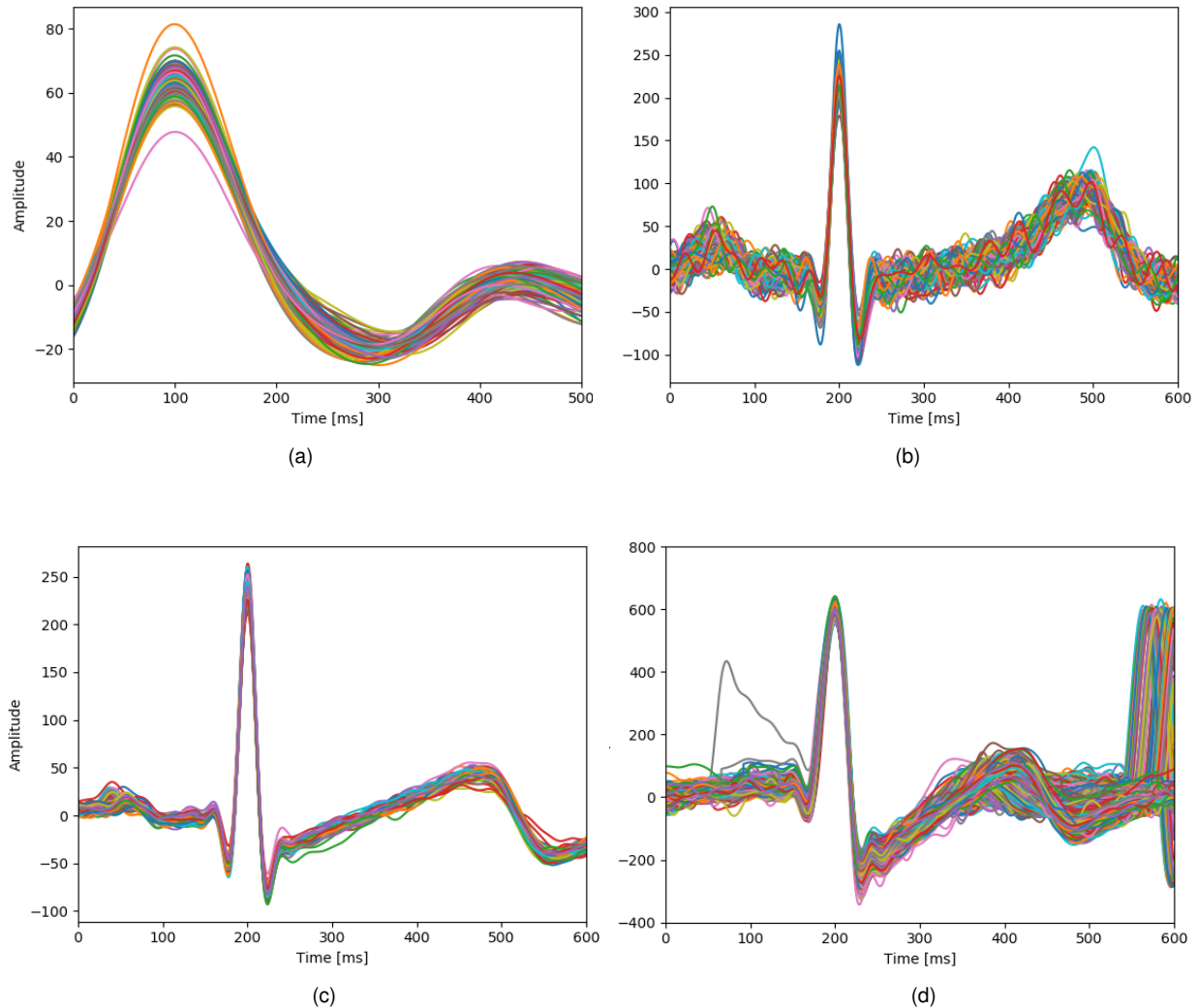


Figure 5.9: Segmentation performed using fixed time windows for (a) BVP, (b) forearm ECG and (c) chest ECG. (d) Example of segmented waves associated with a high heart rate. Each figure shows the overlay of several waves from a single subject.

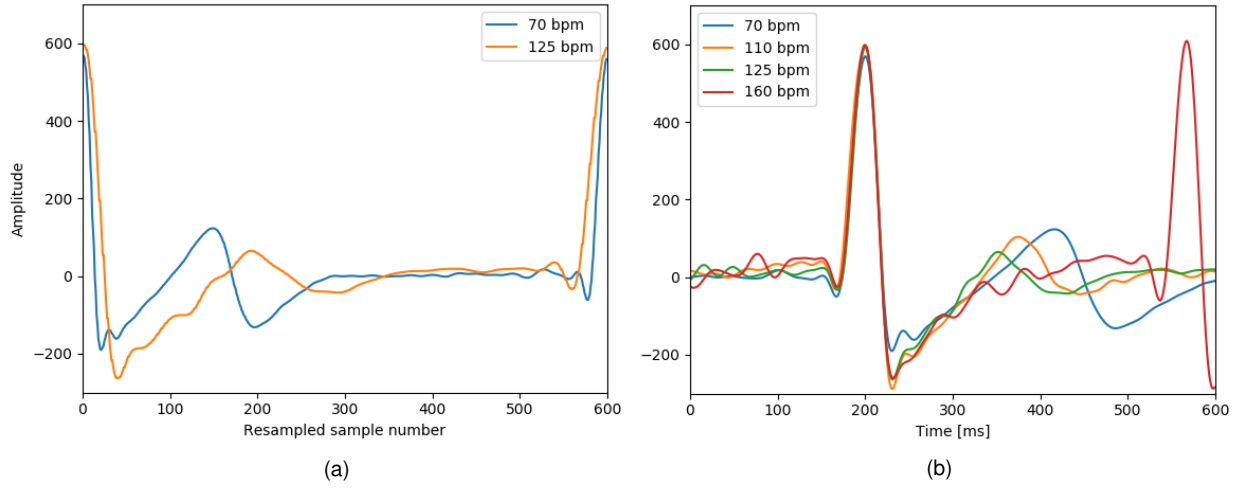


Figure 5.10: (a) Example of two waves with different heart rates mapped using uniform resampling. (b) Waves with different heart rates segmented using the fixed time window method.

experiment confirmed that the QRS complex is robust to the HRV and suffers minor width changes. The segment that is most affected by the HRV is the ST interval, defined by the offset of the S and T waves. With the increase in the heart rate, this segment becomes shorter and the morphology of the T wave can change significantly. These changes are illustrated in Figure 5.10b. However, for resting heart rate values, the main responsible for the changes in the heartbeat duration is the TP segment, defined between the offset of the T wave and the onset of the P wave of the consecutive heartbeat. This segment between consecutive heartbeats is the isoelectric interval of the ECG, since no heart activity is performed in this time interval, and hence carries no particular useful information.

Given that the R-peak is the only fiducial point identified in the heartbeat, a nonuniform resampling method is herein proposed by using a fixed window around the R-peak and then resample the other segments of the wave to the remaining points. As the QRS width varies between 80 to 120 ms in healthy subjects [17], a window [-50, 50] ms centered at the R-peak was used. Some experiments were conducted using a larger window, since for a normal rest heart rate the changes occur predominantly in the TP segment, but this method assumes the subjects are always at rest, which limits the applicability of the method.

Thus, two kinds of heart rate based resampling methods were applied to the ECG: (i) uniform resampling and (ii) nonuniform resampling using a fixed window size centered at the R-peak, [-50, 50] ms. In both methods the waves were resampled to 600 points.

As for the BVP signal, only the uniform method was applied, since no information was found in the literature regarding the changes in length of different segments of the BVP wave promoted by HRV. The experimental observation of the BVP data also yielded no conclusion about this topic.

Figure 5.11 shows examples of the resampling methods used in the segmentation of the waves for the three signals.

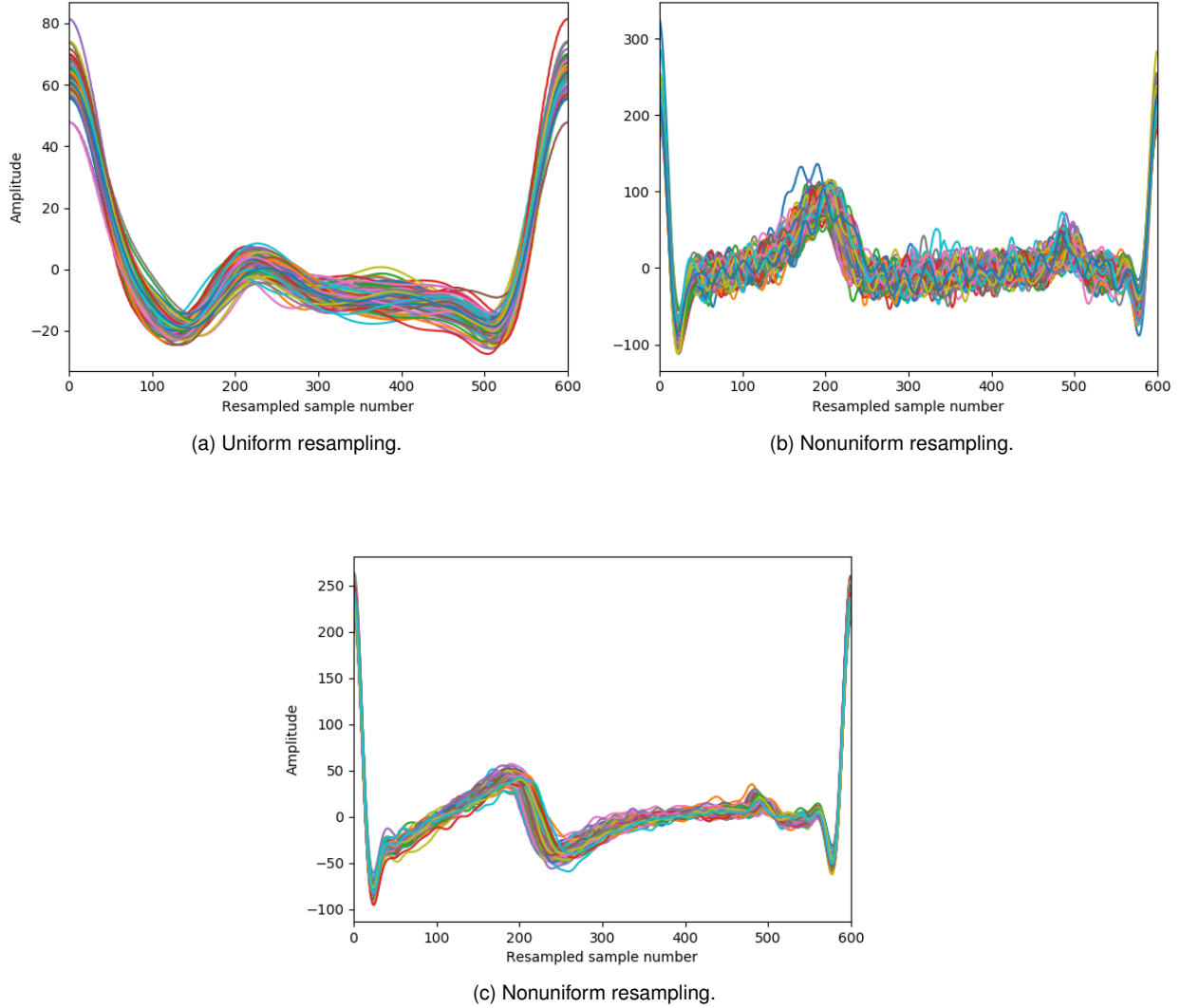


Figure 5.11: Segmentation performed using heart rate based resampling for (a) BVP, (b) forearm ECG and (c) chest ECG. In the case of the BVP, the mapping is done uniformly to 600 points. For the ECG waves, the mapping is done to 600 points with samples maintained over a fixed window size of 100 points [-50, 50] ms, defined relative to the R-peaks, with the remaining segments resampled into a 500 points size mapping.

5.3 Outlier Removal

After the denoising step, some noise components, mainly motion artifacts and contact noise, were not successfully removed. In order to remove waves that do not present a reasonable degree of quality, outlier removal strategies were proposed. The main challenge consists in defining outliers and finding an effective rule, metric or similarity measure to distinguish them from valid waves. In this section, we present some methods that were tested, but deemed unsuccessful, and the method that was applied in the signal processing pipeline.

5.3.1 Tested Methods

Heart Rate and Fiducial Point Amplitude Context based Algorithm

An initial approach was to develop an outlier removal algorithm based on the context information of the heart rate and amplitude of the fiducial points. Fixed ranges for the instantaneous heart rate and fiducial point amplitude were defined. For the instantaneous heart rate, the interval used was [30, 200] bpm, which covers almost completely the physiological human range in bradycardia, rest and tachycardia. The RR interval defined between the R-peak of the current heartbeat and the one from the consecutive heartbeat was used as a measure of the instantaneous heart rate. The same reasoning was considered for the computation of the instantaneous heart rate in the BVP signal using the systolic peaks. For the amplitude of the fiducial point, a fixed range was determined for each modality (BVP, forearm and chest ECG) by computing the histograms of the amplitude values of the fiducial points in the recordings obtained for the task Idle for all subjects ($n=53$). In addition to these fixed range conditions, the algorithm also presented a context based condition: the current wave is only accepted if the amplitude of the fiducial point and the respective instantaneous heart rate belong to an interval defined by the average values of these two parameters computed using a set composed by the last n accepted waves. The set of rules used to validate a wave is shown in Equation 5.1, where x is the current wave, x_{hr} and x_{amp} are the instantaneous heart rate and amplitude of the fiducial point of the wave, respectively, AMP_{range} is the fixed amplitude range for the amplitude values of the fiducial points, specific for each signal, \bar{Y}_{hr} and \bar{Y}_{amp} are the average values of instantaneous heart rate and fiducial point amplitude of the last n accepted waves, and the α and β

parameters are coefficients that weight the average values and define the boundaries of the context interval.

$$Accept\ x\ if \begin{cases} x_{hr} \in [30, 200] \text{ bpm} \\ \wedge \\ x_{amp} \in AMP_{range} \\ \wedge \\ \alpha_{hr}\bar{Y}_{hr} \leq x_{hr} \leq \beta_{hr}\bar{Y}_{hr} \\ \wedge \\ \alpha_{amp}\bar{Y}_{amp} \leq x_{amp} \leq \beta_{amp}\bar{Y}_{amp} \end{cases} \quad (5.1)$$

If a wave is assumed valid, the list of last accepted waves is updated by removing the oldest wave and adding the current wave. In an initial phase, when there are no accepted waves, only the first two conditions presented in Equation 5.1 are used to test new waves. The two context conditions are tested when there is a set of n waves that was accepted previously. When waves are rejected for a certain time interval (resetting time), the dynamics underlying the HRV and the morphology of the signal, and to that extent the amplitude of the fiducial point, can change and, as a consequence, the values associated with the last accepted waves may not represent the current dynamics. Hence, the set of last accepted waves is reset and the process evolves as in the initial phase.

The presented method shows a good performance only when applied to high quality recordings and where the HRV is not significant. However, the algorithm fails in other cases. The dynamics of the ECG and BVP signals are caused by complex stochastic processes, so modeling these dynamics using simple methods as the one presented here may fail to capture the changes in the signals. Several parameters need to be tuned, such as the number of the last accepted waves that are considered, the resetting time, and the α and β coefficients. One has to consider how to compute these coefficients, and decide if they should change as a function of the heart rate or HRV, and be subject-specific, which imply the use of large amounts of data. A poor choice of parameters may lead to the acceptance of outliers as valid waves, which can provide bad estimates of the current heart rate and fiducial point amplitude, and thus lead to the rejection of high quality waves. This is even more crucial in the initial or resetting phases, when the context conditions are not tested.

Template based Algorithms

In order to consider the morphology of the waves, another approach analyzed was to compute a template (or set of templates), *i.e*, a representative prototype of the waves that present an acceptable degree of quality, and use a measure of similarity or dissimilarity between the template(s) and the test waves. If the value of the similarity (dissimilarity) measure is below (above) a defined threshold, the waves are considered outliers.

The template can be computed as the mean wave of the set of all test waves. This can lead to an unrepresentative template if most of the test waves are highly contaminated by noise or if the waves present

significant differences in morphology. To overcome this, a subset of test waves can be used if one knows *a priori* that this subset contains high quality representative waves. Another alternative is to compute the template using a set of waves, different from the test set, that one knows that consists of high quality waves, such as the data collected in the enrollment phase, where the acquisition conditions and quality of the data can be controlled. The topic of template selection is extensively analyzed in the literature and the work conducted in [50] is an example of an approach to the problem.

As for the thresholds, these can be determined using the set of waves used to create the templates. The thresholds can be defined using the cumulative histogram of the values of the similarity (or dissimilarity) measure. Commonly used methods include assigning the threshold to the value associated with the highest slope or a given fraction of the normalized cumulative histogram. These methods are highly dependent on the data used.

Three different similarity measures were tested:

- Cross-correlation: the cross-correlation measures the similarity of two series by displacing one relative to the other. The measure is computed between the test wave and the template and the test wave is accepted as a valid wave if the maximum value of the cross-correlation is between two predefined thresholds, as shown in Equation 5.2, where x is the test wave, y is the template, R_{xy} is the cross-correlation between the two waves, and α and β are predefined thresholds;

$$Accept \ x \ if \ \alpha \leq max(R_{xy}) \leq \beta, \ R_{xy}[k] = \sum_{m=0}^N x[m]y[m-k] \quad (5.2)$$

- Kullback-Leibler (KL) divergence: the squared error between each sample point of the template and the waves that were used to create the template is computed. The same computation is done using the test waves and the template. The normalized histograms of the sample squared error for the two cases are computed and the KL divergence between the two empirical distributions is determined. This measure describes the dissimilarity between two distributions. If the value is below a predefined threshold, the wave is considered valid, as shown in Equation 5.3, where P and Q are the random variables of the squared error of the test wave and of the waves used to compute the template, respectively, $KL(P||Q)$ is the KL divergence between the two distributions of the respective random variables, p and q , and α is a predefined threshold. So that the distribution q is nonzero for every point where p is nonzero, Laplace smoothing was performed with a smoothing factor $s=1$, as shown in Equation 5.4, where N_i is the number of observations for $Q = q_i$, N is the total number of observations, and $|Q|$ is the number of values the random variable Q can take;

$$Accept \ x \ if \ KL(P||Q) \leq \alpha, \ KL(P||Q) = \sum_{i=0}^N p(i) \log \frac{p(i)}{q(i)} \quad (5.3)$$

$$p(Q = q_i) = \frac{N_i + s}{N + s|Q|} \quad (5.4)$$

- Pearson correlation coefficient: this measure is invariant to shifts and scaling, and thus can reflect the differences in morphology between valid waves and waves that are highly contaminated by noise while ignoring differences in amplitude. Equation 5.5 shows the formula of the Pearson correlation coefficient, where x is the test wave, y is the template, $\rho(x, y)$ is the Pearson correlation coefficient between the two waves, and X and Y are the respective random variables.

$$\begin{aligned} \text{Accept } x \text{ if } \rho(x, y) \geq \alpha, \quad \rho(x, y) &= \frac{\sum_{i=1}^N (x_i - \bar{x})(y_i - \bar{y})}{\sqrt{\sum_{i=1}^N (x_i - \bar{x})^2} \sqrt{\sum_{i=1}^N (y_i - \bar{y})^2}} \\ &= \frac{\text{cov}(X, Y)}{\sqrt{\text{var}(X)\text{var}(Y)}} \end{aligned} \quad (5.5)$$

The cross-correlation presents as a disadvantage the fact that one needs to define an upper and a lower thresholds, since, for example, a squared wave that is positive when the template is positive, and negative in the opposite case, gives a higher maximum cross-correlation value than the maximum of the autocorrelation values of the template. As some contact noise promotes the saturation of the signal, this noise can resemble squared waves, and thus be accepted as valid waves. On the other hand, for the KL divergence and Pearson correlation coefficient methods only one threshold needs to be defined.

Although the KL divergence method only requires an upper threshold, the assumption that the sample errors are *i.i.d* does not hold: (i) the sample errors do not need to follow the same distribution. For example, the error of the samples associated with the QRS complex in a heartbeat is much smaller than the error of other segments, given the robustness of the complex to noise and heart rate changes; (ii) the error in one sample may not be independent from the error in previous samples; (iii) if the set of waves used to create the template is small, the empirical distribution that is generated may not be representative of the real distribution.

The Pearson correlation coefficient method does not require the same assumptions as the KL divergence method, and thus can provide better results.

Figure 5.12 shows the values of the KL divergence for a segment of heartbeats acquired at the chest. As the example highlighted in the figure, a low quality heartbeat that was distorted by a motion artifact presented a KL divergence value as low as some high quality heartbeats found in the same segment. Figure 5.13 shows a similar example, but using as similarity measures the cross-correlation and the Pearson correlation coefficient. One can observe how the Pearson correlation coefficient performs better than the cross-correlation. In the examples highlighted, a “flat” heartbeat presents a similar cross-correlation value to those of high quality heartbeats, and another low quality heartbeat contaminated by a motion artifact is associated with an even higher maximum cross-correlation value.

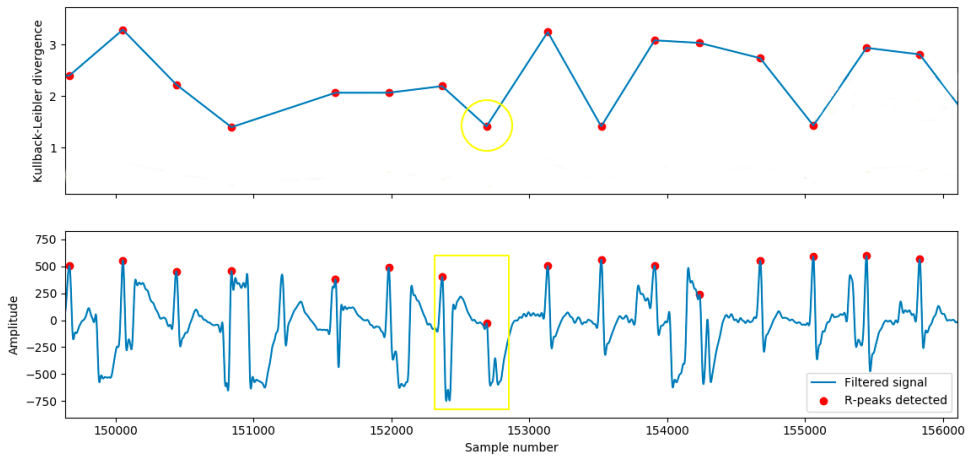


Figure 5.12: KL divergence values (top) associated with the corresponding waves in the segment of chest ECG (bottom).

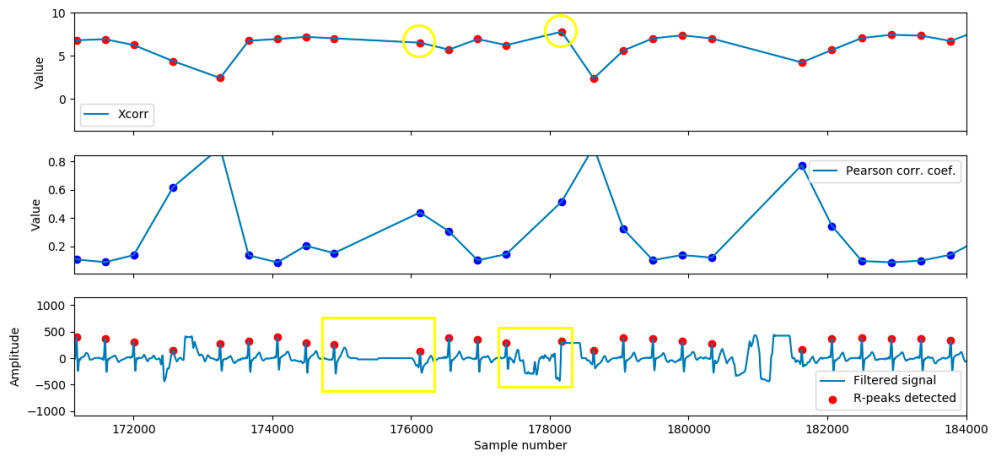


Figure 5.13: Cross-correlation (top) and Pearson correlation coefficient (middle) values associated with the corresponding waves in the segment of chest ECG (bottom).

Clustering based Algorithm

Another approach considered was the use of clustering to investigate if clusters of high quality and low quality waves were produced. Given this, Ensemble Accumulation Clustering (EAC) [30] was used in the form of k -means consensus. This algorithm is an iterative algorithm that runs multiple instances of k -means with different values for k and different initializations for the centers. The algorithm then counts the number of occurrences where each observation ended up in the same cluster as each of all the other observations, producing a co-association matrix on which a hierarchical clustering algorithm is applied to extract the final clusters. One needs to define several parameters: the range of k values to be tested, by choosing the k_{min} and k_{max} values, the number of partitions in the ensemble, *i.e.*, the number of k -means performed, the linkage criterion and the final number of clusters extracted. Increasing the number of partitions in the ensemble can produce better results, but increases the running time of the algorithm.

Tests were conducted using 10, 20, 50, and 100 ensembles, the average linkage as the linkage criterion, the life-time criterion to decide the final number of clusters to extract, and the cosine distance as similarity measure (Equation 5.6), which is invariant to scaling. The range of tested k values was defined using a heuristic: $k_{min} = \frac{\sqrt{n}}{2}$ and $k_{max} = \sqrt{n}$, where n is the number of test waves. To select the valid clusters, a parameter based on the average sample variance between the waves in each cluster was defined. The reasoning is that clusters with low quality waves that are contaminated with noise have a higher sample variance than the ones with waves with an acceptable degree of quality, since the waves are more similar among them. The evaluation parameter is shown in Equation 5.7, where c_i is a cluster produced by the algorithm, μ_i is the value of the evaluation parameter, L is the number of test waves in the cluster, $var(sample_{i,l})$ is the variance associated with sample l across all waves in cluster c_i , and α is a predefined threshold that was empirically derived from analyzing the variance in clusters obtained using the enrollment data.

$$D_c(x, y) = 1 - S_c(x, y), \quad S_c(x, y) = \frac{x \cdot y}{\|x\| \|y\|} \quad (5.6)$$

$$\text{Accept } c_i \text{ if } \mu_i \leq \alpha, \quad \mu_i = \frac{1}{L} \sum_{l=1}^L var(sample_{i,l}) \quad (5.7)$$

The results obtained were not satisfactory. In some cases, the algorithm was able to separate high quality waves from low quality waves into different clusters, but in most cases the separation was unsuccessful. This may be due to at least two factors: (i) in those cases where the recording contains few waves with a reasonable degree of quality, most of the waves are in fact noise. The valid waves are then a small fraction of the total of test waves, and the algorithm fails to produce representative clusters of the data, assigning the valid waves to clusters of low quality waves; (ii) since the QRS complex is robust to noise and changes in the heart rate, this segment presents a low variability. Given this, a cluster can contain high quality waves that due to changes in the heart rate present a different morphology among themselves, leading to a decrease in their similarity, and also low quality waves that can be highly contaminated by noise in all segments except

the QRS complex.

5.3.2 Proposed Method

The previous approaches were unsuccessful in effectively removing outliers, but provided information about the behavior of the noise and the quality of the data, and can serve as a basis to develop other methods that can be more successful in the detection of outliers. The method proposed and applied in this work is composed of two modules: one is applied to the recordings used as enrollment data, and the other is applied to the test recordings from which are extracted the waves for performing identity recognition. The former recordings, given that the subjects are at rest, do not present significant amounts of noise, so most of the signal is composed of high quality waves. As for the latter, these recordings can be highly contaminated by noise to the extent that waves with a reasonable degree of quality consist in a small fraction of the recordings. The algorithms implemented to remove outliers are described below.

Physiology based Exclusion Algorithm

A physiological heart rate range was used to consider as outliers those waves whose instantaneous heart rate did not belong to the interval [30, 200] bpm. In terms of amplitude, a range was defined using the histograms of the maximum and minimum amplitude values of the waves obtained from the enrollment recordings for all subjects and for the three signals. The DMEAN algorithm [51] was applied, using as parameters $\alpha = 0.5$ and $\beta = 1.5$ and as metric the cosine distance, to remove motion artifacts present in the enrollment data before computing the histograms. The computed histograms were used to define acceptable amplitude ranges for the forearm and chest ECG and BVP signals, which were [-400, 600], [-550, 700] and [-250, 400], respectively. Waves whose amplitudes do not belong to these amplitude ranges are considered outliers. With this method, waves contaminated with contact noise that causes the saturation of the signal are removed.

The use of morphological information of the signals was also studied, focusing on some characteristic points of the ECG and BVP: (i) the R-peak and the systolic peak are assumed to be the maxima of the waves, so if these fiducial points are not the points associated with the highest amplitude, the wave is considered an outlier. However, for some subjects, the T wave in the forearm ECG presented a higher amplitude than the R-peak, so this hypothesis cannot be generalized for this signal; (ii) the Q or the S peaks are assumed to be the minimum in the heartbeat, and by defining a [-50, 50] ms window around the R-peak one can include both points. If the minimum is not inside the window, the wave is considered an outlier. Nonetheless, in the forearm ECG, due to noise, particularly EMG, other segments in the wave can present a lower amplitude value than these two fiducial points. Hence, the use of this information to remove outliers in the forearm ECG was not considered. Furthermore, since applying these rules to the BVP and chest ECG signals did not lead to a more effective removal of outliers, this information was not considered in the final algorithm.

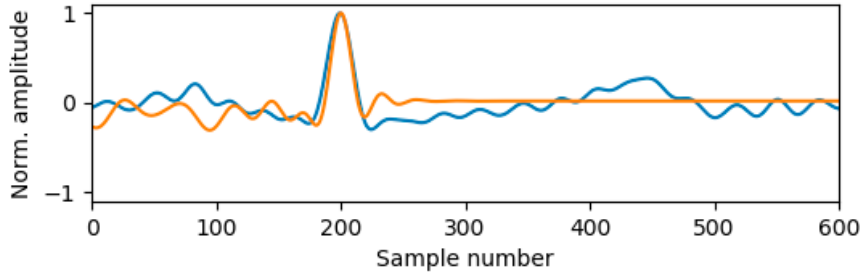


Figure 5.14: Example of flat beat.

Flat Beat Removal Algorithm

In the case of the forearm ECG, “flat” beats can occur when there is a loss of contact during a short time interval between the electrodes and the forearms of the user. These beats are characterized by constant value segments to the left and/or right of the QRS complex. To remove these waves, the waves are first normalized following Equation 5.8, where x is the wave, x_{zm} is the wave where the mean value, μ_x , was removed, and x_{norm} is the normalized wave. A sliding window of 100 ms with a step of 1 ms is applied to the heartbeat and if at least one of these segments presents an amplitude difference between the maximum and minimum values smaller than 0.02, the beat is considered a “flat” beat and is removed. The threshold was defined empirically by extracting examples of “flat” beats from different subjects and studying their properties. Figure 5.14 shows an example of a “flat” beat.

$$\begin{aligned} x_{zm} &= x - \mu_x \\ x_{norm} &= \frac{x_{zm}}{\max(|x_{zm}|)} \end{aligned} \tag{5.8}$$

Template Distance based Exclusion Algorithm

Templates were created as the mean waves of the subjects’ enrollment data. The cosine distance between every wave in the enrollment data and every subject template was computed and the threshold was defined as the average distance. In the recognition phase, the distance between each test wave and every subject template was computed. For each test wave, if the distance to the closest subject template was larger than the threshold, the wave was considered an outlier. The reasoning is that the subjects’ mean waves obtained from the enrollment data are high quality waves with different morphologies that are representative prototypes of high quality waves.

DMEAN Algorithm

The DMEAN algorithm extracts a template as the mean wave of the ensemble of test waves and computes the distance between each wave and the template. The threshold in the distance thr_{dist} is computed as shown in Equation 5.9, where μ_{dist} is the average distance to the template and σ_{dist} the respective standard

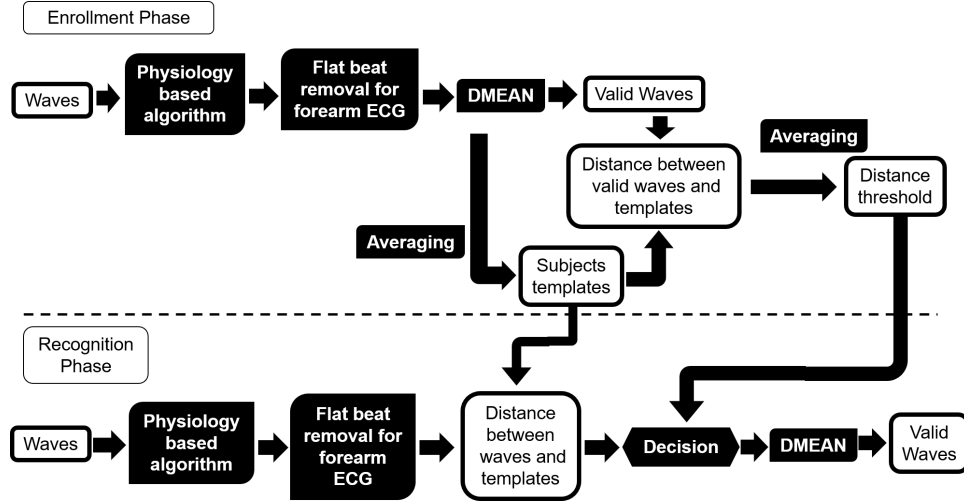


Figure 5.15: Outlier removal pipeline.

deviation. Waves whose distance is above the threshold are considered outliers. Furthermore, those waves whose maximum and minimum values do not belong to the range defined by the median of the maximum and minimum values of the set of waves, weighted by a factor β , are also considered outliers. The DMEAN algorithm works well only when the noise consists in a small fraction of the tested waves.

$$thr_{dist} = \mu_{dist} + \alpha\sigma_{dist} \quad (5.9)$$

Outlier Removal Pipeline

The pipeline used for removing outliers is shown in Figure 5.15 and described below:

- Enrollment phase:
 1. Physiology based exclusion;
 2. Flat beat removal algorithm;
 3. DMEAN: the algorithm was applied using as parameters $\alpha = 0.5$ and $\beta = 1.5$ and as metric the cosine distance.
- Recognition phase:
 1. Physiology based exclusion;
 2. Flat beat removal;
 3. Template distance based exclusion;
 4. DMEAN: the algorithm was used with the same parameters as described in step 3 of the outlier removal process applied to the enrollment data.

The cosine similarity and the Pearson correlation coefficient differ from each other in the fact that in the latter the mean value is subtracted from the waves. Given this, while the cosine similarity is only invariant to scaling, the Pearson correlation coefficient is also invariant to shifts. In the denoising step, the DC component and most of the baseline wandering are effectively removed, causing the denoised waves to be centered at the zero value. Thus, removing the mean should not lead to a significant difference in the results using the two similarity measures. Both similarity measures are more useful than the Euclidean distance in this case, since they take into account only the differences in morphology between valid waves and outliers, and not their differences in amplitude.

Figures 5.16 and 5.17 show the results of applying the outlier removal method described previously to the forearm ECG and BVP data acquired for a subject during the four tasks in one acquisition session. The number of waves considered valid after applying the method is indicated above each plot. For the BVP signal, one can observe that performing any movement related task produces motion artifacts, that increase the variability of the signal, and changes in its amplitude, the latter caused by variations in the local perfusion due to the bending of the index finger. This variability is higher in the two typing tasks. Due to normalization, the change in the amplitude is not visible. As for the forearm ECG, one can observe the effects of motion artifacts and contact noise. The saturation produced by the contact noise is removed by the physiology based exclusion algorithm, and the motion artifacts are partly removed by the algorithm based on the distance to templates. The amount of noise present in the waves increases significantly when the subject is performing tasks that promote the movement of the forearms, and this is a general trend in the recordings collected. Since some of the movements are generated by the combined activity of muscles in the forearms, the EMG noise is also more present in the ECG signal. Figure 5.18 shows an example of the result obtained for the chest ECG data. Given the acquisition site, the conditions for this signal do not change with the task performed. Figure 5.19 shows one example where the method failed to remove all waves, since no wave presented a reasonable degree of quality. In all these figures, to facilitate the visualization of the results, the waves were normalized to the [-1,1] interval using the normalization technique shown in Equation 5.8.

5.4 Amplitude Normalization

Differences in amplitude occur during the acquisitions, so in order to decrease the intrasubject variability, amplitude normalization techniques can be applied to individual waves. On the other hand, applying such techniques to individual waves leads to a loss of information that could be useful when performing identity recognition. Two types of normalization were tested: (i) the scaling described in Equation 5.8 and (ii) z-score normalization, which is shown in Equation 5.10, where x is the non-normalized wave and μ_x and σ_x are the mean and standard deviation of the wave amplitude, respectively.

$$x_{zscore} = \frac{x - \mu_x}{\sigma_x} \quad (5.10)$$

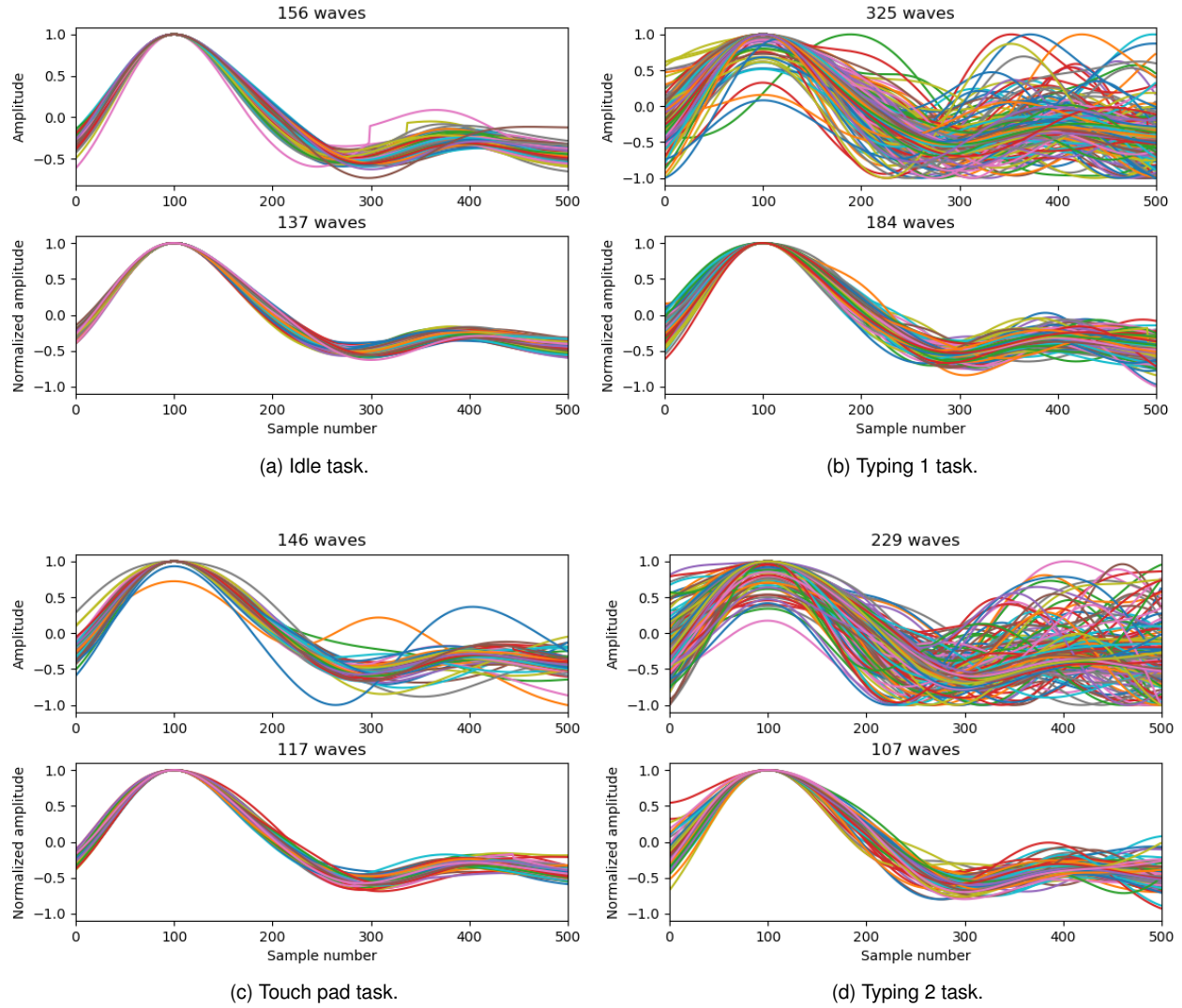


Figure 5.16: Results obtained after removing outliers in tasks (a) Idle, (b) Typing 1, (c) Touch pad and (d) Typing 2 for the BVP signal for one subject in the first acquisition session. Overlaid waves using the fixed time window segmentation. In each figure, from top to bottom: denoised waves before removing outliers; waves obtained after applying the method proposed.

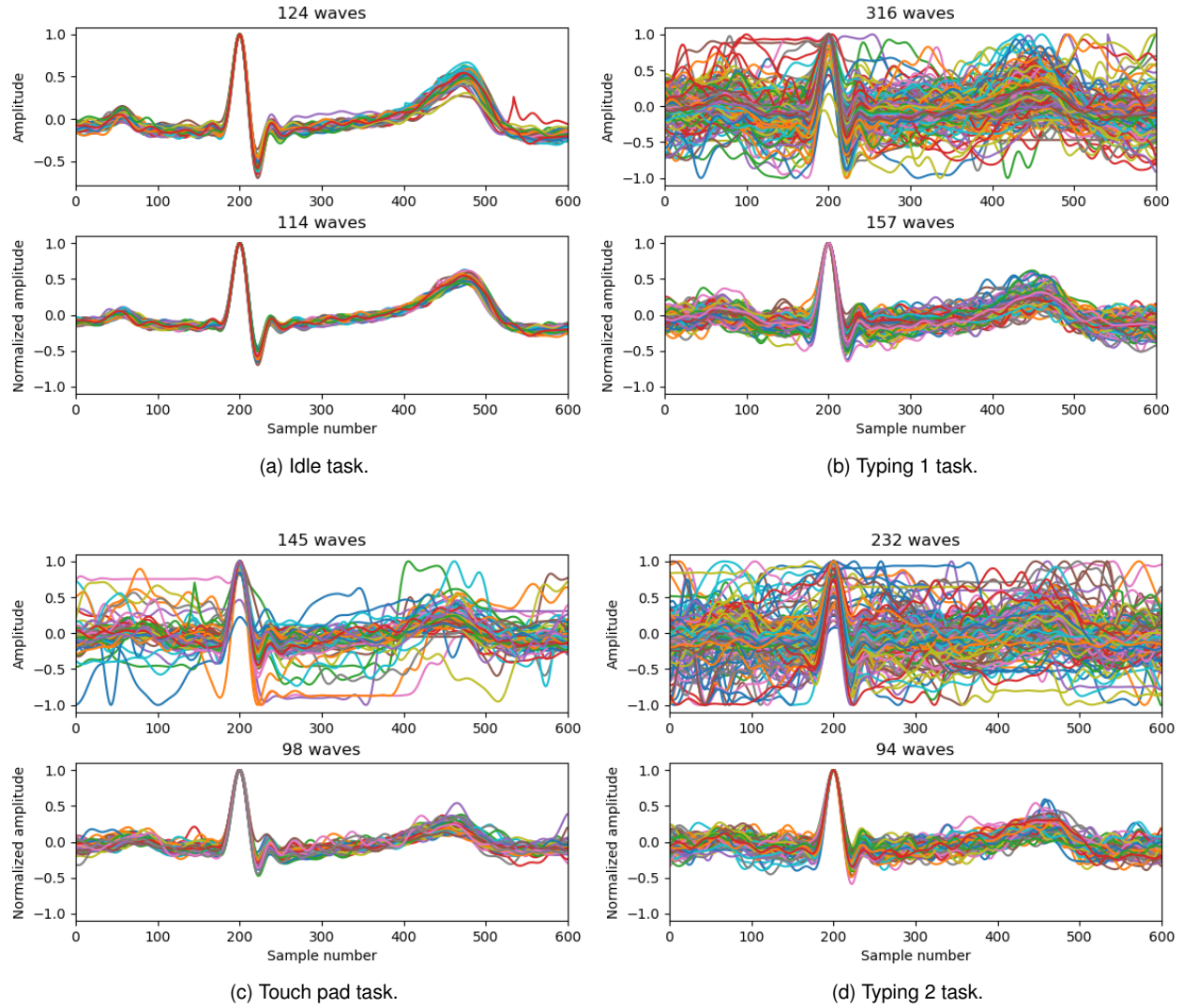


Figure 5.17: Results obtained after removing outliers in tasks (a) Idle, (b) Typing 1, (c) Touch pad and (d) Typing 2 for the forearm ECG signal for one subject in the first acquisition session. Overlaid waves using the fixed time window segmentation. In each figure, from top to bottom: denoised waves before removing outliers; waves obtained after applying the method proposed.

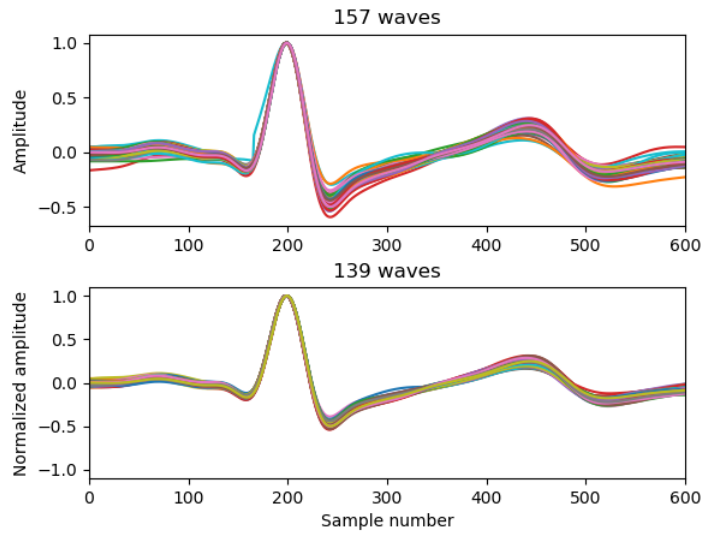


Figure 5.18: Results obtained after removing outliers in the Idle task for the chest ECG signal for one subject in the first acquisition session. Overlaid waves using the fixed time window segmentation. In each figure, from top to bottom: denoised waves before removing outliers; waves obtained after applying the method proposed.

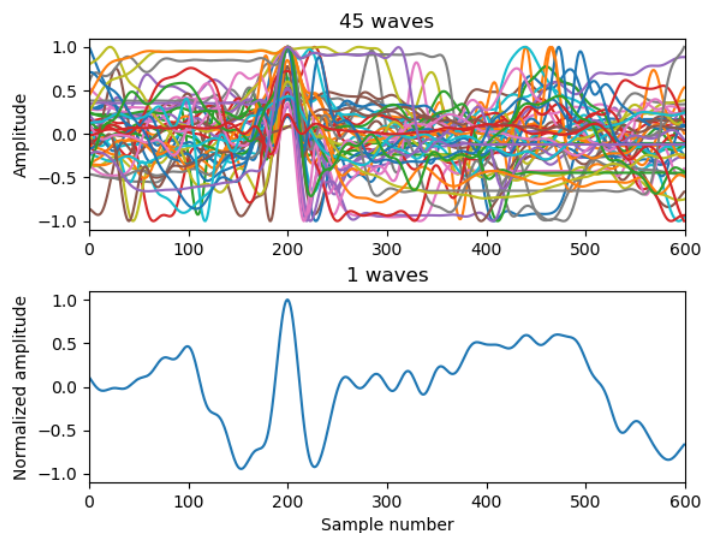


Figure 5.19: Example where the proposed outlier removal method failed to completely remove all outliers in a forearm ECG recording. In each figure, from top to bottom: denoised waves before removing outliers; waves obtained after applying the method proposed.

Chapter 6

Feature Extraction and Classification

In this chapter we describe the kind of features that were extracted and the classification algorithms that used them in the verification and identification tests performed for the data collected in the acquisition sessions.

6.1 Feature Extraction

Since the segmentation of the ECG and BVP signals was conducted at the individual wave cycle, the extracted features must be related to the waves themselves. As previously referred in Chapter 5, the signals contain a significant amount of noise, which makes the process of accurately identifying fiducial points an unreliable task.

In this case, a better approach than using fiducial features was to use the amplitude values of the wave as the feature set. The dimension of the feature set changes depending on the sampling frequency and segmentation used. A higher sampling frequency produces a more detailed version of the waves, which can provide more discriminative information. On the other hand, if no resampling or decimation is performed, the dimension of the feature space can be significantly large. Dimension reduction techniques can be applied to find a subspace of features that can result in an increase in the classification performance. As already mentioned in the previous chapter, two kinds of segmentation were performed. In the case of the segmentation based on a fixed time window, the features are embedded in the time domain, so the feature space corresponds to the fixed window size used. For the BVP signal, a window of 500 ms sampled at 1 kHz was used, which corresponds to 500 sample points. For the two ECG modalities, sampled at the same frequency, the window has a length of 600 ms, which corresponds to 600 sample points. As for the heart rate based resampling method, the waves are mapped from the time domain, where they have different lengths due to the HRV, to a domain where every wave has 600 sample points using a resampling function that samples the original segment in a uniform or nonuniform way, the latter applying a fixed time window specified in Subsection 5.2.3.

6.2 Classification: Identification and Authentication Techniques

In this section we start by describing the classification algorithm used in the context of single modality biometrics for the three signals in study: the forearm and chest ECG, and the BVP. We then focus our attention in how to fuse the information provided by the two modalities that were used in the devised biometric system: the forearm ECG and the BVP.

6.2.1 Single Modality Biometrics

The KNN algorithm was used to perform single modality identification and authentication tests. This classifier is an instance-based learning algorithm where a test sample x is classified by finding the K training samples x_i ($i = 1, \dots, K$) that are closest to it given some metric or similarity measure d such as the Euclidean, cosine or Pearson correlation distances. The class output is decided through majority voting, as shown in Equation 6.1, where A_k is the set of the closest K neighbors to the test sample, y_i is the class label of training sample x_i that belongs to A_k , c_j is a class label from the set of all class labels B_j ($j = 1, \dots, J$), and I is a function that evaluates to 1 when its argument is true, and 0 otherwise.

$$f(x) = \arg \max_{c_j} \frac{1}{K} \sum_{i \in A_k} I(y_i = c_j) \quad (6.1)$$

Although the training phase consists in simply storing the training data, with no explicit computation of the decision boundaries, the classification phase can become computationally intensive when using large training sets, and in this case data structures such as kd-trees can be used to increase the efficiency of the search. In addition to finding an appropriate metric or similarity measure, the number of neighbors used, K , must be specified. The choice of this parameter depends on the data. Increasing K leads to a more robust classification to noise and outliers, preventing overfitting, but also produces less distinct boundaries between classes.

A variant of this learning algorithm, the weighted KNN (W-KNN), was also used. In this case, the neighbors are weighted by their distance to the test sample, so that closer neighbors have a greater influence than those that are further away, as shown in Equation 6.2, where $w_{x_i,x}$ is the weight associated with the training sample x_i .

$$f(x) = \arg \max_{c_j} \frac{1}{K} \sum_{i \in A_k} \frac{1}{w_{x_i,x}} I(y_i = c_j), w_{x_i,x} = d(x_i, x) \quad (6.2)$$

In the identification and authentication tests performed, the training and test sets were composed of individual waves or the mean wave of m consecutive waves. In the case of identification, the predicted subject was given by the W-KNN algorithm for each test sample and the EID was used as performance metric. In terms of authentication, for each subset of training samples pertaining to a given subject, the closest K neighbors to each test sample were computed. A test sample was accepted as belonging to the

claimed identity if the distance (or similarity measure) to the K neighbors is smaller (larger) than a given threshold. This test was conducted for a defined range of threshold values and FAR and FRR curves were computed for each subject. The intersection of these two curves gives the EER for each subject. In order to compute a global EER as performance metric for the authentication tests, these curves were averaged across all subjects.

Regarding the development of a continuous authentication framework, since this classification algorithm is simple, it can be easily adapted to perform continuous authentication. As new data are available from the data stream, based on the output given by the classifier, the training set can be updated by adding new templates and removing or adapting previous ones without any considerable overhead.

6.2.2 Multimodal Biometrics

A Bayesian decision fusion scheme was used to map the decision labels output by the single modality classifiers into probability values. A confusion matrix was computed for each classifier using the training data. Let CM^j be the $N \times N$ confusion matrix for the j^{th} single modality classifier, where N is the number of classes. The entry $cm_{k,l}^j$ of the matrix CM^j corresponds to the number of instances in the training set where a test input belonging to the true class ω_k was assigned to the class ω_l by the j^{th} classifier. Let the total number of instances in the training set be M and the number of patterns that belong to class ω_k be M_k . Let c_j be the class label assigned to a test pattern by the j^{th} classifier. Given this, the value $cm_{k,l}^j/M_k$ is an estimate of the conditional probability $P(c_j|\omega_k)$ and M_k/M can be considered an estimate of the prior probability of class ω_k . From the decision output by the single modality classifiers, we can create a set of decisions $\mathbf{c} = [c_1, \dots, c_J]$, where J is the number of single modality classifiers. We then are interested in computing the posterior probability of class ω_k , $P(\omega_k|\mathbf{c})$. To calculate this probability, we can use the Bayes rule, described in Equation 6.3, where $k = 1, \dots, N$.

$$P(\omega_k|\mathbf{c}) = \frac{P(\mathbf{c}|\omega_k)}{P(\mathbf{c})} P(\omega_k) \quad (6.3)$$

Since the denominator does not depend on the class ω_k , the discriminant function for class ω_k is given by Equation 6.4.

$$g_k = P(\mathbf{c}|\omega_k)P(\omega_k) \quad (6.4)$$

To simplify the computation of the likelihood probability, one can assume conditional independence between the single modality classifiers, which is known as the Naive-Bayes rule. Given this, the $P(\mathbf{c}|\omega_k)$ can be computed following Equation 6.5.

$$P(\mathbf{c}|\omega_k) = P(c_1, \dots, c_J|\omega_k) = \prod_{j=1}^J P(c_j|\omega_k) \quad (6.5)$$

The decision rule is shown in Equation 6.6.

$$f(\mathbf{c}) = \arg \max_k g_k \quad (6.6)$$

The fusion algorithm can be adapted to perform authentication. In this case, a threshold is set on the value of the discriminant function g_k . Assuming that the claimed identity is w_k , the set of decisions output by the single modality classifiers \mathbf{c} is accepted as belonging to w_k if g_k is greater than the defined threshold. A range of threshold values is tested to create the FAR and FRR curves.

Chapter 7

Experimental Results and Discussion

In this chapter we present results using the data obtained according to the experimental setup described in Chapter 4 and processed following the methodology described in Chapter 5. Additionally, we also elaborate and discuss the results achieved.

7.1 Test Protocol

The data acquired during the acquisition sessions were used after the processing step to conduct several performance evaluation tests of the biometric system. Three kinds of analysis were conducted: (i) within-session within-task analysis (WS-WT), where the data from one task were used to create the training and test sets using a Leave-one-out (LOO) strategy; (ii) within-session across-task analysis (WS-AT), where the data from one task were used to create the training set, and the data from other task in the same session were used to create the test set; and (iii) across-session analysis (AS), which is similar to WS-AT analysis, but the data for the training and test sets come from tasks that belong to different sessions. Table 7.1 summarizes these three kinds of analysis.

The WS-AT and WS-WT analyses evaluate the performance of the system in a short-time reference frame, which resembles a scenario of continuous authentication. On the other hand, the AS analysis shows the impact on the performance in the long term due to the varying nature of the biometric modalities and evaluate the permanence of the biometric traits. Table 7.2 shows the labels used for each task.

The choice of the tested subjects depends on the number of valid waves available, after the processing step, for each subject in the tasks from which the data are extracted to create the training and test sets.

Table 7.1: Summary of the types of analysis conducted.

Analysis	Data partitioning	Number of runs
WS-WT	LOO	20
WS-AT	Separate sets	100
AS	Separate sets	100

Table 7.2: Labels assigned to the tasks. x takes the values of 1 or 2 if the task belongs to session 1 or 2, respectively.

Task	Idle	Typing 1	Touch pad	Typing 2
Label	Sx.1	Sx.2	Sx.3	Sx.4

Table 7.3: Composition of the used balanced data sets.

Data set	Training set (per subject)	Test set (per subject)	Number of subjects
D _A	1920(80)	360(15)	24
D _B	1920(80)	150(10)	15

Table C.1 summarizes the type of data collected for each subject in each task and session. In order to create balanced training and test sets, a fixed number of samples was extracted randomly, in each run, from the complete set of samples available for each subject, and the results are then averaged across the runs, whose number was defined previously in Table 7.1. Information regarding the balanced data sets used in the performance evaluation tests conducted is presented in Table 7.3.

The performance evaluation tests were conducted using a distance weighted 3-NN algorithm. With the exception of the tests conducted in Subsection 7.3.1, the mean wave of 5 consecutive waves was used as template for the forearm ECG and BVP modalities, and no averaging was applied to the chest ECG. Additionally, after a preliminary evaluation of the filtering cutoff frequency and its effects on the performance of the biometric system, only the ECG based modalities filtered with the 40 Hz cutoff frequency were used in the rest of the tests. Table 7.4 summarizes information related to the performance evaluation tests conducted.

7.2 System's Usability

The usability of the system depends on the user acceptability and satisfaction. The former can be characterized in terms of the relationship between the time of use of the system and the amount of biometric data collected during that period. Even more important is the relationship between these two parameters and the amount of biometric data that is effectively used to perform identity recognition, since data with a low degree

Table 7.4: Summary of the information regarding the performance evaluation tests conducted. ID and Auth refer to identification and authentication tests, respectively. The tasks used in each test are shown in the last column - training task>test task. x and x' take the values of 1 or 2 if the task belongs to session 1 or 2, respectively. x and x' represent tasks that belong to different sessions, so they cannot be assigned simultaneously the same value.

Type of test	Performance evaluation test	Data set	Analysis
ID	Averaging and ECG cutoff frequency	D _A	WS-WT (S1.1), WS-AT (S1.1>S1.3), AS (S1.1>S2.1)
ID	Normalization techniques and dissimilarity measures	D _A	WS-AT(S1.1>S1.3)
ID	Comparison between tasks	D _B	WS-AT(Sx.1>Sx.2-4), AS (Sx.1>Sx'.1-4)
Auth	Authentication tasks	D _B	WS-AT(S1.1>S1.2-4), AS (S1.1>S2.1)
ID	Multimodal biometrics	D _B	WS-AT(S1.1>S1.3), AS (S1.1>S2.1)

Table 7.5: Averaged fraction of recording effectively used as a result of outlier removal and total time of acquisition in the first session using a fixed time window segmentation.

Task	Modality	Avg. time used (%)	Avg. acquisition time (s)
Idle	BVP	85	120
	Forearm ECG	87	
	Chest ECG	89	
Typing 1	BVP	41	265
	Forearm ECG	26	
	Chest ECG	90	
Touch pad	BVP	65	115
	Forearm ECG	50	
	Chest ECG	90	
Typing 2	BVP	36	180
	Forearm ECG	24	
	Chest ECG	88	

of quality cannot be used by the system. In terms of user satisfaction, the ease of use and the comfort provided by the system are crucial factors when evaluating the possibility for deployment of the biometric system.

7.2.1 User Acceptability

The signal processing pipeline described in Chapter 5 was applied to the data collected during the acquisition sessions. For each task, statistics regarding the number of waves extracted and the corresponding duration of the recordings was computed for each modality and type of segmentation for the total population. Furthermore, in the case of the ECG, the results were also obtained for the two cutoff frequencies tested, 20 and 40 Hz. The values obtained for each subject were used to compute statistics such as the mean and median values. Tables C.2 and C.3 show these results computed for the first acquisition session using a fixed time window segmentation. To have a more compact presentation of the results, the values associated with the ECG using the 20 Hz cutoff frequency are not depicted, since these results are similar to those associated with the 40 Hz cutoff frequency. Table C.2 shows statistics related to the number of waves extracted before and after removing outliers and Table C.3 presents the corresponding results in terms of acquisition duration before and after performing segmentation, and after removing outliers.

Table 7.5 condenses the information shown in Table C.3, showing the average percentage time of valid segments obtained after outlier removal and the average acquisition time for each modality and task for the fixed time window segmentation. The results using the heart rate based resampling method are similar and hence are not shown.

In Table 7.5 one can observe that, for the task Idle, approximately 85% of the recording, on average, achieves a minimum degree of quality to be used in the classification stage. This result gives an estimate of the ability of the system to perform identity recognition when the subjects are idle, without performing significant movements with their arms and fingers. Behaviors that fit into these conditions include reading

and watching some content on the computer without actively using the mouse, touch pad or keyboard. When considering the results obtained for the typing tasks, the values presented are similar for both tasks. In the case of the BVP modality, approximately 40% of the recording is effectively used, with this value decreasing to 25% in the case of the forearm ECG. These values increase to 65% and 50%, respectively, for the task Touch pad. Considering the results obtained, the use of the devised biometric system in a continuous authentication framework is limited, given that the user acceptability only reaches significant values when the subjects are not performing any significant movements. Although this can be restrictive, in the case of a working routine where the user spends long hours on the desk performing some cognitive work that frequently requires idle moments for thinking and reading or watching some content in the computer, the system can effectively acquire data with enough quality to perform identity recognition. In those cases where the user regularly moves his or her arms and fingers, the biometric system can assist the decision provided by another authentication system, or give a decision in a longer time frame. The best results presented in tables C.2 and C.3 show that it is possible to obtain values in the range of 60% to 80% for the non-idle tasks. This is due to two factors: (i) there are some subjects whose behavior allows them to use the biometric system without producing noise that severely degrades a significant fraction of the recording; (ii) there are subjects that are aware of the limitations of the device and this influences their behavior. These results show that, by adapting the behavior of the users, they can increase the effectiveness of the system. On the other hand, this can degrade the user experience.

7.2.2 User Satisfaction

At the end of each acquisition session, the subjects were asked to fill in a questionnaire regarding the comfort and ease of use of the acquisition system, as shown in Figure B.3. The first two questions are related to the comfort using the armrest and wristlet, respectively. The third and last question pertains to the change in the user's behavior while using the two modules with respect to the tasks performed with the computer. Figure 7.1 shows the results of the answers provided by the subjects in the first session.

The results to the questionnaire presented in Figure 7.1 show that the developed acquisition system was well accepted. In terms of comfort, the subjects found the wristlet more comfortable than the armrest. Some users reported that the wristlet caused itching due to the elastic band used. This became more severe with time, especially in warmer days. They also mentioned that the armrest was excessively filled and that caused some discomfort and promoted changes in their behavior, since the keyboard was not at the same height as their hands. The subjects reported some changes in their behavior, but those were not considered significant. The answers given to the questionnaire were based on the use of the sensor modules during sessions that lasted on average approximately half an hour, which cannot be compared to a full day of use. A subset of subjects also performed long time acquisitions of one and two hours. In these long time sessions, the subjects referred that the main cause of discomfort was the wristlet. As for the armrest, some mentioned that they were concerned with keeping the forearms most of the time on the armrest, while others

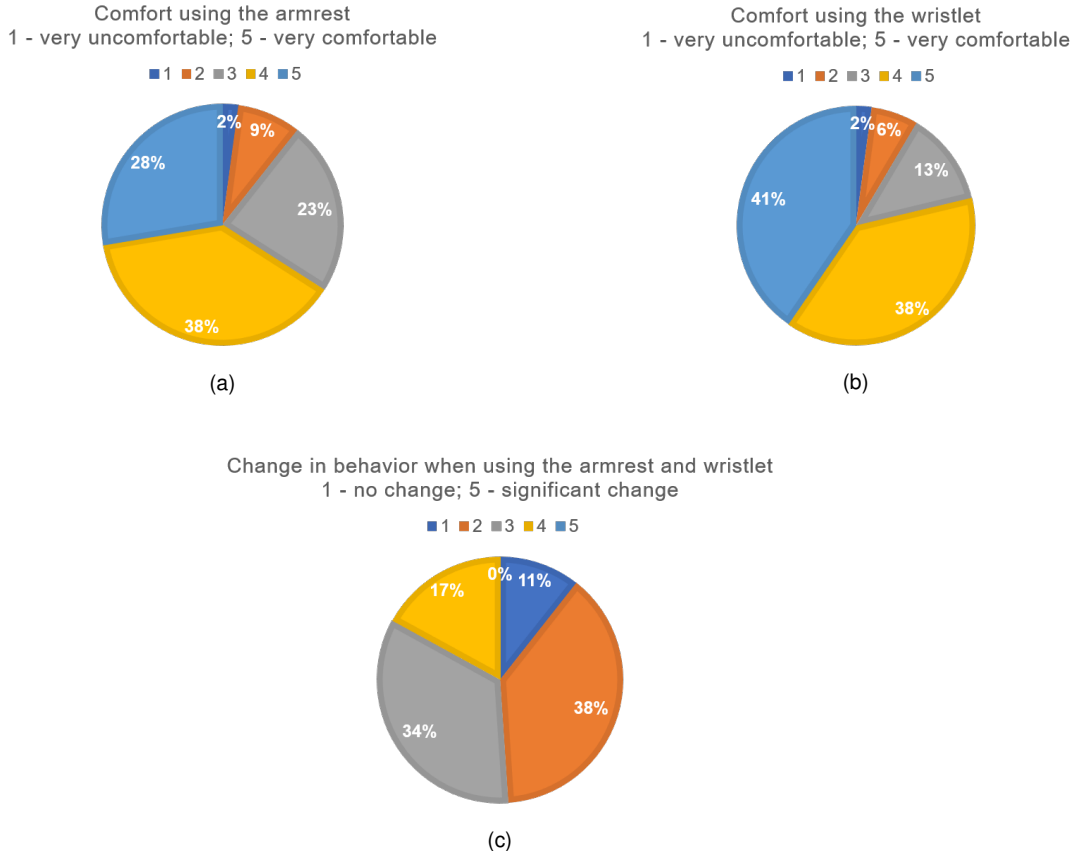


Figure 7.1: Results of the answers to the user satisfaction questionnaire provided by the subjects in the first acquisition session.

mentioned that they became used to this module.

7.3 Identification Results: Single Modalities

The following results concern the tests performed using the single modality approach for performing identification. In this section, we assume a closed-set identification scenario.

7.3.1 Averaging and ECG Cutoff Frequency

In this test, the averaging of m consecutive waves was performed to study the effect of ensemble averaging in removing inter-beat variations produced by noise such as the EMG, with $m = 1, 2, \dots, 15$. Each group of m consecutive waves was replaced by the corresponding mean wave in both training and test sets. The results are presented for two types of segmentation: fixed time window and heart rate based resampling. For the ECG modalities, the results are also presented for the two cutoff frequencies used in the denoising step. The Euclidean distance was used as metric for determining the nearest neighbors and the z-score normalization was applied to the samples. Figure 7.2 shows the results for the WS-AT analysis. The WS-WT and AS results are presented in Figures C.1 and C.2, respectively.

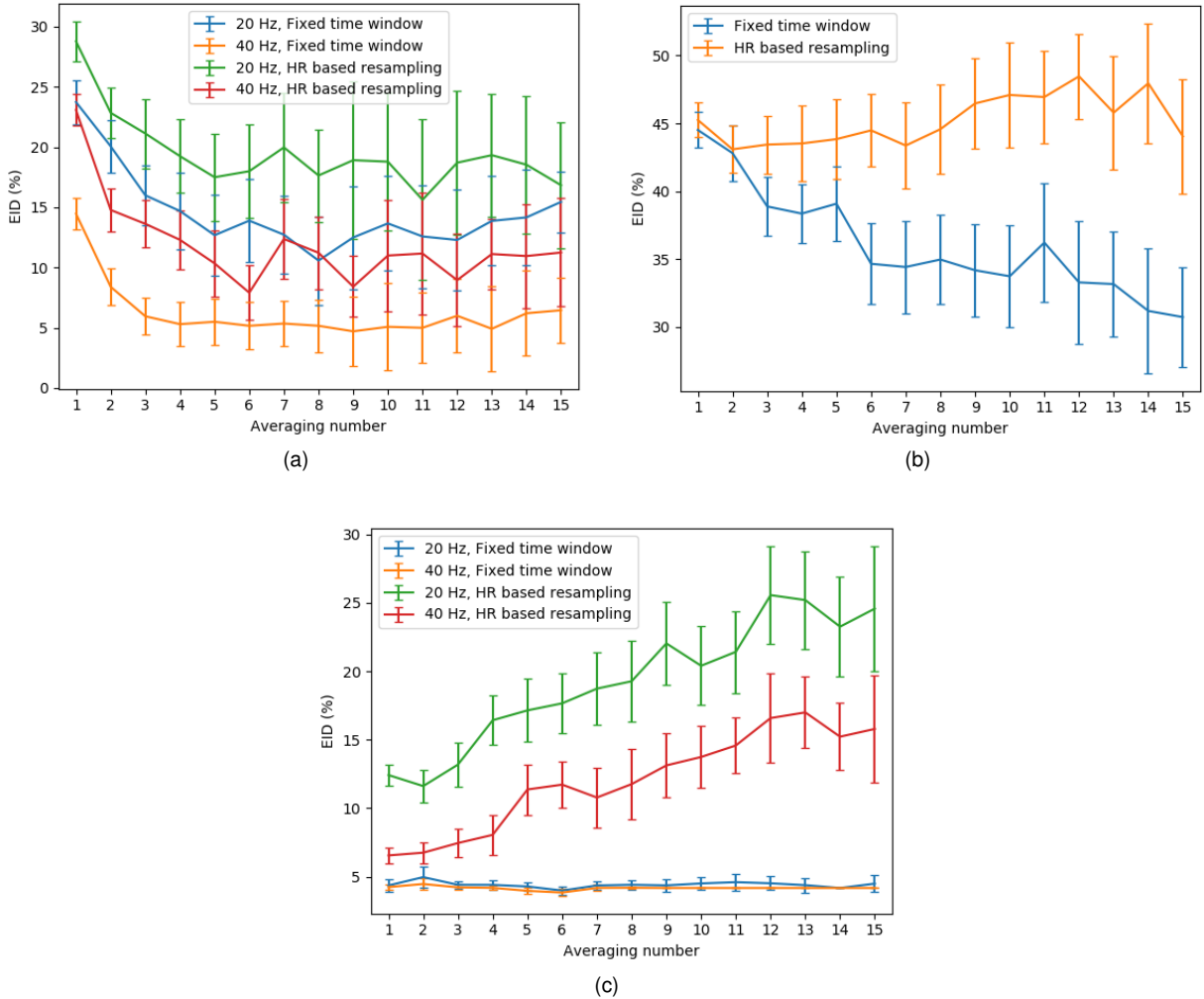


Figure 7.2: Identification results of averaging consecutive waves when performing WS-AT analysis for the (a) forearm ECG, (b) BVP and (c) chest ECG modalities.

The averaging results obtained for the ECG modalities show that the performance is higher when applying a low-pass filter with a cutoff frequency of 40 Hz, as opposed to 20 Hz. Despite removing less components of the EMG noise than the smaller cutoff frequency, the larger cutoff frequency preserves more detail in the heartbeats, which leads to a higher discriminability between subjects. Thus, the effect of EMG noise is less detrimental than removing the ECG information associated with frequencies between 20 Hz and 40 Hz, as shown in Figures 7.2a and 7.2c. Furthermore, the EMG noise can be reduced by performing ensemble averaging (Figure 7.2a).

These results also show that the fixed time window segmentation achieves a better performance than the heart rate based resampling method, as presented in Figures 7.2, C.1 and C.2. This can be explained in part because the assumption that the different segments of the ECG and BVP waves are transformed in the same way as a function of the HRV does not hold. The approximation implemented increases the intra-subject variability and, in some cases, averaging degrades the performance. The accurate localization

of fiducial points such as the Q and S waves in the heartbeat may lead to better results, since one can define more precisely the QRS complex for each subject, as opposed to the use of a fixed window around the R peak, which can be fairly arbitrary. Nonetheless, the development of more robust methods that model the change of the several segments with the HRV is crucial when considering the challenge of decreasing and removing the influence of HRV in the morphology of the waves. A thorough study involving a large population of subjects performing tasks during several sessions that promote changes in the heart rate must be conducted to evaluate how the different segments vary with it. The input of experts in this analysis is fundamental to understand the relationship between the heart rate and the evolution of the morphology and amplitude of the waves.

As expected, in the WS-WT and WS-AT analyses the best performance was achieved for the chest ECG modality, followed by the forearm ECG and, lastly, the BVP. Considering a continuous authentication framework, the WS-AT analysis is the one that most closely resembles it, since the WS-WT tests were performed using data from acquisitions in which the subjects were completely idle. In the WS-AT tests, for the forearm ECG, the average EID decreases from approximately 15% to 5% when using the mean wave of 5 consecutive waves. Assuming a rest heart rate around 80 bpm, 5 consecutive waves correspond to a time interval of approximately 4 seconds, and so a decision can be output in the given amount of time. By taking advantage of a continuous framework, a decision can be provided using also the data previously collected or the decisions output in the past, so that the decision is based in more data and can then be given in a shorter time interval.

7.3.2 Normalization Techniques and Dissimilarity Measures

Table 7.6 shows the results obtained for the WS-AT analysis using the Euclidean, cosine and Pearson correlation distances as dissimilarity measures. In the case of the Euclidean distance, two types of normalization were also tested: the normalization described in Equation 5.8, referred as scaled, and z-score normalization.

Table 7.6: Average EID results obtained when testing different normalization techniques and dissimilarity measures for WS-AT analysis.

Modality	Euclidean	Scaled Euclidean	Euclidean z-score	Cosine	Pearson correlation
BVP	50.07±2.92	39.65±2.75	38.50±2.77	38.20±2.94	38.13±3.04
Forearm ECG	16.13±2.38	8.83±2.30	5.15±1.98	10.83±2.48	4.71±1.93
Chest ECG	4.51±0.19	4.51±0.21	4.46±0.19	4.64±0.19	4.30±0.24

The results achieved show that the Euclidean distance provided the worst performance, especially in the case of the BVP and forearm ECG modalities. As for the two types of normalization tested for the Euclidean distance, the z-score normalization produced marginally better results than the scaling described by Equation 5.8. However, the best results were achieved for the non-normalized waves using the Pearson correlation distance.

7.3.3 Comparison Between Tasks

In this performance evaluation test we compare the results achieved when testing in different tasks. The Pearson correlation distance was used as dissimilarity measure. Tables 7.7 and 7.8 present the results for the WS-AT and AS analyses, respectively, for the fixed time window segmentation. Tables C.4 and C.5 show the same results for the heart rate based resampling method.

Table 7.7: Average EID results obtained for each task when conducting a WS-AT analysis using a fixed time window segmentation. x is assigned to 1 or 2 if the training set belongs to session 1 or 2, respectively.

Test Task	Session 1			Session 2		
	BVP	Forearm ECG	Chest ECG	BVP	Forearm ECG	Chest ECG
Sx.2	57.34±2.73	12.4±5.53	6.87±0.11	64.75±4.66	3.07±2.62	3.00±0.04
Sx.3	25.38±2.84	2.24±1.72	6.46±0.29	30.72±3.41	4.44±1.73	9.18±0.52
Sx.4	63.91±4.13	7.51±2.4	8.31±0.82	65.77±3.87	5.63±2.45	9.51±0.35

Table 7.8: Average EID results obtained for each task when conducting an AS analysis using a fixed time window segmentation. x is assigned to 1 or 2 if the training set belongs to session 2 or 1, respectively.

Test Task	Session 1			Session 2		
	BVP	Forearm ECG	Chest ECG	BVP	Forearm ECG	Chest ECG
Sx.1	65.81±1.06	22.39±1.25	50.65±0.61	64.47±2.03	23.33±1.66	70.4±0.73
Sx.2	84.65±2.91	29.77±4.11	55.14±0.73	71.37±2.19	38.13±8.48	68.17±0.64
Sx.3	70.31±2.76	26.53±1.67	52.88±0.53	67.36±3.09	38.93±3.38	71.49±0.53
Sx.4	82.47±2.83	36.43±3.15	61.93±0.62	72.42±2.79	39.8±4.16	64.58±0.89

Regarding the tests conducted when comparing the performance achieved in the different tasks, the results presented in Tables 7.7 and 7.8 show that the best performance was achieved for the tasks Idle and Touch pad, as expected given the lower presence of noise. The forearm ECG and BVP achieved a minimum EID of approximately 2% and 25%, respectively, in the WS-AT tests. For some tasks, the results obtained with the forearm ECG are better than those obtained with the chest ECG, although these last ones were achieved with no averaging.

According to the results presented in Figure C.2 and Table 7.8, the performance of the three modalities in the AS tests was significantly lower. In the case of the chest ECG, the low performance can be explained due to a different placement of the chest band between sessions for some subjects. Although the experimental protocol was explained to each subject in the beginning of each acquisition session, the placement of the chest band at the 5th intercostal space was not always correctly performed, leading to deviations from the correct position. Given this, the relative position of the electrodes with respect to the electrical vector of the heart changes, and so does the morphology of the ECG signal collected. Figure 7.3 shows the mean waves of the chest ECG and the ECG acquired at the collar bones for the task Idle of the two sessions for one subject. One can observe the significant changes in the slope of the ST segment and amplitude of the R wave in the chest ECG between the two sessions, as opposed to the case of the ECG collected at the collar bones, in which is visible a change in the T wave caused only by a different heart rate.

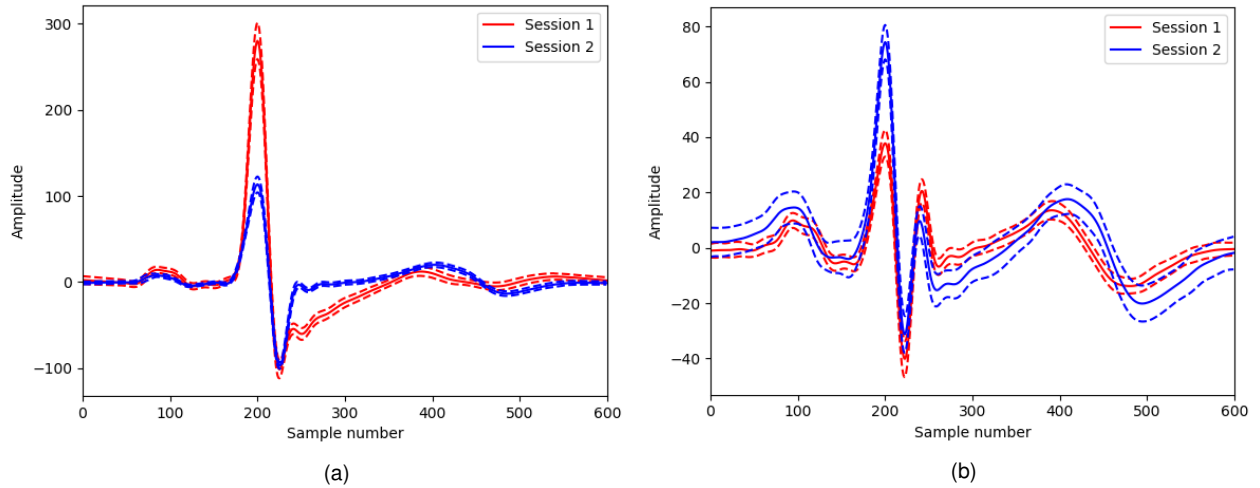


Figure 7.3: Mean waves (\pm std) for the task Idle for the two sessions of one subject. (a) chest ECG and (b) ECG collected at the collar bones.

As for the forearm ECG, the poor performance obtained across-sessions was due mainly to three subjects: subjects 4, 5 and 7 in the confusion matrix shown in Figure 7.4a. Of these three subjects, two presented heartbeats that changed considerably between sessions. Figure 7.4 shows the confusion matrix for the forearm ECG associated with the AS analysis performed in Subsection 7.3.3 using S1.1 and S2.1 as training and test sets, respectively. Additionally, the mean waves of the task Idle for the two sessions of the three subjects are also depicted.

Fixed Time Window

Considering the significant changes in morphology between sessions for some subjects, two smaller fixed time windows were also tested for the forearm ECG modality in addition to the [-200, 400] ms window that includes the PQRST complex: [-200, 50] ms and [-50, 50] ms windows that include the PQRS and QRS complexes, respectively. The results are shown in Table 7.9. The WS-AT analysis was performed using only tasks S1.1 and S1.3 as training and test sets, respectively. As for the AS analysis, only tasks S1.1 and S2.1 were used as training and test sets, respectively.

Table 7.9: Average EID results obtained when conducting WS-AT and AS analyses using fixed time windows with different lengths for the forearm ECG modality.

Analysis	QRS	PQRS	PQRST
WS-AT	12.02 ± 3.11	4.58 ± 1.75	2.09 ± 1.70
AS	22.12 ± 1.15	8.07 ± 1.18	22.38 ± 1.04

In the WS-AT tests, the performance increased when a larger fixed time window is used, ranging from an EID value of approximately 12% for the QRS complex fixed time window to 2% using the larger one that includes the PQRST complex. This was expected given the lower variability of the heartbeats in the

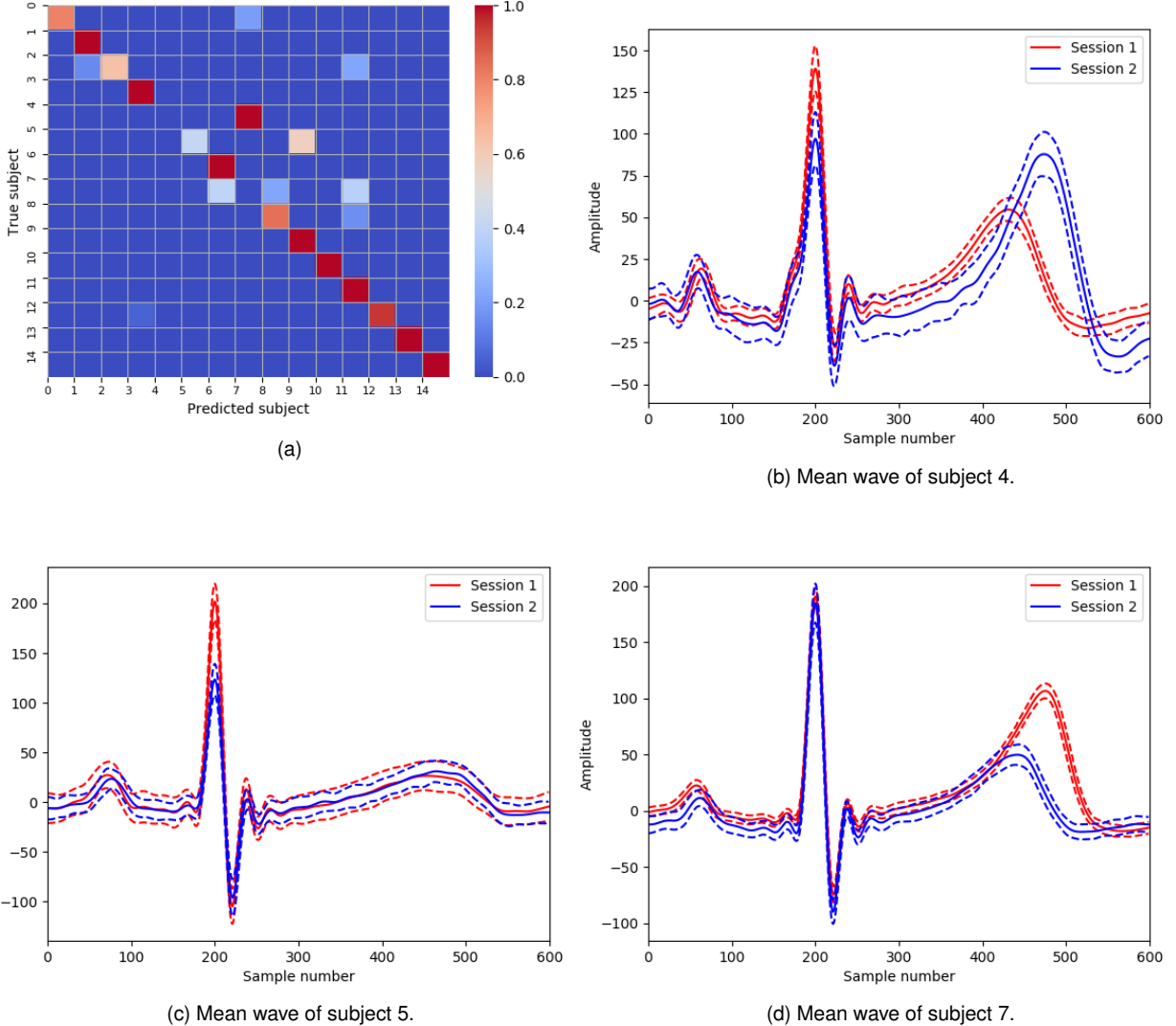


Figure 7.4: (a) Confusion matrix obtained in the AS analysis of Subsection 7.3.3 for the forearm ECG modality using S1.1 and S2.1 as training and test sets, respectively. (b)-(d) show the mean waves ($\pm \text{std}$) obtained for three subjects in the two sessions of the Idle task.

short term and the additional information that the ST segment provides in terms of discriminative capacity. However, in the AS analysis the performance achieved using only the QRS complex window was similar to that obtained using the PQRST complex counterpart, with EID values of approximately 22%. The changes across-sessions that occur at the level of the ST segment degraded the performance. On the other hand, the results obtained for the PQRS complex show that this segment presents a lower degree of variability with time, achieving an EID of approximately 8% across-sessions.

7.4 Authentication Results: Single Modalities

Tests were also performed in terms of authentication using the Pearson correlation distance as dissimilarity measure. The average global EER values are shown in Table 7.10 for the fixed time window segmentation. Table C.6 presents the results for the heart rate based resampling segmentation and Figure 7.5 shows the global ROC curves, averaged across all runs and subjects, for the three modalities when performing WS-AT and AS analyses, for the fixed time window segmentation.

Table 7.10: Average global EER results obtained when conducting WS-AT and AS analyses using a fixed time window segmentation.

Test sets	BVP	Forearm ECG	Chest ECG
S1.2	20.68 ± 1.18	7.24 ± 1.28	6.66 ± 0.04
S1.3	6.84 ± 0.65	4.13 ± 0.8	5.88 ± 0.35
S1.4	22.12 ± 0.77	6.51 ± 0.74	7.53 ± 0.4
S2.1	27.9 ± 0.55	13.42 ± 0.13	32.72 ± 0.4

The results obtained for the forearm ECG were reasonable, even across-sessions. As in the identification tests conducted using the different tasks, the best performance was achieved for the task Touch pad.

7.5 Identification Results: Multimodality

The following results concern the tests performed using the multimodal approach based on fusion at the decision level referred in Section 6.2.2. Equal a priori probabilities were set to all subjects and the same weights were given to the decisions produced by the two single modality classifiers. These used the Pearson correlation distance as dissimilarity measure and the results are presented for the fixed time window segmentation. Similar to a WS-WT analysis, LOO performance estimate was used in the training set to compute the confusion matrices of each single modality classifier. In this section, we assume again a closed-set identification scenario.

7.5.1 Forearm ECG and BVP

In this case, the fusion was performed using the forearm ECG and BVP modalities. The results are shown in Table 7.11.

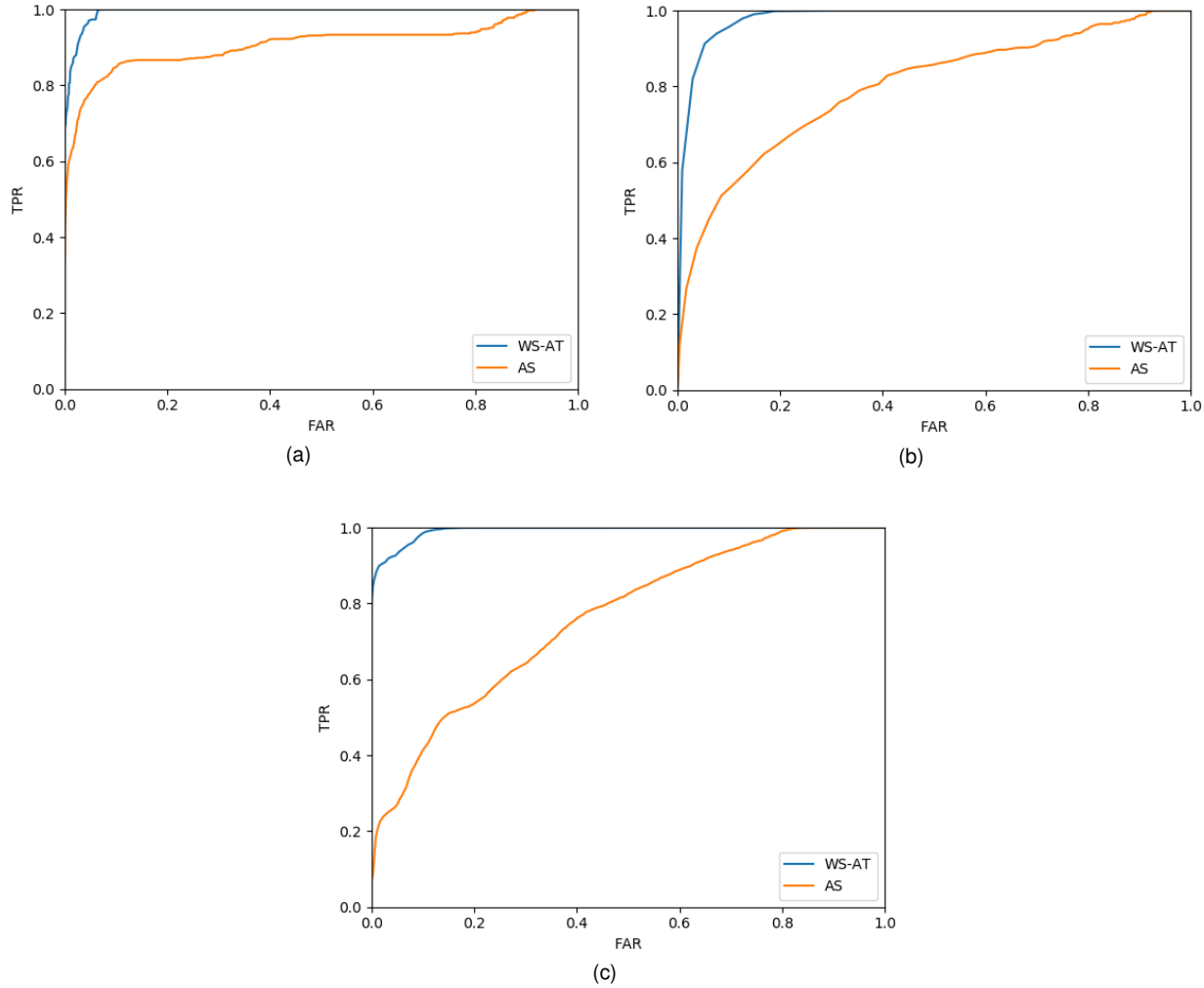


Figure 7.5: ROC curves obtained when performing WS-AT and AS analyses for the (a) forearm ECG, (b) BVP and (c) chest ECG modalities using fixed time window segmentation.

The fusion of the BVP and forearm ECG modalities did not lead to an increase in the performance when compared to the single modality results, as shown in Table 7.11. The average EID values obtained are higher than the ones achieved for the forearm ECG modality. It is clear that the BVP modality degrades the performance of the fusion methodology, even in the WS-AT tests

7.5.2 Forearm ECG

As an alternative to the fusion of the forearm ECG and BVP modalities, the use of two modalities based on the forearm ECG signal was considered: one using the fixed time window already defined that encompasses the PQRST complex for a rest heart rate, [-200, 400] ms; and another one using a smaller window that includes only the QRS complex, [-50, 50] ms, or the PQRS complex, [-200, 50] ms. The results are shown in Table 7.12.

The fusion achieved slightly better results in the across-session analysis, especially in the case of the

Table 7.11: Average EID results obtained when conducting single modality and multimodality tests using the forearm ECG and BVP as input modalities.

Analysis	BVP	Forearm ECG	Fusion
WS-AT	28.78 ± 6.14	3.51 ± 2.41	4.67 ± 3.34
AS	65.58 ± 1.21	22.68 ± 1.32	43.48 ± 1.86

Table 7.12: Average EID results obtained when conducting single modality and multimodality tests using the forearm ECG modality with a combination of different fixed time windows.

Analysis	PQRST	QRS	PQRS	Fusion w/ QRS	Fusion w/ PQRS
WS-AT	2.93 ± 2.46	15.07 ± 3.88	7.47 ± 2.27	8.58 ± 2.95	6.20 ± 2.55
AS	22.66 ± 1.37	21.91 ± 1.6	8.04 ± 1.15	18.60 ± 1.18	7.95 ± 1.13

PQRS complex window, as shown in Table 7.12. Although not particularly significant, the results suggest that using a combination of different fixed time windows may yield an increase in the performance when the identity recognition is performed across-sessions. Although the forearm ECG modality presents a higher degree of discriminability when using a fixed time window that includes the PQRST complex, the use of QRS and PQRS complexes windows is more robust to changes with time. By combining these modalities, an increase in the performance can be achieved when the elapsed time between the enrollment and recognition phases is significant.

7.6 Benchmarking

Few biometric studies investigate the use of modalities such as the ECG and BVP in settings in which the noise contamination is significant. In most cases, the subjects are in a seated position, at rest, and without performing movements that can produce noise. Furthermore, most of the tests are conducted using data from a single session and that are collected from sites such as the fingertips and the hand palms. Given this, comparing the results achieved in this work with the research conducted is a difficult task. In [64], Pinto *et al* studied the implementation of a continuous biometric system based on the ECG signal collected at the hands in driving settings. They performed authentication and identification tests using excerpts of ECG recordings extracted from two trips of six drivers, acquired over a period of six days. They randomly selected two excerpts for each subject, each with duration of 169-367 seconds, from the two trips, and combined them in succession. The signal acquisition included periods of highway and city driving, driver swaps and idle periods, so the recordings presented a low quality. The best identification results were achieved using as features coefficients from the Haar wavelet transform combined with a SVM classifier (EID of 5.11%). In terms of authentication, the use of DCT coefficients combined with a SVM classifier and a user-tuned threshold led to a minimum EER of 2.66%. However, they did not mention the amount of signal that was effectively used during the driving settings to assert the performance in terms of user acceptability. Although they have achieved a performance in the identification and authentication tests similar to that obtained in studies conducted in medical settings, they provided results for a small number of subjects and used training

and test sets that contained more data than the tests performed in this thesis. Additionally, they merged data from different sessions to create the training and test sets.

Chapter 8

Conclusions

In this final chapter we summarize the work developed and give an overview of the results obtained. We also address the future work, defining guidelines for the next research steps.

8.1 Main Results

We explored the use of two physiological signals, the ECG and BVP, as biometric traits to perform identity recognition in a computer interaction setup, following a semi off-the-person approach. With this in mind, we devised a set of representative tasks that simulated the usual behavior of a user when using a computer in a work environment, and collected data for a group of subjects. Since active research is being developed in the area of multimodality to overcome the challenges faced by single modality approaches, we developed a fusion method based on the decisions produced by the single modality classifiers.

The BVP modality revealed an overall poor performance, even when performing within-session analysis. Although the BVP presents a lower discriminative capacity than the ECG counterpart, the significant amount of noise in the collected BVP data degrades considerably the performance. Considering the setup developed, with the BVP sensor attached on the index finger, the movements produced by the fingers severely contaminate the signal with motion artifacts, and removing this noise becomes a considerable challenge. The research developed in the field of BVP biometrics shows that this modality can be used as a biometric trait. However, most of the studies are conducted in controlled conditions, where the subjects are at rest and seated, and only within-session tests are performed. Considering the results obtained in this thesis, the BVP can be used to provide information regarding the heart rate and HRV, since the systolic peaks are well defined even if the wave is distorted by noise. Furthermore, the evaluation performed in terms of user acceptability showed that the amount of BVP signal available is larger than that of the ECG.

In the case of the ECG modality collected with the armrest, the use of the ECG as a biometric trait is limited, since the amount of signal effectively collected depends on the behavior of the user when interacting with the computer. Passive activities, such as reading and watching some content on the computer, can provide conditions for the acquisition of sufficient signal with a reasonable degree of quality and without

significant interruptions. The effective use of the system in other conditions, in which the user performs non-passive activities with the computer, depends significantly on the ability of the user to conform and adapt to the system. In the scenario where the users do not adapt to the system, the system can be used to assist other biometric system or, in an extreme case, ask the user to provide biometric data with a reasonable degree of quality.

The work conducted in this thesis lays the foundations for exploring off-the-person biometrics in a computer interaction setup. Further improvements, especially in terms of sensor development and integration, and implementation of robust denoising techniques and continuous authentication frameworks, must be investigated. To our knowledge there are currently no studies performed in similar conditions. The methodology developed was able to recognize a small set of individuals from signals acquired in a computer interaction setup and is a step towards robust continuous ECG and multimodality based biometrics.

8.2 Future Work

The work conducted in this thesis provides a basis for the study and development of a biometric system in a semi off-the-person approach integrated in a computer interaction setup. Further developments are described below:

Use more than one wave. Previous studies have shown that using the combined information of several waves leads to an increase in the performance of ECG-based biometrics [32]. This requires larger test time frames, but this does not constitute a problem in the context of continuous validation;

Validation using long term acquisitions. An additional validation of the biometric system based on tests performed using long term acquisitions (several hours, similar to a regular workday) is crucial to evaluate the performance of the system in a continuous authentication scenario;

Test other types of representation and classification methods. Explore other types of representation of the discriminative characteristics of the traits and collect more data such that the templates become more representative of the characteristics of those traits for each subject. This is an essential step to approach the problems faced in terms of trait permanence and HRV. Additionally, explore hierarchical strategies using different types of features or classification fusion based on different data representation for the same signal;

Study adaptive frameworks. Investigate adaptive strategies that continuously change the gallery of templates associated with each subject to reflect the changes in the short and long terms;

Explore more effective denoising approaches. Study and implement noise removal approaches that are more effective, such as model-based techniques;

Improvement of the performance of the BVP modality. Test other sites for the acquisition of the BVP signal that are less affected by noise, such as the neck [98] and earlobe [90] [41]. Additionally, investigate the use of HRV as biometric trait, which can be easily extracted from the BVP acquired with the wristlet. Although the HRV has been actively studied by the medical research community to predict and diagnose several diseases, for example, its use in the field of biometrics has yet to be effectively explored [6];

Improvement of the armrest module. Develop new iterations of the armrest following the feedback given by the subjects and the accumulated experience.

Appendix A

Tools

The work developed in this thesis was accomplished using a group of software tools, both for the writing of the thesis and for the scientific computation.

Most of the tools used are Open Source software, and we thank the community for providing the tools to perform scientific work in an open platform.

A.1 Thesis Writing

The writing of the thesis was accomplished using the \LaTeX environment and using the editor *TeXstudio*. When conducting research on the literature, *Google Scholar* was the main tool for accessing studies and articles.

A.2 Scientific Computation

The main tool used for coding was the *Python* environment and *PyCharm* was used as IDE. The *Python* modules used include *matplotlib*, *numpy*, *biosppy*, *scikit-learn*, *seaborn* and *scipy*. The software *OpenSignals* was used as a complementary visualization tool of the data acquired in real-time, mostly used in the beginning of the work, since we then developed a real-time plotting application in *Python* to visualize the acquisition during the experiment performed using modules that include *PyQtGraph*.

Appendix B

Acquisition System and Experimental Setup

This appendix contains information related to the experimental setup and protocol followed.

B.1 Interface of the Signal Acquisition Application

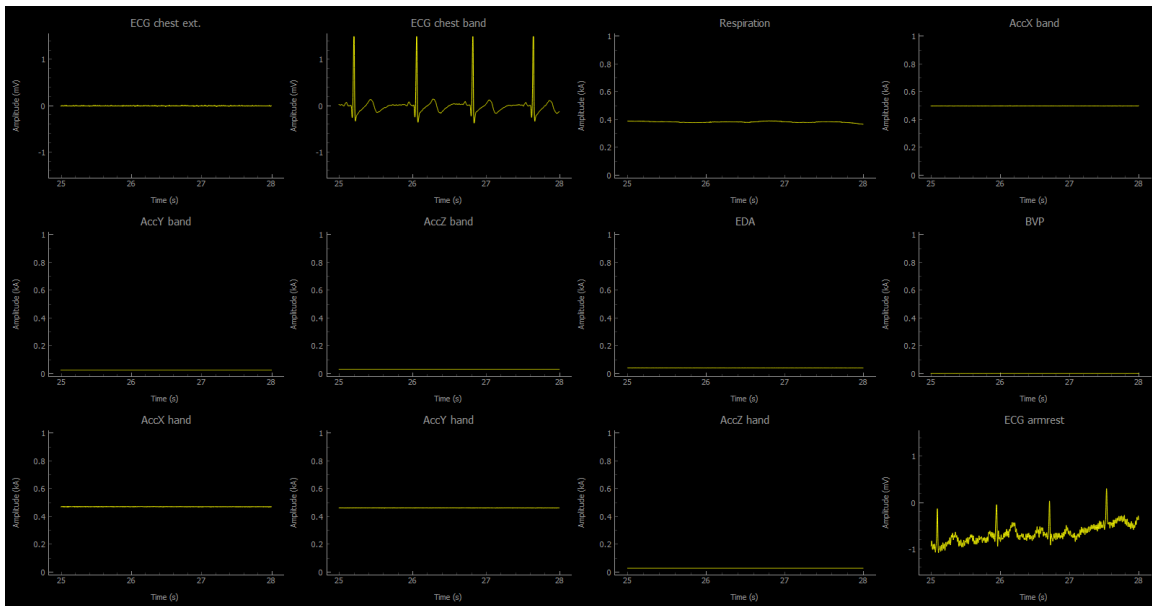


Figure B.1: Real-time plots produced by the application.

B.2 Text Associated with the Task Typing 1

There is a crime here that goes beyond denunciation. There is a sorrow here that weeping cannot symbolize. There is a failure here that topples all our success. The people come with nets to fish for potatoes in the river, and the guards hold them back. And they stand still and watch the potatoes float by, listen to the screaming pigs being killed in a ditch and covered with quick-lime, watch the mountains of oranges slop down to a putrefying ooze; and in the eyes of people there is the failure; and in the eyes of the hungry there is a growing wrath. In the souls of the people grapes of wrath. In the souls of the people the grapes of wrath are filling and growing heavy, growing heavy for the vintage.

Figure B.2: Excerpt used in task Typing 1 taken from *Grapes of Wrath*, Steinbeck [83].

B.3 Informed Consent Form

Informed Consent Form

We are performing a study on **biometric recognition** based on the fusion of two biosignals.

Your participation in our study is fundamental to help expand the knowledge in the field.

<http://www.it.pt>

★★★★★

Sensors Data Results +You more ►

Materials

A differential electrocardiography (ECG) sensor will be used for data acquisition at the hands and forearms.

Another differential ECG sensor will be used for data acquisition at the torso.

A blood volume pulse sensor (BVP) will be used for data acquisition at the base of the index finger (proximal phalanx).

An electrodermal activity sensor (EDA) will be used for data acquisition at the wrist.

Conductive fabrics will be used as electrodes to acquire the ECG on the hands and forearms and are placed on an [armrest](#).

A computer will be used to [record the data](#).

Sensors more ▼

Objectives

Assess the quality of [ECG](#), [BVP](#) and [EDA](#) signals at the referred acquisition sites when the user interacts with a computer setup.

Evaluate [signal processing algorithms](#) used for biometric recognition with ECG data collected in a heart rate varying context.

Study of continuous user authentication through physiological multimodality (ECG/BVP).

Build a [non-intrusive](#) and [semi off-the-person](#) database.

Design an adaptive system to continuously [authenticate](#) and [monitor](#) the user in a computer setup of a work environment.

Results more ▼

Methods

All sensors have a [non-intrusive placement](#).

All sensors only have a [measurement function](#).

All acquired signals will be used [anonimously](#).

You can decide to interrupt the study at anytime.

Data more ▲

About You

Name: _____

E-Mail: _____ Age: _____

+You more ►

Thanks!

We greatly appreciate your time and support.

If you have additional questions about the study contact us:

mig.js.martinho@gmail.com | afred@lx.it.pt

more ▼

Signature

I acknowledge to have been informed about this study and accept to participate as a volunteer:

____ / ____ / ____

Notes and Comments

Questionnaire

On a mark of 1-5, how would you rate:

Comfort resting the forearms on the armrest.
(1 - very uncomfortable, 5 - very comfortable)

Comfort using the wristlet.
(1 - very uncomfortable, 5 - very comfortable)

Change in your behavior in a computer setup given the use of the armrest and wristlet.
(1 - no change, 5 - significant change)

Figure B.3: Informed consent form and questionnaire about user satisfaction given to the subjects involved in the experiment.

Appendix C

Additional Results

In this appendix, additional results regarding the set of performance evaluation tests conducted are presented.

C.1 Test Protocol

Table C.1: Data collected for each subject in each task and session and elapsed time between sessions. a, b, c and d refer to the acquisition of forearm ECG, BVP, chest ECG and collar bones ECG, respectively. Those tasks where no acquisition was performed are marked with an x.

Subject	Session 1				Session 2				Elapsed time (days)
	1	2	3	4	1	2	3	4	
0	a,b,c	a,b,c	a,b,c	a,b,c	a,b,c	a,b,c	a,b,c	a,b,c	75
1	a,b,c	a,b,c	a,b,c	a,b,c	a,b,c,d	a,b,c,d	a,b,c,d	a,b,c,d	63
2	a,b,c	a,b,c	a,b,c	a,b,c	-	-	-	-	-
3	a,b,c	a,b,c	a,b,c	a,b,c	a,b,c	a,b,c	x	a,b,c	53
4	a,b,c	a,b,c	a,b,c	a,b,c	a,b,c	a,b,c	a,b,c	a,b,c	26
5	a,b,c,d	a,b,c,d	a,b,c,d	a,b,c,d	-	-	-	-	-
6	a,b,c	a,b,c	a,b,c	a,b,c	-	-	-	-	-
7	a,b,c,d	a,b,c,d	a,b,c,d	a,b,c,d	a,b,c,d	a,b,c,d	a,b,c,d	a,b,c,d	41
8	a,b,c,d	a,b,c,d	a,b,c,d	a,b,c,d	a,b,c,d	a,b,c,d	a,b,c,d	a,b,c,d	3
9	a,b,c,d	a,b,c,d	a,b,c,d	a,b,c,d	a,b,c,d	a,b,c,d	a,b,c,d	a,b,c,d	18
10	a,b,c	a,b,c	a,b,c	a,b,c	a,b,c,d	a,b,c,d	a,b,c,d	a,b,c,d	47
11	a,b,c	a,b,c	a,b,c	a,b,c	a,b,c,d	a,b,c,d	a,b,c,d	a,b,c,d	43
12	a,b,c	a,b,c	a,b,c	a,b,c	a,b,c,d	a,b,c,d	a,b,c,d	a,b,c,d	49
13	a,b,c	a,b,c	a,b,c	a,b,c	a,b,c,d	a,b,c,d	a,b,c,d	a,b,c,d	67
14	a,b,c	a,b,c	a,b,c	x	a,b,c	a,b,c	a,b,c	a,b,c	64
15	a,b,c	a,b,c	a,b,c	a,b,c	a,b,c	a,b,c	a,b,c	a,b,c	50
16	a,b,c,d	a,b,c,d	a,b,c,d	a,b,c,d	a,b,c,d	a,b,c,d	a,b,c,d	a,b,c,d	22
17	a,b,c	a,b,c	a,b,c	a,b,c	a,b,c,d	a,b,c,d	a,b,c,d	a,b,c,d	76

18	a,b,c	46								
19	a,b,c	a,b,c	a,b,c	a,b,c	a,b,c,d	a,b,c,d	a,b,c,d	a,b,c,d	a,b,c,d	73
20	a,b,c,d	41								
21	a,b,c	a,b,c	a,b,c	a,b,c	a,b,c,d	a,b,c,d	a,b,c,d	a,b,c,d	a,b,c,d	58
22	a,b,c	a,b,c	a,b,c	a,b,c	a,b,c,d	a,b,c,d	a,b,c,d	a,b,c,d	a,b,c,d	49
23	a,b,c	a,b,c	a,b,c	a,b,c	a,b,c,d	a,b,c,d	a,b,c,d	a,b,c,d	a,b,c,d	77
24	a,b,c	a,b,c	a,b,c	a,b,c	a,b,c,d	a,b,c,d	a,b,c,d	a,b,c,d	a,b,c,d	53
25	a,b,c	42								
26	a,b,c	a,b,c	a,b,c	x	a,b,c,d	a,b,c,d	a,b,c,d	a,b,c,d	a,b,c,d	57
27	a,b,c	2								
28	a,b,c	a,b,c	a,b,c	a,b,c	a,b,c,d	a,b,c,d	a,b,c,d	a,b,c,d	a,b,c,d	59
29	a,b,c	61								
30	a,b,c	a,b,c	a,b,c	a,b,c	a,b,c,d	a,b,c,d	a,b,c,d	a,b,c,d	a,b,c,d	26
31	a,b,c	a,b,c	a,b,c	a,b,c	a,b,c,d	a,b,c,d	a,b,c,d	a,b,c,d	a,b,c,d	61
32	a,b,c	a,b,c	a,b,c	a,b,c	a,b,c,d	a,b,c,d	a,b,c,d	a,b,c,d	a,b,c,d	76
33	a,b,c	a,b,c	a,b,c	a,b,c	a,b,c,d	a,b,c,d	a,b,c,d	a,b,c,d	a,b,c,d	63
34	a,b,c,d	87								
35	a,b,c,d	a,b,c,d	a,b,c,d	a,b,c,d	-	-	-	-	-	-
36	a,b,c	a,b,c	a,b,c	x	a,b,c	a,b,c	a,b,c	a,b,c	a,b,c	67
37	a,b,c	a,b,c	a,b,c	a,b,c	-	-	-	-	-	-
38	a,b,c	a,b,c	a,b,c	a,b,c	a,b,c,d	a,b,c,d	a,b,c,d	a,b,c,d	a,b,c,d	50
39	a,b,c,d	14								
40	a,b,c,d	28								
41	a,b,c,d	a,b,c,d	a,b,c,d	a,b,c,d	-	-	-	-	-	-
42	a,b,c,d	a,b,c,d	a,b,c,d	a,b,c,d	-	-	-	-	-	-
43	a,b,c,d	42								
44	a,b,c,d	a,b,c,d	a,b,c,d	a,b,c,d	-	-	-	-	-	-
45	a,b,c,d	a,b,c,d	a,b,c,d	a,b,c,d	-	-	-	-	-	-
46	a,b,c,d	a,b,c,d	a,b,c,d	a,b,c,d	-	-	-	-	-	-
47	a,b,c,d	a,b,c,d	a,b,c,d	a,b,c,d	-	-	-	-	-	-
48	a,b,c,d	41								
49	a,b,c,d	a,b,c,d	a,b,c,d	a,b,c,d	-	-	-	-	-	-
50	a,b,c,d	a,b,c,d	a,b,c,d	a,b,c,d	-	-	-	-	-	-
51	a,b,c,d	a,b,c,d	a,b,c,d	a,b,c,d	-	-	-	-	-	-
52	a,b,c,d	a,b,c,d	a,b,c,d	a,b,c,d	-	-	-	-	-	-

C.2 User Acceptability

Table C.2: Information regarding the number of waves extracted and waves accepted as valid after outlier removal for the total population in the first session using a fixed time window segmentation. The symbols indicated over each column correspond to the following: Mean - average number of waves across the population; Std - standard deviation of the number of waves across the population; Median - median of waves across the population; IQR - interquartile range; Q1 - first quartile; Q3 - third quartile, Max - maximum number of waves per subject in the population; Min - minimum number of waves per subject in the population.

Task	Modality	Total number of waves	Mean	Std	Median	IQR	Q1	Q3	Max	Min
Idle	BVP	Detected	145.774	26.273	144	30	130	160	213	98
		Valid	124.245	25.7	123	30	108	138	203	63
	Forearm ECG	Detected	144.76	26.523	145.5	32.5	126.5	159	214	92
		Valid	125.76	24.463	126	26.75	110.25	137	194	72
	Chest ECG	Detected	146.25	28.176	145.5	34.75	125.5	160.25	215	91
		Valid	131.115	26.397	126.5	29.25	113.75	143	205	71
Typing 1	BVP	Detected	313.472	74.303	314	89	263	352	539	170
		Valid	136.283	89.393	110	137	69	206	373	31
	Forearm ECG	Detected	329.12	86.685	328.5	120.75	266.25	387	573	165
		Valid	82.82	81.583	64	105.25	18.25	123.5	344	1
	Chest ECG	Detected	343.269	102.015	334	120	286	406	612	156
		Valid	307.308	98.964	299.5	133.25	240.75	374	547	135
Touch pad	BVP	Detected	139.453	48.973	138	62	106	168	263	51
		Valid	93.604	42.08	93	58	65	123	169	3
	Forearm ECG	Detected	137.46	51.409	135.5	60.5	106.5	167	267	45
		Valid	69.1	44.479	68	58.5	35.85	93.75	193	1
	Chest ECG	Detected	141.019	51.46	146	67.25	104.5	171.75	285	52
		Valid	126.365	48.594	122.5	65.75	88	153.75	271	49
Typing 2	BVP	Detected	206.88	32.753	207	43	185.75	228.75	280	134
		Valid	80.86	48.96	67.5	87.5	37.5	125	188	12
	Forearm ECG	Detected	227.383	28.032	228	38.5	206.5	245	291	168
		Valid	53.478	45.288	45	66.5	10.5	77	186	1
	Chest ECG	Detected	233.66	45.484	231.5	55.5	204	259.5	398	142
		Valid	206.56	46.592	209	38.75	185.25	224	312	17

Table C.3: Information regarding the duration of the signal acquisitions in the first session using a fixed time window segmentation. The obtained values relate to the total duration of each acquisition, and the corresponding duration associated with the waves extracted before and after outlier removal. The symbols indicated over each column correspond to the following: Mean - average acquisition duration across the population; Std - standard deviation of the acquisition duration across the population; Median - median of acquisition duration across the population; IQR - interquartile range; Q1 - first quartile; Q3 - third quartile, Max - maximum acquisition duration per subject in the population; Min - minimum acquisition duration per subject in the population.

Task	Modality	Duration(s)	Mean	Std	Median	IQR	Q1	Q3	Max	Min
Idle	BVP	Total	119.547	2.484	120	0	120	120	120	103
		Detected	119.019	2.553	119.542	0.596	119.211	119.807	120	102.241
		Valid	101.563	11.312	102.478	15.237	95.528	110.765	118.806	65.118
	Forearm ECG	Total	119.52	2.555	120	0	120	120	120	103
		Detected	118.508	2.856	119.303	0.645	118.946	119.591	120	101.554
		Valid	104.026	11.705	107.501	14.992	97.27	112.263	119.013	70.755
	Chest ECG	Total	119.538	2.507	120	0	120	120	120	103
		Detected	118.855	2.669	119.338	0.502	119.105	119.607	120	101.601
		Valid	107.074	8.162	108.505	12.152	102.11	114.262	116.683	86.793
Typing 1	BVP	Total	265.749	54.989	262	76	224	300	402.6	166.6
		Detected	264.736	55.083	259.889	75.819	223.5	299.319	402.77	166.429
		Valid	108.512	63.693	88.662	79.973	59.726	139.699	292.434	26.944
	Forearm ECG	Total	264.894	56.332	259.25	78.175	221.375	299.55	402.6	166.6
		Detected	263.932	56.254	258.856	78.637	219.963	298.6	401.436	165.191
		Valid	68.297	64.37	51.089	86.92	15.617	102.537	244.764	0.661
	Chest ECG	Total	265.304	55.384	261.75	77.525	223.125	300.65	402.6	166.6
		Detected	264.464	55.378	260.584	77.408	222.877	300.285	402.087	165.185
		Valid	238.234	58.431	233.76	90.147	193.359	283.506	378.28	98.305
Touch pad	BVP	Total	115.372	45.842	110.5	49.9	84.5	134.4	257.5	48.6
		Detected	114.596	45.839	110.541	48.248	84.016	132.264	257.134	48.027
		Valid	74.51	33.361	77.874	45.11	51.551	96.661	141.415	2.619
	Forearm ECG	Total	115.586	46.483	111.75	51.2	82.85	134.05	257.5	48.6
		Detected	114.366	46.619	110.751	52.23	81.389	133.619	256.166	47.315
		Valid	57.824	38.301	57.077	46.609	31.155	77.764	192.372	0.896
	Chest ECG	Total	115.294	46.277	110.5	50.675	83.875	134.55	257.5	48.6
		Detected	114.614	46.36	110.056	50.896	83.377	134.274	256.812	47.948
		Valid	103.767	44.634	98.864	55.449	69.967	125.416	235.045	44.737
Typing 2	BVP	Total	179.956	5.603	180	0	180	180	180	151.5
		Detected	179.301	5.753	179.584	0.757	179.19	179.948	179.985	150.52
		Valid	65.745	35.743	50.593	59.043	36.644	95.687	143.012	10.31
	Forearm ECG	Total	180	3.998	180	0	180	180	180	177.2
		Detected	179.411	4.348	179.159	1.065	178.508	179.573	179.677	172.686
		Valid	43.691	36.096	39.199	59.988	8.517	68.505	128.046	0.796
	Chest ECG	Total	179.976	5.503	180	0	180	180	180	152.5
		Detected	179.214	5.684	179.326	0.585	179.084	179.669	179.781	150.487
		Valid	159.121	23.786	163.407	16.48	153.958	170.438	179.067	15.062

C.3 Identification Results: Single Modalities

C.3.1 Averaging and ECG Cutoff Frequency

Additional results are shown below regarding the averaging of m consecutive waves, with $m = 1, 2, \dots, 15$, for the WS-WT and AS analyses. Each group of m consecutive waves was replaced by the corresponding mean wave in both training and test sets. The results are presented for two types of segmentation: fixed time window and heart rate based resampling. For the ECG modalities, the results are also presented for the two cutoff frequencies used in the denoising step. Figures C.1 and C.2 show the results for the WS-WT and AS analyses, respectively.

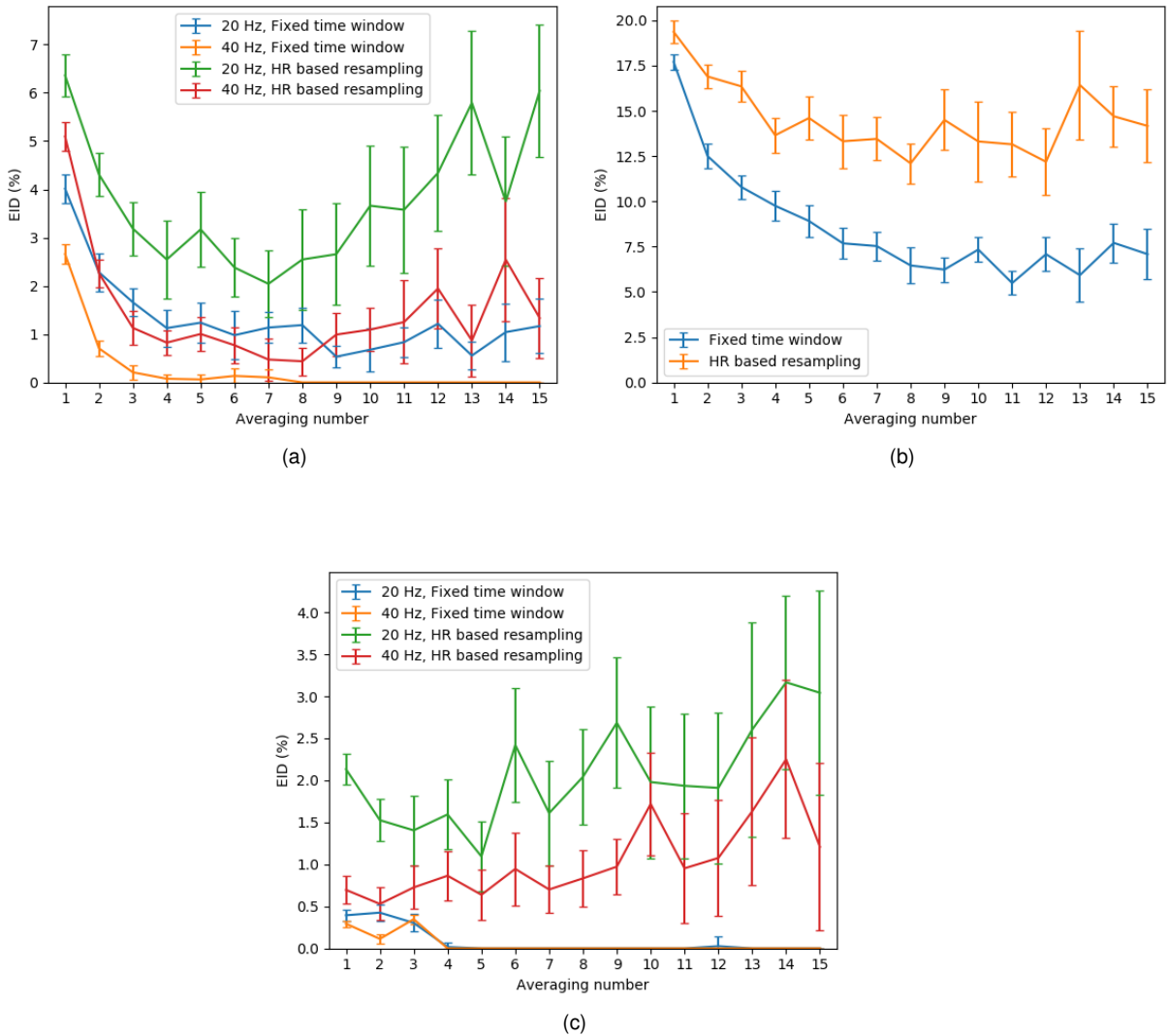


Figure C.1: Identification results of averaging consecutive waves when performing WS-WT analysis for the (a) forearm ECG, (b) BVP and (c) chest ECG modalities.

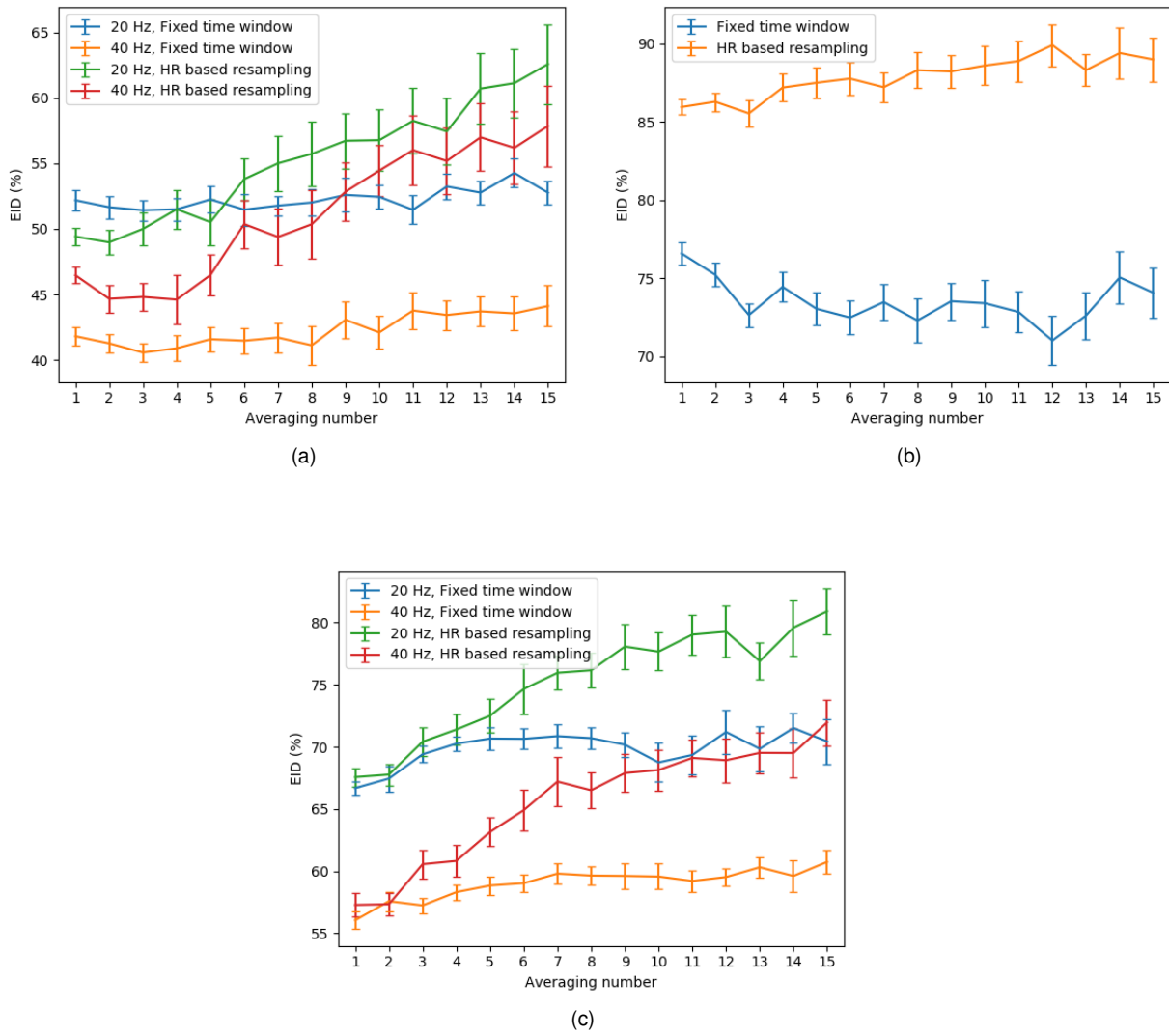


Figure C.2: Identification results of averaging consecutive waves when performing AS analysis for the (a) forearm ECG, (b) BVP and (c) chest ECG modalities.

C.3.2 Comparison Between Tasks

Table C.4: Average EID results obtained for each activity when conducting an WS-AT analysis using the heart rate based resampling segmentation.

Task	Session 1			Session 2		
	BVP	Forearm ECG	Chest ECG	BVP	Forearm ECG	Chest ECG
Sx.2	62.08±3.52	25.93±6.49	5.31±0.37	57.93±10.28	12.07±4.12	1.27±0.2
Sx.3	28.56±3.52	9.58±3.01	5.91±0.84	33.06±2.42	14.1±4.13	13.58±0.48
Sx.4	63.91±4.13	15.83±4.95	8.03±0.85	64.67±10.14	16.73±6.67	10.52±0.39

Table C.5: Average EID results obtained for each activity when conducting an AS analysis using the heart rate based resampling segmentation.

Task	Session 1			Session 2		
	BVP	Forearm ECG	Chest ECG	BVP	Forearm ECG	Chest ECG
Sx.1	87.59±1.53	32.58±1.7	49.92±0.87	79.26±1.96	37.51±2.17	61.16±0.48
Sx.2	83.67±7.18	43.63±5.15	56.73±0.81	84.08±2.61	55.33±9.01	62.73±0.41
Sx.3	81.26±2.72	27.33±4.95	52.45±1.19	80.81±2.56	49.2±4.24	68.3±0.89
Sx.4	80.47±5.78	46.93±7.46	53.99±0.97	85.12±2.19	53.03±6.18	63.73±1.33

C.4 Authentication Results

Table C.6: Average global EER results obtained when conducting WS-WT and AS analyses using the heart rate based resampling segmentation.

Test sets	BVP	Forearm ECG	Chest ECG
S1.2	23.38±1.09	13.27±4.59	5.2±0.21
S1.3	7.86±1.05	5.28±1.05	5.11±0.33
S1.4	23.34±1.69	6.29±1.06	9.57±0.61
S2.1	29.54±0.97	16.02±0.55	35.49±0.21

References

- [1] Bosphorus Database. <http://bosphorus.ee.boun.edu.tr/>. Accessed: 2018-02-9.
- [2] Foteini Agrafioti, Francis M Bui, and Dimitrios Hatzinakos. Medical biometrics: The perils of ignoring time dependency. In *Biometrics: Theory, Applications, and Systems, 2009. BTAS'09. IEEE 3rd International Conference on*, pages 1–6. IEEE, 2009.
- [3] Foteini Agrafioti, Jiexin Gao, and Dimitrios Hatzinakos. Heart biometrics: Theory, methods and applications. In *Biometrics*. InTech, 2011.
- [4] Foteini Agrafioti and Dimitrios Hatzinakos. ECG based recognition using second order statistics. In *Communication Networks and Services Research Conference, 2008. CNSR 2008. 6th Annual*, pages 82–87. IEEE, 2008.
- [5] Foteini Agrafioti and Dimitrios Hatzinakos. Fusion of ECG sources for human identification. In *Communications, Control and Signal Processing, 2008. ISCCSP 2008. 3rd International Symposium on*, pages 1542–1547. IEEE, 2008.
- [6] Nazneen Akhter, Sumegh Tharewal, Vijay Kale, Ashish Bhalerao, and KV Kale. Heart-Based Biometrics and Possible Use of Heart Rate Variability in Biometric Recognition Systems. In *Advanced Computing and Systems for Security*, pages 15–29. Springer, 2016.
- [7] Osamah Al-Hamdani, Ali Chekima, Jamal Dargham, Sh-Hussain Salleh, Fuad Noman, Hadri Hussain, A Ariff, and A Mohd Noor. Multimodal biometrics based on identification and verification system. *Journal of Biometrics & Biostatistics*, 4(2):1–8, 2013.
- [8] John Allen. Photoplethysmography and its application in clinical physiological measurement. *Physiological measurement*, 28(3):R1, 2007.
- [9] HC Bazett. An Analysis of the Time-relation of Electrocardiograms. *Annals of Noninvasive Electocardiology*, 2(2):177–194, 1997.
- [10] Lena Biel, Ola Pettersson, Lennart Philipson, and Peter Wide. ECG analysis: a new approach in human identification. In *Instrumentation and Measurement Technology Conference, 1999. IMTC/99. Proceedings of the 16th IEEE*, volume 1, pages 557–561. IEEE, 1999.

- [11] Battista Biggio and Fabio Roli. Wild Patterns: Ten Years After the Rise of Adversarial Machine Learning. *arXiv preprint arXiv:1712.03141*, 2017.
- [12] University of Toronto Biometrics Security Lab. BioSec PPG Dataset. http://www.comm.utoronto.ca/~biometrics/PPG_Dataset/data_desc.html. Accessed: 2018-02-8.
- [13] Marcin D Bugdol and Andrzej W Mitas. Multimodal biometric system combining ECG and sound signals. *Pattern Recognition Letters*, 38:107–112, 2014.
- [14] Samik Chakraborty and Saurabh Pal. Photoplethysmogram signal based biometric recognition using linear discriminant classifier. In *Control, Instrumentation, Energy & Communication (CIEC), 2016 2nd International Conference on*, pages 183–187. IEEE, 2016.
- [15] Adrian DC Chan, Mohyeldin M Hamdy, Armin Badre, and Vesal Badee. Wavelet distance measure for person identification using electrocardiograms. *IEEE transactions on instrumentation and measurement*, 57(2):248–253, 2008.
- [16] Ivaylo I Christov. Real time electrocardiogram QRS detection using combined adaptive threshold. *Biomedical engineering online*, 3(1):28, 2004.
- [17] Gari D Clifford, Francisco Azuaje, and P McSharry. Advanced methods and tools for ECG data analysis, 2006.
- [18] David Pereira Coutinho, Ana LN Fred, and Mário AT Figueiredo. ECG-based Continuous Authentication System using Adaptive String Matching. In *Biosignals*, pages 354–359, 2011.
- [19] Hugo Plácido da Silva, José Guerreiro, André Lourenço, Ana LN Fred, and Raúl Martins. BITalino: A Novel Hardware Framework for Physiological Computing. In *PhyCS*, pages 246–253. Citeseer, 2014.
- [20] Hugo Plácido Da Silva, André Lourenço, Ana Fred, Nuno Raposo, and Marta Aires-de Sousa. Check Your Biosignals Here: A new dataset for off-the-person ECG biometrics. *Computer methods and programs in biomedicine*, 113(2):503–514, 2014.
- [21] Philip De Chazal, Maria O’Dwyer, and Richard B Reilly. Automatic classification of heartbeats using ECG morphology and heartbeat interval features. *IEEE transactions on biomedical engineering*, 51(7):1196–1206, 2004.
- [22] Willem Einthoven. Ueber die Form des menschlichen Electrocardiogramms. *Pflügers Archiv European Journal of Physiology*, 60(3):101–123, 1895.
- [23] World Famous Electronics. BVP sensor datasheet. https://cdn.shopify.com/s/files/1/0100/6632/files/Pulse_Sensor_Data_Sheet.pdf?14358792549038671331. Accessed: 2018-02-10.

- [24] Mohamed Elgendi. On the analysis of fingertip photoplethysmogram signals. *Current cardiology reviews*, 8(1):14–25, 2012.
- [25] Mohamed Elgendi, Ian Norton, Matt Brearley, Derek Abbott, and Dale Schuurmans. Systolic peak detection in acceleration photoplethysmograms measured from emergency responders in tropical conditions. *PLoS One*, 8(10):e76585, 2013.
- [26] Shih-Chin Fang and Hsiao-Lung Chan. Human identification by quantifying similarity and dissimilarity in electrocardiogram phase space. *Pattern Recognition*, 42(9):1824–1831, 2009.
- [27] Shih-Chin Fang and Hsiao-Lung Chan. QRS detection-free electrocardiogram biometrics in the reconstructed phase space. *Pattern Recognition Letters*, 34(5):595–602, 2013.
- [28] Mike Folk, Gerd Heber, Quincey Koziol, Elena Pourmal, and Dana Robinson. An overview of the HDF5 technology suite and its applications. In *Proceedings of the EDBT/ICDT 2011 Workshop on Array Databases*, pages 36–47. ACM, 2011.
- [29] Antonio Fratini, Mario Sansone, Paolo Bifulco, and Mario Cesarelli. Individual identification via electrocardiogram analysis. *Biomedical engineering online*, 14(1):78, 2015.
- [30] Ana LN Fred and Anil K Jain. Combining multiple clusterings using evidence accumulation. *IEEE transactions on pattern analysis and machine intelligence*, 27(6):835–850, 2005.
- [31] LS Fridericia. The duration of systole in an electrocardiogram in normal humans and in patients with heart disease. *Annals of Noninvasive Electrocardiology*, 8(4):343–351, 2003.
- [32] Hugo Gamboa. *Multi-modal behavioral biometrics based on HCI and electrophysiology*. PhD thesis, PhD thesis, Universidade Técnica de Lisboa, Instituto Superior Técnico, 2008.
- [33] Hugo Gamboa and Ana Fred. A behavioral biometric system based on human-computer interaction. In *Biometric Technology for Human Identification*, volume 5404, pages 381–393. International Society for Optics and Photonics, 2004.
- [34] Ary L Goldberger, Luis AN Amaral, Leon Glass, Jeffrey M Hausdorff, Plamen Ch Ivanov, Roger G Mark, Joseph E Mietus, George B Moody, Chung-Kang Peng, and H Eugene Stanley. Physiobank, physiotoolkit, and physionet. *Circulation*, 101(23):e215–e220, 2000.
- [35] Mouhcine Guennoun, Najoua Abbad, Jonas Talom, Sk Md Mizanur Rahman, and Khalil El-Khatib. Continuous authentication by electrocardiogram data. In *Science and Technology for Humanity (TIC-STH), 2009 IEEE Toronto international conference*, pages 40–42. IEEE, 2009.
- [36] Pat Hamilton. Open source ECG analysis. In *Computers in Cardiology, 2002*, pages 101–104. IEEE, 2002.

- [37] Anil K Jain, Sarat C Dass, and Karthik Nandakumar. Can soft biometric traits assist user recognition? In *Biometric Technology for Human Identification*, volume 5404, pages 561–573. International Society for Optics and Photonics, 2004.
- [38] Anil K Jain, Karthik Nandakumar, and Arun Ross. 50 years of Biometric Research: Accomplishments, challenges, and opportunities. *Pattern Recognition Letters*, 79:80–105, 2016.
- [39] Anil K Jain, Arun Ross, and Sharath Pankanti. Biometrics: a tool for information security. *IEEE transactions on information forensics and security*, 1(2):125–143, 2006.
- [40] Anil K Jain, Arun A Ross, and Karthik Nandakumar. *Introduction to Biometrics*. Springer Science & Business Media, 2011.
- [41] Gu-Young Jeong, Kee-Ho Yu, and Nam-Gyun Kim. Continuous blood pressure monitoring using pulse wave transit time. *measurement*, 4(7), 2005.
- [42] A Reşit Kavsaoglu, Kemal Polat, and M Recep Bozkurt. A novel feature ranking algorithm for biometric recognition with PPG signals. *Computers in biology and medicine*, 49:1–14, 2014.
- [43] Ibrahim Khalil and Fahim Sufi. Legendre polynomials based biometric authentication using QRS complex of ECG. In *Intelligent Sensors, Sensor Networks and Information Processing, 2008. ISSNIP 2008. International Conference on*, pages 297–302. IEEE, 2008.
- [44] Sander Koelstra, Christian Muhl, Mohammad Soleymani, Jong-Seok Lee, Ashkan Yazdani, Touradj Ebrahimi, Thierry Pun, Anton Nijholt, and Ioannis Patras. Deap: A database for emotion analysis; using physiological signals. *IEEE Transactions on Affective Computing*, 3(1):18–31, 2012.
- [45] Samaneh Kouchaki, Adeleh Dehghani, Sara Omranian, and Reza Boostani. ECG-based personal identification using empirical mode decomposition and Hilbert transform. In *Artificial Intelligence and Signal Processing (AISP), 2012 16th CSI International Symposium on*, pages 569–573. IEEE, 2012.
- [46] Ruggero Donida Labati, Vincenzo Piuri, Roberto Sassi, Fabio Scotti, and Gianluca Sforza. Adaptive ECG biometric recognition: a study on re-enrollment methods for QRS signals. In *Computational Intelligence in Biometrics and Identity Management (CIBIM), 2014 IEEE Symposium on*, pages 30–37. IEEE, 2014.
- [47] Ruggero Donida Labati, Roberto Sassi, and Fabio Scotti. ECG biometric recognition: Permanence analysis of QRS signals for 24 hours continuous authentication. In *Information Forensics and Security (WIFS), 2013 IEEE International Workshop on*, pages 31–36. IEEE, 2013.
- [48] Xiaoming Liu, Tsuhan Chen, and Susan M Thornton. Eigenspace updating for non-stationary process and its application to face recognition. *Pattern Recognition*, 36(9):1945–1959, 2003.

- [49] Justin Leo Cheang Loong, Khazaimatol S Subari, Rosli Besar, and Muhammad Kamil Abdullah. A new approach to ECG biometric systems: a comparative study between LPC and WPD systems. *World Acad Sci Eng Technol*, 68:759–64, 2010.
- [50] André Lourenço, Carlos Carreiras, Hugo Silva, and Ana Fred. ECG biometrics: A template selection approach. In *Medical Measurements and Applications (MeMeA), 2014 IEEE International Symposium on*, pages 1–6. IEEE, 2014.
- [51] André Lourenço, Hugo Silva, Carlos Carreiras, et al. Outlier detection in non-intrusive ECG biometric system. In *International Conference Image Analysis and Recognition*, pages 43–52. Springer, 2013.
- [52] André Lourenço, Hugo Silva, and Ana Fred. Unveiling the biometric potential of finger-based ECG signals. *Computational intelligence and neuroscience*, 2011:5, 2011.
- [53] André Lourenço, Hugo Silva, Paulo Leite, Renato Lourenço, and Ana LN Fred. Real Time Electrocardiogram Segmentation for Finger based ECG Biometrics. In *Biosignals*, pages 49–54, 2012.
- [54] Jaakko Malmivuo and Robert Plonsey. *Bioelectromagnetism: principles and applications of bioelectric and biomagnetic fields*. Oxford University Press, USA, 1995.
- [55] Patrick E McSharry, Gari D Clifford, Lionel Tarassenko, and Leonard A Smith. A dynamical model for generating synthetic electrocardiogram signals. *IEEE transactions on biomedical engineering*, 50(3):289–294, 2003.
- [56] Julie Mennell and Ian Shaw. The future of forensic and crime scene science: Part I. A UK forensic science user and provider perspective. *Forensic Science International*, 157:S7–S12, 2006.
- [57] Ikenna Odinaka, Po-Hsiang Lai, Alan D Kaplan, Joseph A O’Sullivan, Erik J Sirevaag, Sean D Kristjansson, Amanda K Sheffield, and John W Rohrbaugh. ECG biometrics: A robust short-time frequency analysis. In *Information forensics and security (wifs), 2010 ieee international workshop on*, pages 1–6. IEEE, 2010.
- [58] Ikenna Odinaka, Po-Hsiang Lai, Alan D Kaplan, Joseph A O’Sullivan, Erik J Sirevaag, and John W Rohrbaugh. ECG biometric recognition: A comparative analysis. *IEEE Transactions on Information Forensics and Security*, 7(6):1812–1824, 2012.
- [59] University of Nottingham. Cardiology Teaching Package. <https://www.nottingham.ac.uk/nursing/practice/resources/cardiology/function/index.php>. Accessed: 2018-04-25.
- [60] Lawrence O’Gorman. Comparing passwords, tokens, and biometrics for user authentication. *Proceedings of the IEEE*, 91(12):2021–2040, 2003.
- [61] Sharath Pankanti, Ruud M Bolle, and Anil Jain. Biometrics: The future of identification. *Computer*, 33(2):46–49, 2000.

- [62] Erik Peper, Rick Harvey, I-Mei Lin, Hana Tylova, and Donald Moss. Is there more to blood volume pulse than heart rate variability, respiratory sinus arrhythmia, and cardiorespiratory synchrony? *Biofeedback*, 35(2), 2007.
- [63] Koksoon Phua, Jianfeng Chen, Tran Huy Dat, and Louis Shue. Heart sound as a biometric. *Pattern Recognition*, 41(3):906–919, 2008.
- [64] João Ribeiro Pinto, Jaime S Cardoso, André Lourenço, and Carlos Carreiras. Towards a Continuous Biometric System Based on ECG Signals Acquired on the Steering Wheel. *Sensors*, 17(10):2228, 2017.
- [65] Konstantinos N Plataniotis, Dimitrios Hatzinakos, and Jimmy KM Lee. ECG biometric recognition without fiducial detection. In *Biometric Consortium Conference, 2006 Biometrics Symposium: Special Session on Research at the*, pages 1–6. IEEE, 2006.
- [66] PLUX. Accelerometer sensor datasheet. http://bitalino.com/datasheets/ACC_Sensor_Datasheet.pdf. Accessed: 2018-02-10.
- [67] PLUX. BITalino board datasheet. http://bitalino.com/datasheets/BITalino_Board_Datasheet.pdf. Accessed: 2018-02-10.
- [68] PLUX. ECG sensor datasheet. http://bitalino.com/datasheets/ECG_Sensor_Datasheet.pdf. Accessed: 2018-02-10.
- [69] PLUX. EDA sensor datasheet. http://bitalino.com/datasheets/EDA_Sensor_Datasheet.pdf. Accessed: 2018-02-10.
- [70] PLUX. Respiration sensor datasheet. http://bitalino.com/datasheets/PZT_Sensor_Datasheet.pdf. Accessed: 2018-02-10.
- [71] Fabienne Porée, Antoine Gallix, and Guy Carrault. Biometric identification of individuals based on the ECG. Which conditions? In *Computing in Cardiology, 2011*, pages 761–764. IEEE, 2011.
- [72] Shahrzad Pouryayevali, Saeid Wahabi, Siddarth Hari, and Dimitrios Hatzinakos. On establishing evaluation standards for ECG biometrics. In *Acoustics, speech and signal processing (icassp), 2014 ieee international conference on*, pages 3774–3778. IEEE, 2014.
- [73] Charles H. Romine. The Current and Future Applications of Biometric Technologies. <https://www.nist.gov/speech-testimony/current-and-future-applications-biometric-technologies>. Accessed: 2018-02-6.
- [74] Arun A Ross, Karthik Nandakumar, and Anil K Jain. *Handbook of Multibiometrics*, volume 6. Springer Science & Business Media, 2006.

- [75] Alex Sagie, Martin G Larson, Robert J Goldberg, James R Bengtson, and Daniel Levy. An improved method for adjusting the QT interval for heart rate (the Framingham Heart Study). *American Journal of Cardiology*, 70(7):797–801, 1992.
- [76] Ashima Sahoo, P Manimegalai, and K Thanushkodi. Wavelet based pulse rate and Blood pressure estimation system from ECG and PPG signals. In *Computer, Communication and Electrical Technology (ICCCET), 2011 International Conference on*, pages 285–289. IEEE, 2011.
- [77] Reza Sameni, Mohammad B Shamsollahi, Christian Jutten, and Gari D Clifford. A nonlinear Bayesian filtering framework for ECG denoising. *IEEE Transactions on Biomedical Engineering*, 54(12):2172–2185, 2007.
- [78] Marta S Santos, Ana LN Fred, Hugo Silva, and André Lourenço. Eigen Heartbeats for User Identification. In *BIOSENSE*, pages 351–355, 2013.
- [79] Abhijit Sarkar, A Lynn Abbott, and Zachary Doerzaph. Biometric authentication using photoplethysmography signals. In *Biometrics Theory, Applications and Systems (BTAS), 2016 IEEE 8th International Conference on*, pages 1–7. IEEE, 2016.
- [80] Abhijit Sarkar, A Lynn Abbott, and Zachary Doerzaph. Biometric authentication using photoplethysmography signals. In *Biometrics Theory, Applications and Systems (BTAS), 2016 IEEE 8th International Conference on*, pages 1–7. IEEE, 2016.
- [81] Petros Spachos, Jixin Gao, and Dimitrios Hatzinakos. Feasibility study of photoplethysmographic signals for biometric identification. In *Digital Signal Processing (DSP), 2011 17th International Conference on*, pages 1–5. IEEE, 2011.
- [82] Statex. Conductive metallized nylon fabric Zell. <https://www.sparkfun.com/datasheets/DevTools/LilyPad/ripstopzell.pdf>. Accessed: 2018-02-11.
- [83] John Steinbeck. *The grapes of wrath*. na, 1939.
- [84] Mohamed M Tawfik, Hany Selim, and Tarek Kamal. Human identification using time normalized QT signal and the QRS complex of the ECG. In *Communication Systems Networks and Digital Signal Processing (CSNDSP), 2010 7th International Symposium on*, pages 755–759. IEEE, 2010.
- [85] Randa Boukhris Trabelsi, Alima Damak Masmoudi, and Dorra Sellami Masmoudi. A new multimodal biometric system based on finger vein and hand vein recognition. *International Journal of Engineering and Technology*, 4:3175, 2013.
- [86] Mitchell Trauring. Automatic comparison of finger-ridge patterns. *Nature*, 197(4871):938, 1963.

- [87] Bert Vandenberk, Eline Vandael, Tomas Robyns, Joris Vandenberghen, Christophe Garweg, Veerle Foulon, Joris Ector, and Rik Willems. Which QT correction formulae to use for QT monitoring? *Journal of the American Heart Association*, 5(6):e003264, 2016.
- [88] N Venkatesh and Srinivasan Jayaraman. Human electrocardiogram for biometrics using DTW and FLDA. In *Pattern recognition (icpr), 2010 20th international conference on*, pages 3838–3841. IEEE, 2010.
- [89] Galen S Wagner. *Marriott's practical electrocardiography*. Lippincott Williams & Wilkins, 2001.
- [90] Lei Wang, Benny PL Lo, and Guang-Zhong Yang. Multichannel reflective PPG earpiece sensor with passive motion cancellation. *IEEE transactions on biomedical circuits and systems*, 1(4):235–241, 2007.
- [91] Yongjin Wang, Foteini Agrafioti, Dimitrios Hatzinakos, and Konstantinos N Plataniotis. Analysis of human electrocardiogram for biometric recognition. *EURASIP journal on Advances in Signal Processing*, 2008(1):148658, 2007.
- [92] Levi B Wood and H Harry Asada. Low variance adaptive filter for cancelling motion artifact in wearable photoplethysmogram sensor signals. In *Engineering in Medicine and Biology Society, 2007. EMBS 2007. 29th Annual International Conference of the IEEE*, pages 652–655. IEEE, 2007.
- [93] Jianchu Yao and Steve Warren. A short study to assess the potential of independent component analysis for motion artifact separation in wearable pulse oximeter signals. In *Engineering in Medicine and Biology Society, 2005. IEEE-EMBS 2005. 27th Annual International Conference of the*, pages 3585–3588. IEEE, 2005.
- [94] Can Ye, Miguel Tavares Coimbra, and BVK Vijaya Kumar. Investigation of human identification using two-lead electrocardiogram (ECG) signals. In *Biometrics: Theory Applications and Systems (BTAS), 2010 Fourth IEEE International Conference on*, pages 1–8. IEEE, 2010.
- [95] Yilong Yin, Lili Liu, and Xiwei Sun. SDUMLA-HMT: a multimodal biometric database. In *Chinese Conference on Biometric Recognition*, pages 260–268. Springer, 2011.
- [96] Zhaomin Zhang and Daming Wei. A new ECG identification method using Bayes' theorem. In *Tencon 2006. 2006 ieee region 10 conference*, pages 1–4. IEEE, 2006.
- [97] Zhilin Zhang, Zhouyue Pi, and Benyuan Liu. TROIKA: A general framework for heart rate monitoring using wrist-type photoplethysmographic signals during intensive physical exercise. *IEEE Transactions on Biomedical Engineering*, 62(2):522–531, 2015.
- [98] Yizhou Zhong, Yun Pan, Ling Zhang, and Kwang-Ting Cheng. A wearable signal acquisition system for physiological signs including throat PPG. In *Engineering in Medicine and Biology Society (EMBC), 2016 IEEE 38th Annual International Conference of the*, pages 603–606. IEEE, 2016.

- [99] W Zong, T Heldt, GB Moody, and RG Mark. An open-source algorithm to detect onset of arterial blood pressure pulses. In *Computers in Cardiology, 2003*, pages 259–262. IEEE, 2003.